

**Development And Improvement Of Subsonic Wind Tunnel In
Universiti Teknologi Petronas
(Air Flow Quality Testing)**

by

Syahril b Salleh

Dissertation submitted in partial fulfillment of
the requirements for the
Bachelor of Engineering (Hons)
(Mechanical Engineering)

JANUARY 2004

Universiti Teknologi PETRONAS
Bandar Seri Iskandar
31750 Tronoh
Perak Darul Ridzuan

CERTIFICATION OF APPROVAL

**Development And Improvement Of Subsonic Wind Tunnel In
Universiti Teknologi Petronas
(Air Flow Quality Testing)**

by

Syahril B Salleh

A project dissertation submitted to the
Mechanical Engineering Programme
Universiti Teknologi PETRONAS
in partial fulfillment of the requirement for the
BACHELOR OF ENGINEERING (Hons)
(MECHANICAL ENGINEERING)

Approved by,



(Pn Azuraian bt Japper@Jaafar)

UNIVERSITI TEKNOLOGI PETRONAS

TRONOH, PERAK

JANUARY 2004

CERTIFICATE OF ORIGINALITY

This is to certify that I am responsible for the work submitted in this project, that the original work is my own except as specified in the references and acknowledgements, and that the original work contained herein have not been undertaken or done by unspecified sources or persons.



SYAHRIL B SALLEH

ABSTRACT

This dissertation is compiled on the study of Development and Improvement on subsonic wind tunnel developed in Universiti Teknologi Petronas (herein after is called UTP). The objective of this study is to design and develop a new open circuit subsonic wind tunnel that can operate under 11 m/s ~ 15 m/s. Basically, the project was divided onto two phases. In Phase I, the scope of study was to cover the literature review on theory regarding the sub sonic wind. The guidelines for the design then were selected and compiled to engineer a new sub sonic wind tunnel that meets the criteria given. The study in Phase I also covered the justification on fan selection and proper contraction ratio. In Phase II, the air flow quality such as turbulence intensity and velocity variations were investigated to verify the developed wind tunnel. The scope of study in Phase II included the understanding of working principle of hot wire anemometer as the tool needed to measure velocity and turbulence intensity. The methodology of approach to achieve the objective started from the literature review related to the airflow quality. Based on the literature review in phase II, an experiment was conducted to determine the velocity variation and the turbulence intensity in the test section. A constant temperature anemometer as one type hot wire anemometer is being used throughout the experiment. The result is obtained by using the Streamline/Streamware software. The sensor used for the experiment was 1D(55P11-Gold Plated Miniature wire probe) sensor due to the unavailable 2D(55P61-X wire probe) sensor during the experiment. . Based on the results obtained, it showed that the velocity of air throughout the test section was about 11 m/s ~ 12 m/s which meet the first objective of the project. The turbulence level was quite low although exceed the constraint of less than 0.1%. This was basically due to the absent of the honeycomb in the settling chamber. However, the project can be concluded to be successful as it meet one of the design constraint which to operate under 10 m/s ~ 15 m/s.

ACKNOWLEDGEMENT

Firstly, the author would like to forward my deepest gratitude to the supervisor, Pn Azuraïen Japper @ Jaafar for the continuous guidance to the author to ensure the project to be completed by the mean time. The author would like also to thanks the Mechanical Program Head, Dr Fakhruddin Mohd Hashim, for his support and not to forget the mechanical technicians, En Kamarul, En. Nizam, En. Zairi, En. Hafiz and En. Sani for their time helping and guiding the author to complete the project.

Special gratitude also to the author's parents who have encouraged the author throughout the moral support. The author will always be grateful for their sacrifices, sincerity and love. Finally, special thanks to colleagues for the understanding and support towards project completion.

TABLE OF CONTENTS

CERTIFICATION OF APPROVAL	i
CERTIFICATION OF ORIGINALITY	ii
ABSTRACT	iii
ACKNOWLEDGEMENT	iv
TABLE OF CONTENTS	v
LIST OF FIGURES	viii
LIST OF TABLES	ix
ABBREVIATION AND NOMENCLATURE	x
CHAPTER 1 : INTRODUCTION	1
1.1 Background. Of .Study	1
1.2 Problem Statement	1
1.3 Objective and Scope of Study.	2
CHAPTER 2 : LITERATURE REVIEW AND THEORY	3
2.1 Over view of Wind Tunnel	3
2.2 Wind Tunnel Classification	4
2.2.1 Closed Circuit.	4
2.2.2 Open Circuit	5
2.3 Design Rules	8
2.4 Fan Selection	9

2.5	Material Selection.	. . .	10
2.6	Air Flow Quality	10
	2.6.1 Reynolds Number	10
	2.6.2 Turbulence Intensity	12
2.7	Laser Doppler and Hot Wire Working Principles		14
2.8	Hot Wire Theory and Working Principle	17
CHAPTER 3 :	METHODOLOGY/PROJECT WORK	12
3.1	Procedure Identification	12
3.2	Phase I-Engineering Design Approach.	17
3.3	Phase II-Identify Type Of Experiment For Air Flow Quality Evaluation	
3.4	Turbulence Intensity Method Of Calculation		
3.5	Tool And Equipment	
3.6	Software	
CHAPTER 4 :	RESULTS AND DISCUSSION	27
4.1	Technical Drawing	27
4.2	Fan Selection.	32
4.3	Material Selection.	34
4.4	Cost	35
4.5	Analysis on Low Speed Wind Tunnel.	36
4.6	Experimental Analysis on Wind Tunnel	36

CHAPTER 5 :	CONCLUSION AND RECOMMENDATION.	45
	5.1 Conclusion	45
	5.2 Recommendation	45
REFERENCES	47
APPENDIX	48

LIST OF FIGURES

FIGURE 2.1	Types of wind tunnel	4
FIGURE 2.2	Close circuit wind tunnel	4
FIGURE 2.3	Open Circuit wind tunnel	5
FIGURE 2.4	Open circuit wind tunnel	6
FIGURE 2.5	Example of Fan capacity diagram	9
FIGURE 2.6	boundary Layer growth nozzle-diffuser configurations	11
FIGURE 2.7	Mean velocity at turbulence velocity.. . . .	12
FIGURE 2.8	Typical velocity and shear distribution in turbulent flow near wall.	13
FIGURE 2.9	Laser Doppler Basic operations.	14
FIGURE 2.10	hot wire anemometers	15
FIGURE 3.1	Probe Position.	20
FIGURE 3.2	Position of testing area from inlet of test section.	21
FIGURE 3.3	Experimental setup	21
FIGURE 3.4	Example of velocity reading	22
FIGURE 3.5	Hot wire anemometer	24
FIGURE 3.6	1-D sensor	25
FIGURE 4.1	Lengths of each section for designed wind tunnel.	27
FIGURE 4.2	The arrangement of honeycomb and screens within the setting Chamber	28
FIGURE 4.7	Comparison on velocity variation at left side of test section	33
FIGURE 4.3	Honeycomb size	29
FIGURE 4.4	CATIA 3D generated design	31
FIGURE 4.5	Fan system for wind tunnel	33
FIGURE 4.6	Velocity distribution for the flow of a Newtonian fluid between two parallel plates	37
FIGURE 4.7	Velocity variations on left side of test section.	38
FIGURE 4.8	Velocity variations on middle side of test section	38
FIGURE 4.9	Velocity variations on right side of test section	38
FIGURE 4.10	Comparison between results of equation 3.1 and 3.2 (Left side)	39

FIGURE 4.11	Comparison between results of equation 3.1 and 3.2 (Middle)	40
FIGURE 4.12	Comparison between results of equation 3.1 and 3.2 (Right side)	41
FIGURE 4.13	Turbulence intensity distributions in test section	42

LIST OF TABLES

TABLE 2.3	Open circuit wind tunnel part and its function	7
TABLE 2.4	Design rules for small low speed wind tunnel.	8
TABLE 3.1	Group of position	20
TABLE 3.3	Tools needed in Phase I	26
TABLE 3.3	Tools needed in Phase II	26
TABLE 4.1	Material use in settling chamber	34
TABLE 4.2	Material use in test section and overall part.	34
TABLE 4.3	Cost for constructing the wind tunnel.	35
TABLE 4.4	Turbulence intensity for both method of calculation.	41

ABBREVIATION AND NOMENCLATURE

Re	Reynolds number	ke	kinetic energy
ρ	Density	U_{ref}	Reference velocity
V	Velocity	T_w	Temperature of wire
L	Length	T_f	Temperature of fluid
μ	Dynamic viscosity	I	Input current
\bar{u}	Mean fluctuated velocity	R	Wire resistance
T	Time taken	a	Thermal coefficient
τ	Turbulent shear stress	h	Heat transfer coefficient
I	Turbulence intensity	NU	Main stream velocity

CHAPTER 1

INTRODUCTION

1. INTRODUCTION

1.1 Background of Study

The study of this project mainly was to develop an open circuit wind tunnel in UTP. The project was divided into two phases. Phase I of the project covered the understanding of working principle of open circuit wind tunnel. Then the theories of the designed were compiled in order to deliver a suitable open circuit wind tunnel for this project. Phase I also covered the justification of the drive system. Phase II of the project began immediately after the wind tunnel was completely fabricated and assembled. Under Phase II, the project was to determine the velocity in the test section and also the turbulence intensity in three sections of the test section namely right, middle and left side. The study also covers the experimental method to measure the velocity variation and turbulence intensities in the test section.

1.2 Problem Statement

The main task on this project is to develop a sub sonic wind tunnel which follows the following condition:

- The test section area must be 30 cm X 30 cm
- The flow speed in the test section in range of 10 m/s-15m/s

The term subsonic means that the wind tunnel will be operated below 0.3 mach or below 134 m/s.

1.2 Objective and Scope of Study

Generally, a wind tunnel is used to study aerodynamic properties of an object in a stationary manner including pressures, forces, velocities, and vibrations. Currently, UTP does not have a proper wind tunnel. Thus, for the ease of study, the existed wind tunnel will be redeveloped.

Currently, UTP has a small scale wind tunnel with improper operating condition. The main goal of this project is to redevelop a small scale wind tunnel which can operate under 10m/s ~ 15 m/s for the use in UTP .By redeveloping this wind tunnel, hopefully it can be fully utilize by the lecturers to visualize the flow characteristic to the students.

The other objective for this project was to determine the velocity variations and turbulence intensity in the test section. The result of the experiment was being analyzed so that further recommendation and improvement will be stated later.

Basically, the development of sub sonic wind tunnel will manipulate the pure mechanical principles such as Fluids Mechanic, Heat Transfer and Computer Aided Design. So, this project also will help us to integrate the knowledge on engineering, management and financial principles.

This project is divided into two phase. Under phase I (August – November), this project will cover the study and design over the function of each part in wind tunnel The prototype of the wind tunnel will be constructed at the end of phase I.

The phase II (January – April) of this project is to cover the study of the flow quality in the test section. Basically, the study will involve the understanding over Hot wire anemometer (CTA) and how to properly select the sensor and the experiment for procedure in order to obtained an accurate results.

Gantt Chart for both Phase I and Phase II can be referred at **Appendix A-1** and **A-2**

CHAPTER 2

LITERATURE REVIEW AND THEORY

2.1 Overview of Wind Tunnel

The wind tunnel actually a replacement of whirling arm and the first wind tunnel was built by Frank H. Wenham (1824-1908), a Council Member of the Aeronautical Society of Great Britain, in 1871.

Generally, the wind tunnel is used to study aerodynamic properties of an object in a stationary manner including pressures, forces, velocities, and vibrations. Wind tunnel offer a rapid, economical, and accurate means for aerodynamic research. It is widely used in automotive and aeronautical fields to test the performance of objects such as car and plane wing.

Wind tunnel also is used for research, in which experiments are done to investigate the microstructure of (turbulent) flows. Either by natural turbulence or by artificial generation, flow structures are analyzed in order to understand the flow system.

2.2 Wind Tunnel Classification

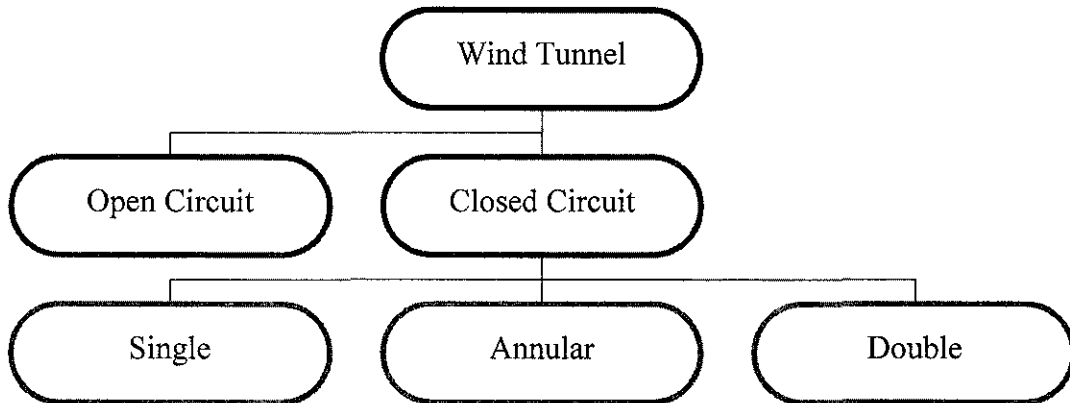


Figure 2.1 : Types of wind tunnel

Mainly there are two types of wind tunnel which are the Open circuit and the close circuit wind tunnel. In a Closed Circuit wind tunnel, the air that passes through the test section is drawn back into the fan and sent through the test section again and again. Please refer to figure 2 . Close circuit wind tunnel can be divided by 3 types which are single, annular and double return.

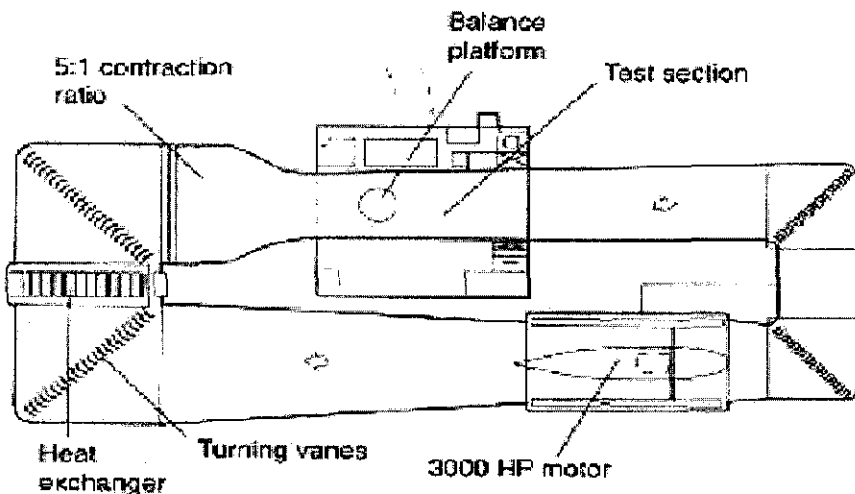


Figure 2.2 : Closed circuit wind tunnel¹

¹Kas Kasravi, 19th August 2003, <[http:// www. Kasravi/cmu/tech452/aerodynamics](http://www.Kasravi/cmu/tech452/aerodynamics)>

Here are the summary of the advantages and disadvantages of close circuit wind tunnel

Table 2.1 : Advantages and disadvantages of close circuit wind tunnel

Advantages	Disadvantages
- In a well designed Closed Circuit wind tunnel, some energy is recovered due to constant ambient condition. A smaller motor can be used.	- Closed Circuit Wind Tunnels are much more expensive to build due to the construction of the additional air return system
- Closed Circuit Wind Tunnels are completely enclosed, and so are shielded from rain and cold weather.	- The air in a Closed Circuit Vertical Wind Tunnel is full of dust and debris from clothing, cushions, etc. This is constantly recirculated, and is very difficult to remove.

The project is more focused on developing small scale open circuit wind tunnel for this project. In an Open Circuit Wind Tunnel, fresh air is drawn into the machine. The air that passes through the test section is discharged from the machine. Please refer top figure.

The term small scale wind tunnel or low speed meaning that the wind tunnel that is currently develop will operate with speed less than 0.3 mach.

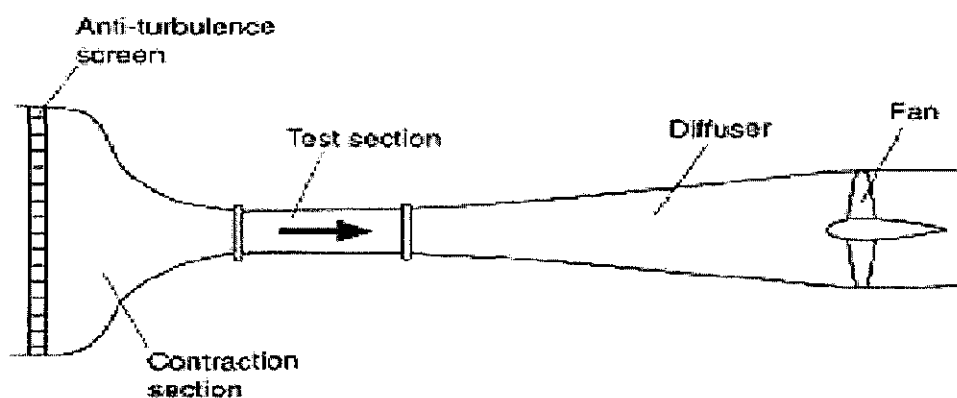


Figure 2.3: Open circuit wind tunnel²

² Kas Kasravi, 19th August 2003, <[http:// www. Kasravi/cmu/tech452/aerodynamics](http://www.Kasravi/cmu/tech452/aerodynamics)>

Here are the summary of the advantages and disadvantages of open circuit wind tunnel.

Table 2.2 : Advantages and disadvantages of open circuit wind tunnel

Advantages	Disadvantages
An Open Circuit Wind Tunnel is much less expensive to build.	not accurate - prone to changes in atmosphere and can require more power
Saving space	There may be dirt and insect coming through the wind tunnel
	Noisy due to fan.

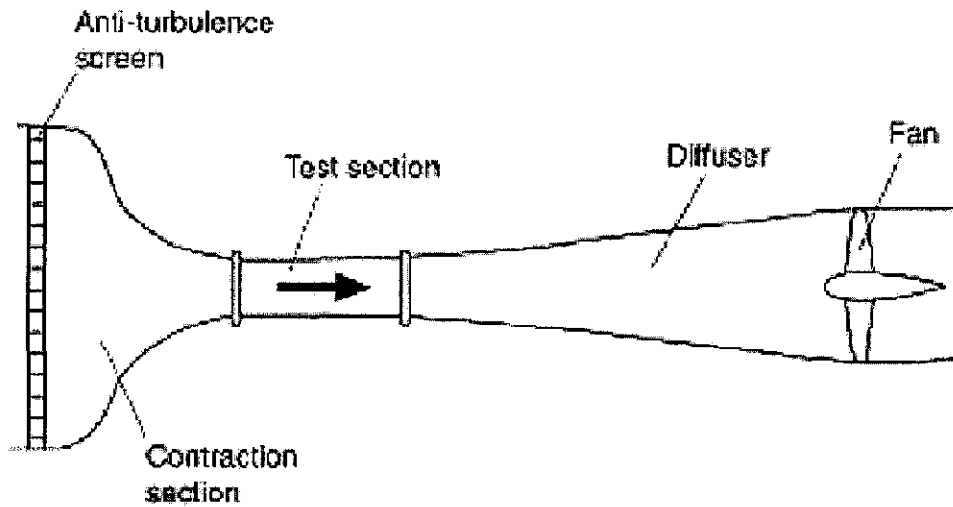


Figure 2.4 : Open circuit wind tunnel.

Basically, a wind tunnel consists of several parts which are a settling chamber, a contraction cone, a test section, a diffuser and also a drive system. (Please Refer to Figure 2.4)

The functions of each part in the wind tunnel are shown in Table 2.3 below.

Table 2.3 : Open circuit wind tunnel part and it function

Section		Function
Settling chamber	Honeycomb	Straighten the air flow
	Air screen filter	Filter dust and reduce turbulence effect
Contraction cone		To take a large volume of low-velocity air and reduce it to a small volume of high-velocity air. Venture effect.
Test Section		Models of wings or planes are placed in the test section. As airflow is brought to the desired velocity, sensors measure forces, such as lift and drag, on the test article.
Diffuser		Where the air coming out of the test section slows down prior to exhausting or recirculating. The air slows down due to the shape of the diffuser. By reducing power, the operating costs are reduced.
Extraction Fan		The drive section provides the force that causes air to move through the tunnel. This force normally comes from fans.

2.3 Small Scale Wind tunnel design rules

The research was continued to find the suitable design including the design size by referring from the technical data and the books wrote by the respective peoples in this area. Table below lists the general rules for the wind tunnel designed.

Table 2.4: Design rules for small low speed wind tunnel

Sections	Design rules
<p style="text-align: center;">Settling chamber length</p>	<p>The settling chamber length of $\frac{1}{2}$ times the inlet diameter is often used. The screen spacing (x) that equivalent to about 0.2 of the settling chamber diameter performs successfully. Also, the distance between last screen and the contraction entry (z) has also been found to be about 0.2 of the cross sectional diameters.³</p>
<p style="text-align: center;">Contraction cone</p>	<p>Contraction ratios between about 6 and 9 are normally used at least for the smaller tunnel³</p> <p>In common practice, the recommended length of the nozzle is , $l_n = 1 \times$ inlet radius</p>
<p style="text-align: center;">Test section</p>	<p>The test section, which may be closed, open, partially open or convertible. The test section length to hydraulic diameter ratio may be typically chosen to be 2 or more⁴</p>

³ Mehta and Bradshaw, 1979, Design Rules for small low speed wind tunnels

⁴ Jewel B. Barlow, 1999, Low Speed Wind Tunnel Testing, John Wiley and Sons

<p>Diffuser</p>	<p>A diffuser of at least three or four test section lengths. The typical equivalent cone angle is range of $2 - 3.5^\circ$ with the smaller angle being more desirable. The area ratio is typically 2-3, again with the smaller values be more desirable ⁵</p>
------------------------	---

2.4 Fan Selection

The fan for the wind tunnel system can be selected by using Fan Capacity Curve.

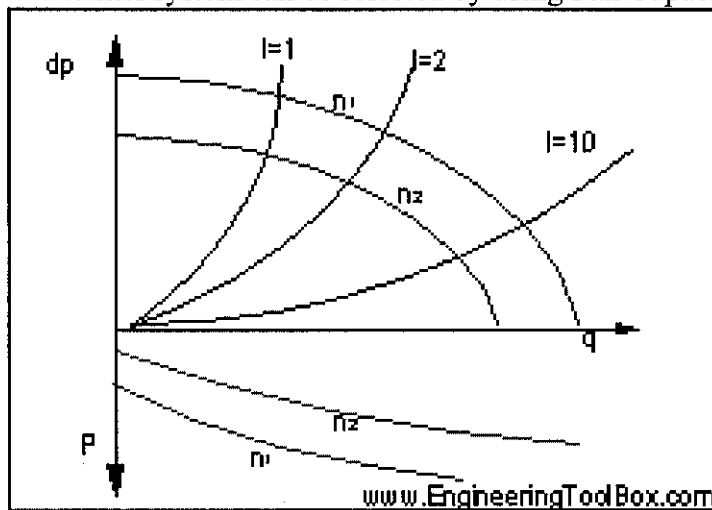


Figure 2.5: Example of fan capacity diagram⁶

The system curve is plotted to our requirement and then compare it to the manufacturer curve which will result to several fans that match up to our specification.

2.5 Material selections

⁵ Jewel B. Barlow, 1999, Low Speed Wind Tunnel Testing, John Wiley and Sons

⁶ The Engineering Toolbox, 5 October 2003, <http://www.engineeringtoolbox.com/hvac.htm>

Basically, there are 4 general criteria that we need to consider in selecting appropriate material for the wind tunnel, which are:

1. Performance characteristics, which selecting materials with suitable properties
2. Processing characteristics, such as finding the suitable process to form the material
3. Environmental profile
4. Budget, in term of material cost and processing cost

Basically, the main material that we had in mind to construct the wind tunnel with is actually the wood. Overall frames and walls of the wind tunnel will be made of wood, including the contraction's walls and diffuser's walls.

2.6 Air flow quality

2.6.1 Reynolds Number

The dimensionless Reynolds number is the primary parameter correlating the viscous behavior of all Newtonian fluids.

$$\text{Re} = \frac{\text{inertia force}}{\text{Viscous force}} = \frac{\rho V l}{\mu} \quad (2.1)$$

Where V = velocity

P = density

μ = viscosity

l = length.

Reynolds number indicates type of flow in test section of wind tunnel whether it is turbulent, laminar or in the transition region. Turbulence is due to the nonuniformity flow. The figure below shows the boundary layer growth and separation in nozzle-diffuser configuration.

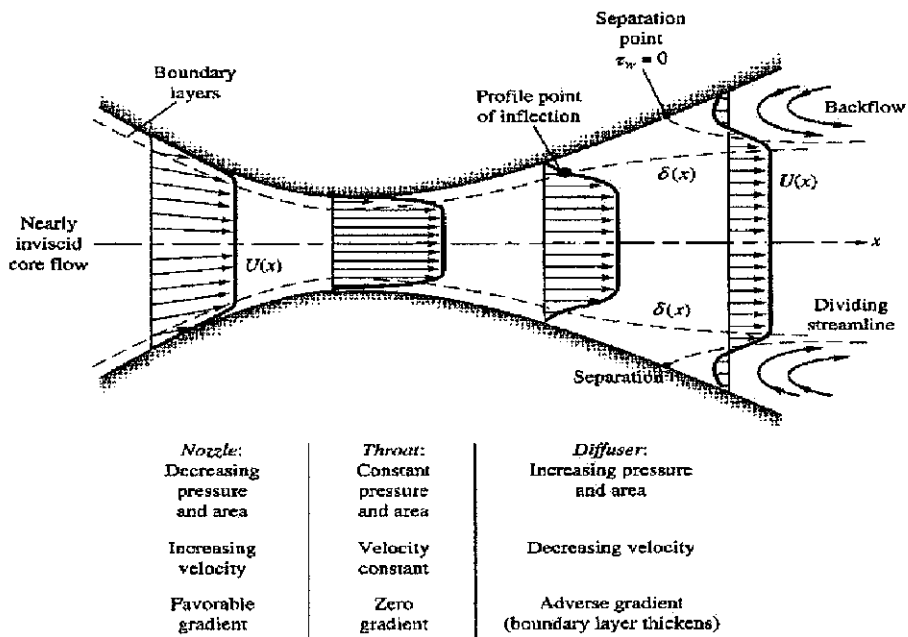


Figure 2.6 Boundary layer growth I nozzle-diffuser configuration⁷

Figure 2.3 above shows that parameters such as pressure, area, velocity and gradient are variables that change in values at different points or locations. Velocity increases when approaching through the nozzle to the throat. Throughout the nozzle, velocity is approximately constant. However, velocity decreases when approaching diffuser from the throat. Velocity of airflow may influence turbulence level. For instance, low velocity leads to boundary layer separation, and later leads to turbulence.

⁷ Frank, M. White, 1999, Fluid Mechanics, 4th edition, McGrawhill International Editions, United States

2.6.2 Turbulence Intensity

According to Osborne Reynolds (1895) rewriting the continuity and momentum equation, the time mean \bar{u} of a turbulent function $u(x,y,z,t)$ is defined by

$$\bar{u} = \frac{1}{T} \int_0^T u \, dt \quad (2.2)$$

where T is an averaging period taken to be longer than any significant period of the fluctuations themselves. The mean values of turbulent velocity is illustrates in figure 5 below.⁸

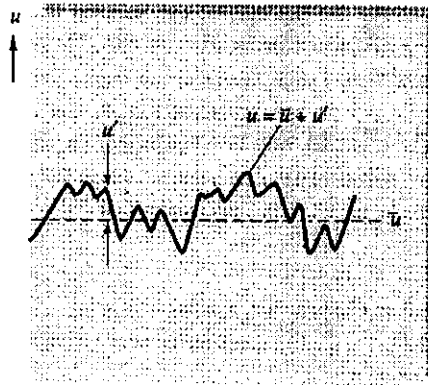


Figure 2.7 Mean values of turbulent velocity

The measure of turbulent intensity is

$$\overline{u'^2} = \frac{1}{T} \int_0^T u'^2 \, dt \neq 0 \quad (2.3)$$

However, each component of momentum equation, after time averaging, will contain mean values plus three mean products or correlation or fluctuating velocities. It reduces to the form of

⁸ Frank, M. White, 1999, Fluid Mechanics, 4th edition, McGrawhill International Editions, United States

$$\rho \frac{d\bar{u}}{dt} = -\frac{\partial \bar{p}}{\partial x} + \rho g_x + \frac{\partial}{\partial x} \left(\mu \frac{\partial \bar{u}}{\partial x} - \overline{\rho u'^2} \right) + \frac{\partial}{\partial y} \left(\mu \frac{\partial \bar{u}}{\partial y} - \overline{\rho u' v'} \right) + \frac{\partial}{\partial z} \left(\mu \frac{\partial \bar{u}}{\partial z} - \overline{\rho u' w'} \right) \quad (2.4)$$

From this equation, turbulent shear equation could be reduced in the form of

$$\tau = \mu \frac{\partial \bar{u}}{\partial y} - \overline{\rho u' v'} \quad (2.5)$$

Figure below shows the distribution of turbulent shear from typical measurements across a turbulent shear layer near a wall. These experimental facts are useful for the velocity distribution across a turbulent wall layer.

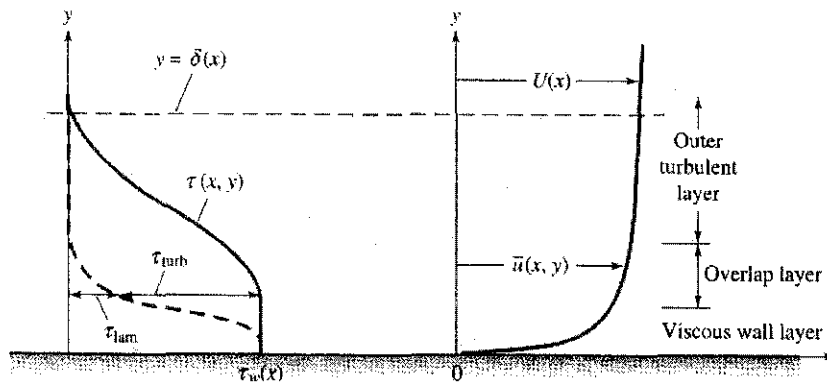


Figure 2.8 Typical velocity and shear distribution in turbulent flow near a wall⁹

For wind tunnel, the turbulence intensity in the test section without model should be kept as lower as possible. Ideally, there is no turbulence occurred in the test section. However, the turbulence level should be not exceed 0.1 % in order to maintain near zero turbulence level.¹⁰

⁹ Frank, M.White,1999, Fluid Mechanics, 4th edition, McGrawhill International Editions, United States

¹⁰ Rafan,Nur Aidawaty,June 2003, Improvement on Subsonic Wind Tunnel in Universiti Teknologi Petronas

2.7 Laser Doppler Anemometer and Hot Wire Anemometer working principles

The laser Doppler velocimeter sends a monochromatic laser beam toward the target and collects the reflected radiation. According to the Doppler Effect, the change in wavelength of the reflected radiation is a function of the targeted object's relative velocity. Thus, the velocity of the object can be obtained by measuring the change in wavelength of the reflected laser light, which is done by forming an interference fringe pattern

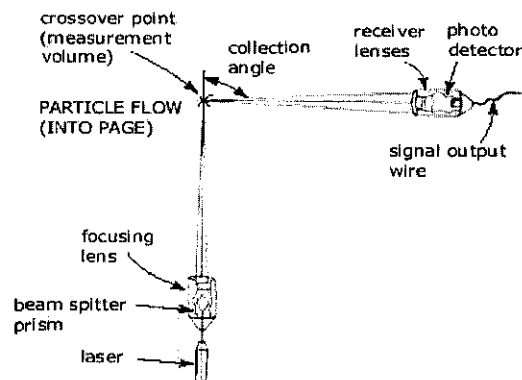


Figure 2.9 : Laser Doppler basic operation¹¹

A laser power source is the essential part of a laser Doppler velocimeter (LDV). Typically, a Helium-Neon (HeNe) or Argon ion laser with a power of 10 mW to 20 W is used. Lasers have many advantages over other radiation/wave sources, including excellent frequency stability, small beam diameter (high coherence), and highly-focused energy.

Laser Dopplers can be configured to act as flow meters or anemometers, by detecting the velocity of reflective particles entrained within a transparent flow field.

¹¹ Engineering Fundamental, <www.efunda.com/designstandards/sensors/hot_wire/laser_doppler_intro>

The Hot-Wire Anemometer is the most well known thermal anemometer, and measures a fluid velocity by noting the heat convected away by the fluid. The core of the anemometer is an exposed hot wire either heated up by a constant current or maintained at a constant temperature (refer to the schematic below). In either case, the heat lost to fluid convection is a function of the fluid velocity.

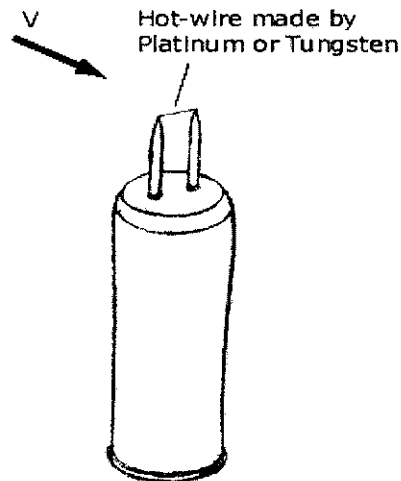


Figure 2.10 : Hot wire anemometer¹²

By measuring the change in wire temperature under constant current or the current required to maintain a constant wire temperature, the heat lost can be obtained. The heat lost can then be converted into a fluid velocity in accordance with convective theory.

Typically, the anemometer wire is made of platinum or tungsten and is $4 \sim 10 \mu\text{m}$ ($158 \sim 393 \mu\text{in}$) in diameter and 1 mm (0.04 in) in length.

Typical commercially available hot-wire anemometers have a flat frequency response ($< 3 \text{ dB}$) up to 17 kHz at the average velocity of 9.1 m/s (30 ft/s), 30 kHz at 30.5 m/s (100 ft/s), or 50 kHz at 91 m/s (300 ft/s).

¹² Engineering Fundamental < www.efunda.com/designstandards/sensors/hot_wire/hot_wires_intro.cfm >

2.8 Hot Wire working principle

Consider a wire that's immersed in a fluid flow. Assume that the wire, heated by an electrical current input, is in thermal equilibrium with its environment. The electrical power input is equal to the power lost to convective heat transfer,

$$I^2 R_w = h \cdot A_w (T_w - T_f)$$

where I is the input current, R_w is the resistance of the wire, T_w and T_f are the temperatures of the wire and fluid respectively, A_w is the projected wire surface area, and h is the heat transfer coefficient of the wire.

The wire resistance R_w is also a function of temperature according to,

$$R_w = R_{Ref} [1 + \alpha (T_w - T_{Ref})]$$

where α is the thermal coefficient of resistance and R_{Ref} is the resistance at the reference temperature T_{Ref} .

The heat transfer coefficient h is a function of fluid velocity v_f according to King's law,

$$h = a + b \cdot v_f^c$$

where a , b , and c are coefficients obtained from calibration ($c \sim 0.5$).

Combining the above three equations eliminate the heat transfer coefficient h ,

$$\begin{aligned} a + b \cdot v_f^c &= \frac{I^2 R_w}{A_w (T_w - T_f)} \\ &= \frac{I^2 R_{Ref} [1 + \alpha (T_w - T_{Ref})]}{A_w (T_w - T_f)} \end{aligned}$$

Continuing, the fluid velocity,

$$v_f = \left\{ \left[\frac{I^2 R_{Ref} [1 + \alpha (T_w - T_{Ref})]}{A_w (T_w - T_f)} - a \right] / b \right\}^{1/c}$$

Two types of thermal (hot-wire) anemometers are commonly used: constant-temperature and constant-current.

The constant-temperature anemometers are more widely used than constant-current anemometers due to their reduced sensitivity to flow variations. Noting that the wire must

be heated up high enough (above the fluid temperature) to be effective, if the flow were to suddenly slow down, the wire might burn out in a constant-current anemometer. Conversely, if the flow were to suddenly speed up, the wire may be cooled completely resulting in a constant-current unit being unable to register quality data.

CHAPTER 3

METHODOLOGY/ PROJECT WORK

3. METHODOLOGY/PROJECT WORK

3.1 Procedure Identification

The study is conducted in two phases. Phase I is a literature review and planning for the design and fabrication of the wind tunnel. Phase II is the improvement and testing period to achieve the objective. The methodology flow chart of project work is show in figure 3.4.

3.2 Phase I - Engineering Design Approach

3.2.1 Problem Definition

The client need was being defined and well justified before the planning of the project begun. In this case, UTP was being considered as the client. The need and the constraint of the project was been identified through the task given

3.2.2 Information Gathering

Then, the information regarding the project was obtained through library, interview with technician and also from visit to the lab. The information also being acquired from the catalogues and brochures from the Internet. A visit to Universiti Sains Malaysia also was made in order to get a clear picture of the wind tunnel.

3.2.3 Concept Generation

Under concept generation, the step involved was brainstorming. Group members gathered together to evoke ideas. The mind mapping techniques was used to branch out the idea from the main problems. Then, parts of the wind tunnel were decomposed and being visualize through the assembly chart.

3.2.4 Concept Evaluation

The concept of the design was being evaluated using the guidelines from the expert that recite their finding in journals and article over internet and books.

3.2.5 Design Configuration

In configuration design, the shape and the general dimensions of components were established. The material used was also being selected under this stage

3.2.6 Parametric Design and detail Drawing

The attributes of parts identified in configuration design now being enhanced in this stage. The design now also count the reliability factors and the tolerances use for the design. The final drawing in CAD was done during this final stage

3.2.7 Fabrication

The fabrication of the prototype was done at the end phase 1, where mostly the assembly and fabrication works has been done in the workshop by the guidance of respective technicians. The fabrication involves for the wind tunnel was the sheet metal and welding process.

3.3 Phase II- Identify type of experiment for air flow quality evaluation

The experiment to evaluate the air flow quality in the wind tunnel was being identified. The experiment was being conducted with the aid of Hot Wire Anemometer (CTA) which integrated with Streamline/Streamware software. Before the experiment can be conducted, the probe stand is designed to hold the probe support so that the probe wire will be at 90 degree against the airflow. In order to allow the probe holder going through the test section, upper side of test section should be drilled. Three holes are drilled

in order to test airflow in three different positions, which allocate the left, center and right side. The probe of hot wire anemometer should be placed perpendicular to the airflow. The probe position in test section is shown in **Appendix A-3**.

Then, velocity of air and turbulence intensity in test section is measured using hot wire anemometer. The reading is taken with several measurements at one specified point. There are few points have been assigned in order to study the velocity profile and turbulence intensity. The points assigned are shown in figure 3.1 below. The testing area is 30 cm from the inlet, which is in the middle of test section as figure 3.2. The probe is assigned at 7cm from the wall and the center is at 15 cm. The distance of probe position assigned in test section is shown in figure 3.1. The experimental setup also is shown in figure 3.3.

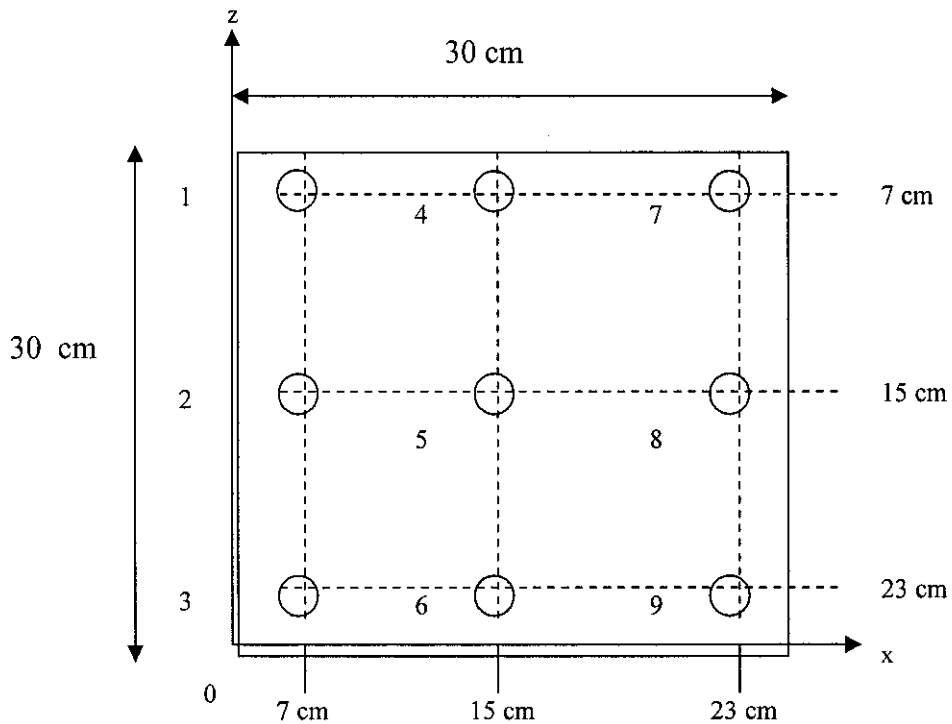


Figure 3.1 Probe position

Table 3.1 Group of position

Group	Position
Left side	1, 2, 3
Center	4, 5, 6
Right side	7, 8, 9

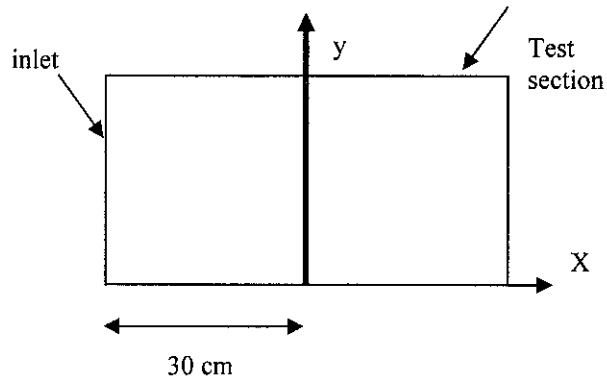


Figure 3.2 Position of testing area from inlet of test section

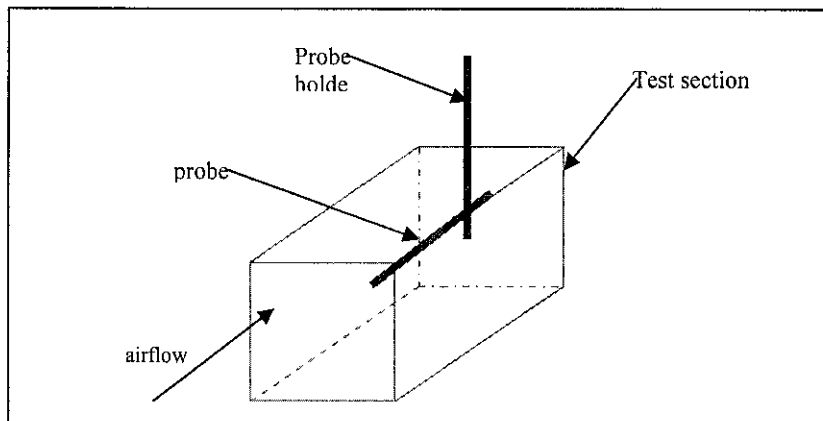


Figure 3.3 Experimental Setup¹³

¹³ Rafan, Nur Aidawaty, June 2003, Improvement on Subsonic Wind Tunnel in Universiti Teknologi Petronas (pg 15)

3.4 Turbulence Intensity method of calculation

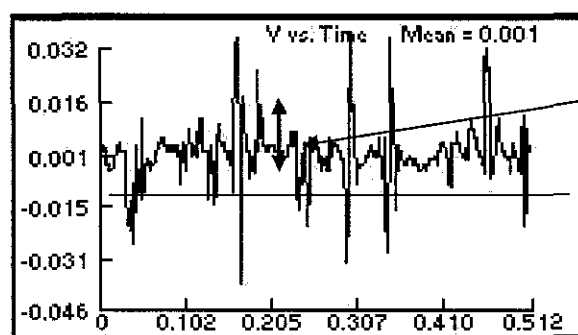
One of the most important aspects of the flow quality in a wind-tunnel is the level of turbulence intensity. During the design of the wind-tunnel, a lot of work was devoted to ensure that the parts used for turbulence damping, such as screens, honeycomb and contraction would work well,(see section 2.5). The measurement of the turbulence intensity in both the streamwise and crossstream directions were made to verify the quality of the design of these parts.

The turbulence intensity is defined as $\frac{\sqrt{I_x^2 + I_y^2 + I_z^2}}{U}$ where I_x , I_y and I_z are the turbulence intensities in the streamwise, the crossstream vertical and the cross-stream horizontal directions, respectively, and U is the streamwise mean velocity.

For wind tunnel, the turbulence intensity in the test section without model should be kept as lower as possible. Ideally, there is no turbulence occurred in the test section. However, the turbulence level should be not exceed 0.1 % in order to maintain near zero turbulence level.¹⁴

For this study, the steps taken by the previous student will be followed in order to determine the turbulence intensity in the wind tunnel.

Turbulence intensity was obtained using two difference equation . First equation defined urbulence intensity as the ratio of the RMS value of velocity component to its mean value.¹⁵



Fluctuated velocity

Figure 3.4 : example of velocity reading

¹⁴ Rafan,Nur Aidawaty,June 2003, Improvement on Subsonic Wind Tunnel in Universiti Teknologi Petronas(pg 33)

¹⁵ Finn,E.Jorgensen,2002, How to Measure Turbulence With Hot Wire Anemometer, Dantec Dynamic

$$\text{Turbulence Intensity, } I = \frac{U_{RMS}}{U_{mean}} \quad (3.1)$$

Where ,

$$U_{mean} = \frac{1}{N} \sum_1^N U_i$$

$$U_{RMS} = \left(\frac{1}{N-1} \sum_1^N (U_i - U_{mean})^2 \right)^{0.5}$$

For Streamware/Streamline software, N = no. of samples

Second equation defines turbulence intensity, I as

$$I = \frac{\left(\frac{2}{3} ke \right)^{\frac{1}{2}}}{U_{ref}} \quad (3.2)$$

where reference velocity, $U_{ref} = (U^2_{mean} + V^2_{mean} + W^2_{mean})^{1/2}$

and

kinetic energy, $ke = \frac{1}{2} (\overline{u^2} + \overline{v^2} + \overline{w^2})$ where \overline{u} , \overline{v} , \overline{w} are mean fluctuated velocity .

A sample calculation of turbulence intensities is shown in **Appendix A-1** .

The result obtained will be in term of velocity graph against distance at near wall and across the test section. The comparison between the two methods were being analyzed and compared.

3.5 Tool and Equipment

For this research study, the tool needed to measure velocity is hot wire anemometer. Hot wire anemometer is the most well known thermal anemometer and measures a fluid velocity by noting the heat conected away. Hot wire anemometer has high frequency response.

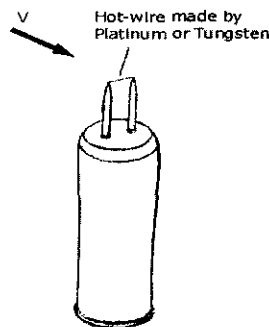


Figure 3.5 Hot wire anemometer¹⁶

3.5.1 Hot Wire Anemometer

The hot wire anemometer used is constant temperature anemometer. The model of hot wire anemometer is Flowpoint Velocity Measuring System with the software of Streamline/Streamware. This model is a Dantec Dynamics product. The probe used is 2 dimensional which is more accurate compared to the 1 dimensional direction. The maximum frequency response is 10 kHz. The typical velocity range is 0.15 to 100 m/s in air or 0.03 to 10 m/s in water. All key flow parameters can be shown, in user selectable units of measure, with real time graphical display. Mean velocity and turbulence intensity are displayed immediately. The analysis is done by using software Streamline/

¹⁶ Engineering Fundamental, <www.efunda.com/designstandards/sensors/hot_wire/hot_wires_intro.cfm>

StreamWare Analysis. The steps taken to operate the hot wire anemometer are shown in **Appendix C-2**. The components of hot wire anemometer are shown in **Appendix C-3**.

3.5.2 Probe selection

Probes are primarily selected on basis of

- Fluid medium
- Number of velocity components to be measured (1-, 2- or 3)
- Expected velocity range
- Quantity to be measured (velocity, wall shear stress etc.)
- Required spatial resolution
- Turbulence intensity and fluctuation frequency in the flow
- Temperature variations
- Available space around the measuring point (free flow, boundary layer flows, confined flows).

3.5.3 Sensors

Probes are available in one-, two- and three-dimensional versions as single-, dual and triple sensor probes referring to the number of sensors. Since the sensors (wires or fibre-films) respond to both magnitude and direction of the velocity vector, information about both can be obtained , only when two or more sensors are placed under different angles to the flow vector[14]. This experiment was conducted using 1 D(55P11) sensor since 2 D sensor was broken and unavailable to be use.

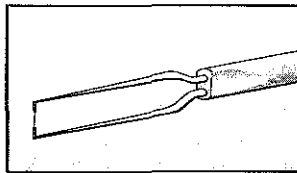


Figure 3.6 : 1D sensors¹⁷

¹⁷ Finn,E.Jorgensen,2002, How to Measure Turbulence With Hot Wire Anemometer, Dantec Dynamic

3.6 Software

The software used for both phases were summarized as below. CATIA solution was used to produce the engineering drawing complete with the dimensions. In second phase, Streamline/Streamware software was used to analyze the data acquired from the hot wire anemometer. Microsoft Excel was used to generate graph and to do calculations regarding turbulence intensity and fluctuated velocity.

Phase 1

Table 3.2 : Tools needed in phase 1

Stage	Tools needed
Literature	PC equipped with word processing software and internet access, digital camera
Design	PC equipped with CAD especially CATIA

Phase 2

Table 3.3 : Tools needed in phase 2

Stage	Tools needed
Literature	PC equipped with word processing software and internet access, digital camera
implementation	Streamline/Streamware(Data Acquiring) , Microsoft Excel(Analysis)

CHAPTER 4

RESULTS AND DISCUSSIONS

4.0 Result and discussion

4.1 Technical drawing

Figure 4.1 below visualize the design engineered using the law that been quoted earlier in Section 2. Details calculations for each part are listed below. The engineering drawing generated by CATIA can be referred at **Appendix A-4**

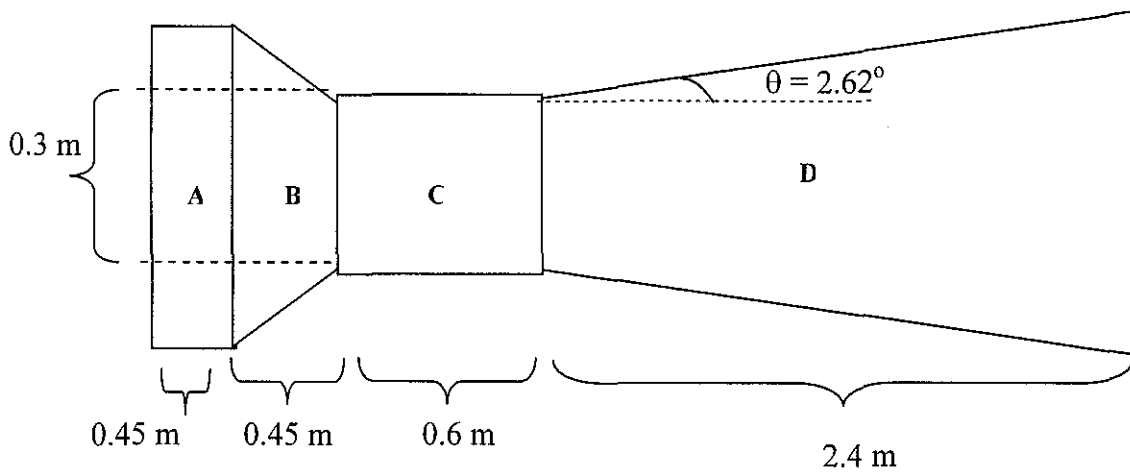


Figure 4.1: Length of each section for designed wind tunnel

Legend

A = Settling chamber

B = Contraction cone

C = Test section

D = Diffuser

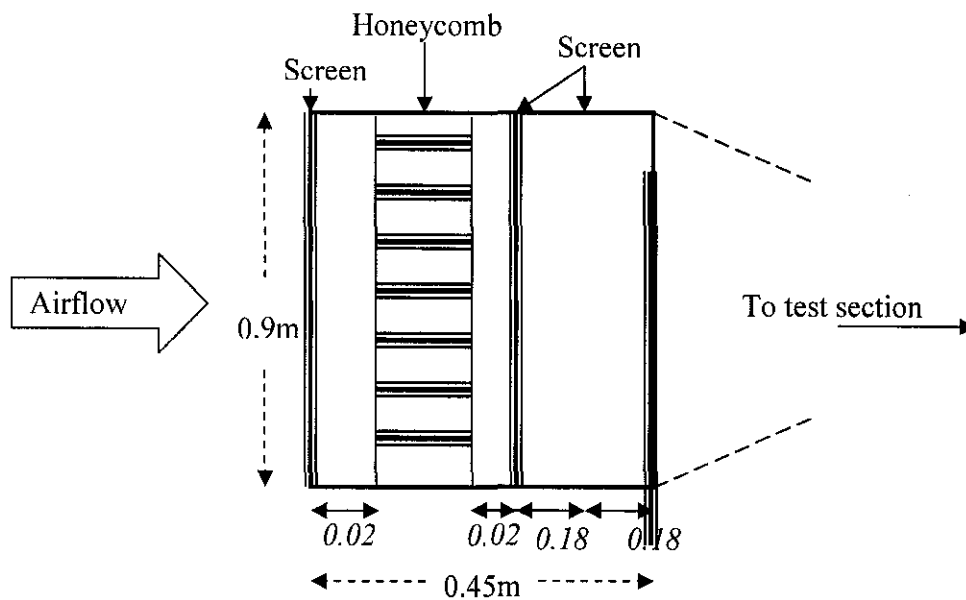


Figure 4.2: The arrangement of honeycomb and screens within the settling chamber

Calculation for wind tunnel design (please refer to figure 4.1 and 4.2)

A) Settling chamber length

The settling chamber length of $\frac{1}{2}$ times the inlet diameter is often used.

Inlet hydraulic diameter calculation (since the inlet is noncircular).

For given Contraction ratio, $Cr = 9$

Inlet area, $A_{in} = Cr \times (\text{test section area})$

$$= 9 \times 0.09 \text{ m}^2$$

$$= 0.81 \text{ m}^2$$

so, hydraulic diameter, $Dh = \frac{4A}{P}$

$$= \frac{4(0.81)}{3.6}$$

$$= 0.9 \text{ m}$$

Settling chamber length, $l_{sc} = 0.5 \times 0.9 \text{ m} = 0.45 \text{ m}$

The screen spacing (x) that equivalent to about 0.2 of the settling chamber diameter performs successfully. Also, the distance between last screen and the contraction entry (z) has also been found to be about 0.2 of the cross sectional diameters.

So, spacing between screens, $x = (0.2) \times 0.9\text{m}$

$$= 0.18 \text{ m}$$

also, known $z = x$

thus, $z = 0.18 \text{ m}$ (Please refer to figure 3)

Honeycomb size calculation

For maximum benefit, the cell length should be about 6-8 times its diameter. The cell size should be smaller than the smallest lateral wavelength of the velocity variation thoroughly 150 cells per settling chamber diameter¹⁸

So, the cell size is equal by $= 0.9 \text{ m} / 150 \text{ cell per settling chamber diameter}$

$$= 6 \text{ mm per cell size}$$

$$\text{cell length} = 8 \times 6 = 48 \text{ mm} \approx 50 \text{ mm}$$

The cell length should be approximately about 8 times of the cell size. From the calculation, we had determined the cell size approximately 6 mm where will result of the cell length of 50 mm. The cell size of 6mm is about the size of a common straw. So, we decide to list the straw as one of the alternative to overcome the honeycomb price problem in case we could not find additional fund to this project.

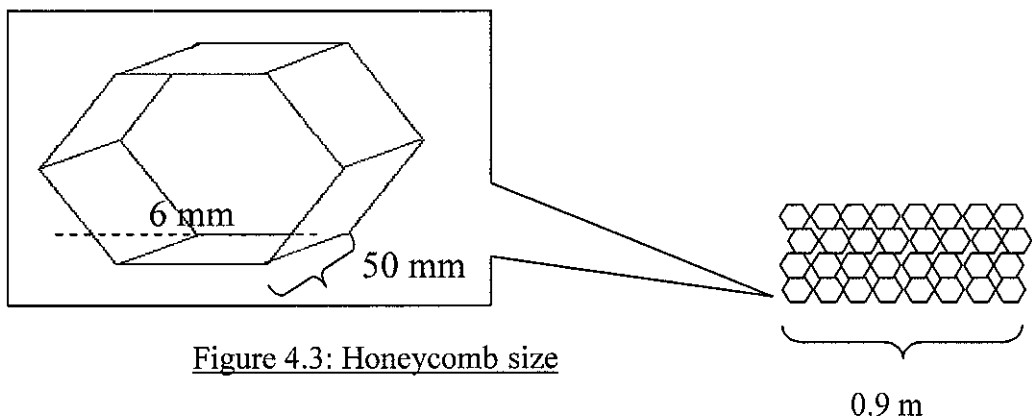


Figure 4.3: Honeycomb size

¹⁸ Mehta and Bradshaw, 1979, Design Rules for small low speed wind tunnels

B) Contraction cone

Contraction ratios between about 6 and 9 are normally used at least for the smaller tunnel¹⁹

In common practice, the recommended length of the nozzle is, $l_n = 1 \times$ inlet radius

Since inlet $D_h = 0.9$ m,

So, inlet radius, $r_{in} = 0.45$ m

Thus, nozzle length, $l_n = 1 \times 0.45$ m
= 0.45 m

C) Test section

The test section, which may be closed, open, partially open or convertible. *The test section length to hydraulic diameter ratio may be typically chosen to be 2 or more*, in contrast to the shorter test sections earlier era tunnel²⁰

D_h for test section = 0.3 m

So, $\frac{l_{ts}}{D_h} = 2$

Thus, $l_{ts} = 2 \times 0.3$ m
= 0.6 m

D) Diffuser

A diffuser of at least three or four test section lengths. The typical equivalent cone angle is in the range of 2 – 3.5° with the smaller angle being more desirable. The area ratio is typically 2-3, again with the smaller values to be more desirable²¹

Diffuser length, $l_d = 4 \times 0.6$ m
= 2.4 m

Selected area ratio for diffuser, $A_r = 3$

Thus, $A_{exit} = 3 \times A_{ts}$
 $= 3 \times 0.09 \text{ m}^2$
 $= 0.27 \text{ m}^2$

¹⁹ Mehta and Bradshaw, 1979, Design Rules for small low speed wind tunnel

²⁰ Jewel B. Barlow, 1999, Low Speed Wind Tunnel Testing, John Wiley and Sons

to find contraction angle, θ ,

$$l_{\text{exit}} = \sqrt{0.27} \text{ m}^2 \\ = 0.52 \text{ m}$$

$$\text{so, contraction angle, } \theta = \tan^{-1} \left[\frac{(0.52 - 0.3)/2}{2.4} \right] \\ = 2.62^\circ$$

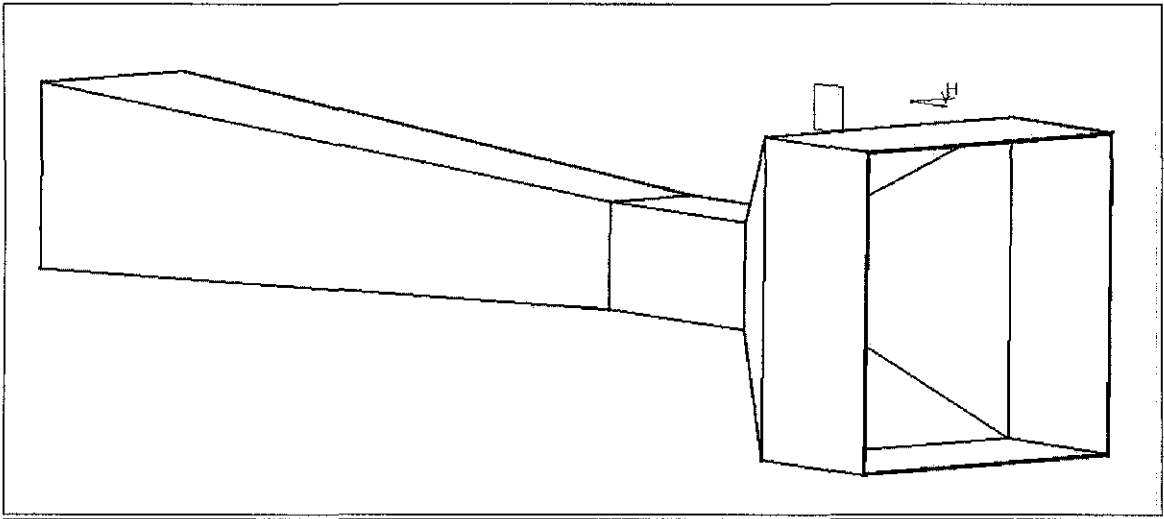


Figure 4.4: CATIA 3D Generated Design

4.2 Fan Selection

At first, the selection was made by using the air flow rate characteristic. It was because the fan that on market can be bought by stating the air flow rate needed. Thus an assumption that the flow rate for the fan must be equal to the flow rate in the test section was made which is about :

$$0.09 \text{ m}^2 \times 15 \text{ ms}^{-1} = 1.35 \text{ m}^3/\text{s} \text{ or } 81 \text{ m}^3/\text{m}. \text{ (test section area x air speed)}$$

But this assumption was not appropriate according to Mr. Shiraz, Thermal System Design lecturer. According to him, by doing that, the function of the diffuser which mainly to reduce the power needed to extract the air will be neglected.

The meeting ends up with a recommendation to use the Fan Capacity curve in order to determine the suitable fan needed. To plot the graph, the assumption made was not to neglect the pressure lost due to friction and velocity drop. (The static and the dynamic pressure)

The equation involve is

$$P2 = P1 \left(\frac{Q2}{Q1} \right)^2$$

Where P2 = dynamic pressure at exit of diffuser

P1 = dynamic pressure at exit of test section

Q1= Flowrate at exit of test section

Q2 = Flowrate at diffuser

Graph 1 : Pressure vs Flowrate

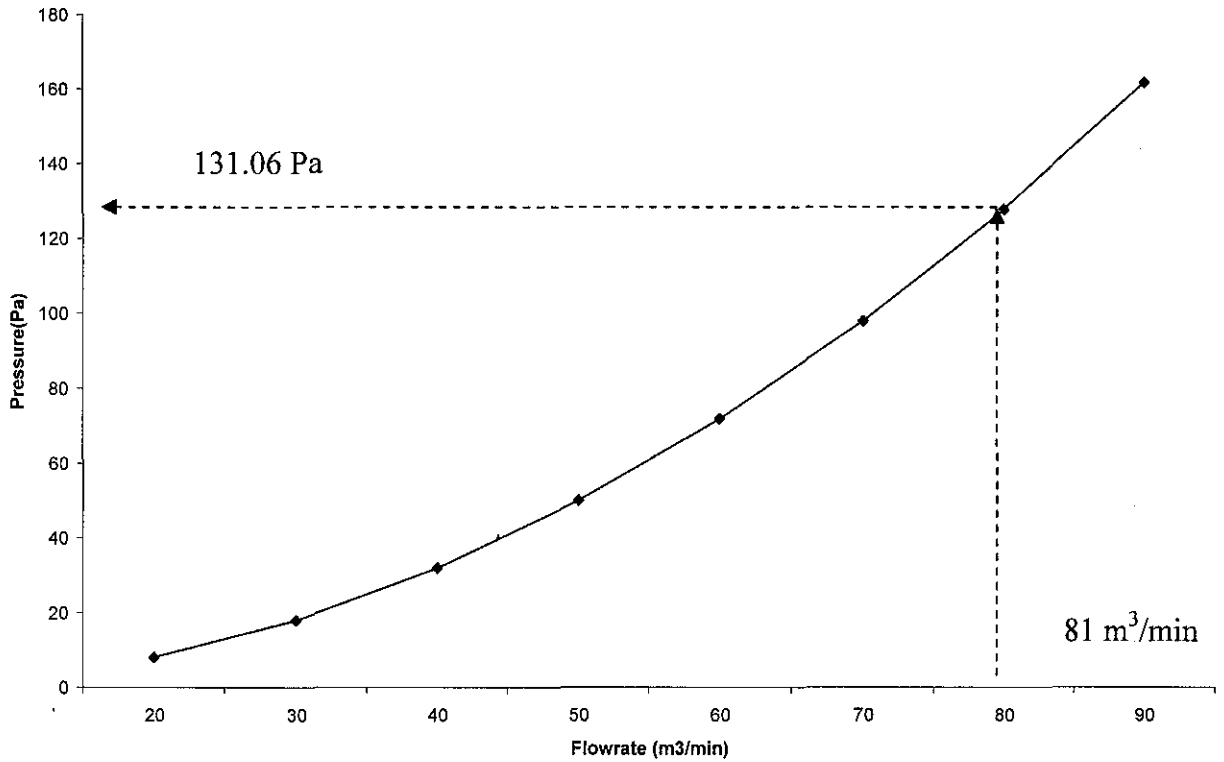


Figure 4.5 : Fan System for the wind tunnel

The System curve will be suited with the manufacturer fan curve to determine the suitable extraction fan needed to extract 81m³/m air flow rate from the test section. From the manufacturer curve, few fans will be listed. From there, the selected fan will be choose on several constraint which are:

1. Air flow rate characteristic – can extract air to the test section in range of 80 to 85 m³/min
2. Size – not bigger than 0.52 m X 0.52 m
3. Cost – around RM 500

Second alternative is to buy the motor and blade from the second hand shop. By this means, the cost can be reduced. But it will jeopardize the availability of the system.

4.3 Material selection

The suggested material for the wind tunnel is summarized below

Settling chamber

Table 4.1: Materials use in settling chamber

Parts	Materials
Chamber Wall	Plywood or aluminum sheet or Zinc
Honeycomb	Phenolic or Aluminum or Zinc or straws
Screens	Nylon Mesh or Metal Mesh

Test section

Table 4.2: Materials use in test section and overall parts

Parts	Materials
Test Section Frame	Wooden Frame
Sides, Top And Bottom Panels	Plexiglas

4.4 Cost

Table 4.3 below summarized the cost to fabricate the wind tunnel.

Table 4.3: Cost for constructing the wind tunnel

No.	Description	Purpose	Quantity	Price (RM)
1	<u>Construction</u>			
	C plate (0.8 mm thickness)	Wind Tunnel Body sheet	5	400
	Wind Tunnel stand Workmanship	Support Wind Tunnel		200 400
2	<u>Accessories</u>			
	Straw	Honeycomb	30 packets	9
	Wayarmesh Screen (4'X3')	Screens	1	22
	Perspex	See through section	1	40
	Exhaust Fan	Main driver	1	235
	<u>Specifications</u>			
	Type : Single Phase Size : 20 " Speed : 1440 RPM Flowrate : 95 m ³ /min			
¼ X ¾ Bolts Glu & Blue Board		1.3 Kg	6.50 16.70	
	Total			1325.20

Unfortunately, the honeycomb was being vandalized during its construction in the common room.

4.5 Analysis on Low Speed Wind Tunnel

Designing parameter of wind tunnel is influenced by the achievable Reynolds Number. From equation 2.1, the Reynolds Number is given by:

$$R = \frac{\rho V l}{\mu}$$

Where ρ = air density , 1.22 kg/m³

μ = viscosity , 1.8 x 10⁻⁵ N sec/m²

V = air velocity

l = test section length

Reynolds number is not appropriate to use for this study. It is because that to use this equation, the length of the test section should be a constant while the speed is a variable. The velocity should not be reduced since that lower velocity will leads to separation that increase in turbulence. Because of different variable in the parameter that being studied, it is concluded that the turbulence intensity will be determined experimentally using hot wire anemometer instead of using Reynolds equation.

However, the max achievable Reynolds number can be determined using Reynolds equation for given velocity and diameter in the test section.

4.6 Experimental Analysis on Wind Tunnel

The procedure to run the experiment was based on the manual of Streamline/Streamware Software.(Setup can be referred at **Appendix C-1, C-2 and C-3**) The velocity is displayed in term of fluctuated velocity. The graph of velocity for each point is shown in **Appendix D-1**. Velocity profile when the distance is increased can be obtained by plotting graph based on data for each point. Based on the velocity reading obtained while running the experiment, a graph is plotted. As a result, the graph shows the behavior of velocity when distance is vertically decreased in each side.

Theoretically, velocity variations in the test section can be described in the figure 4.6 below.

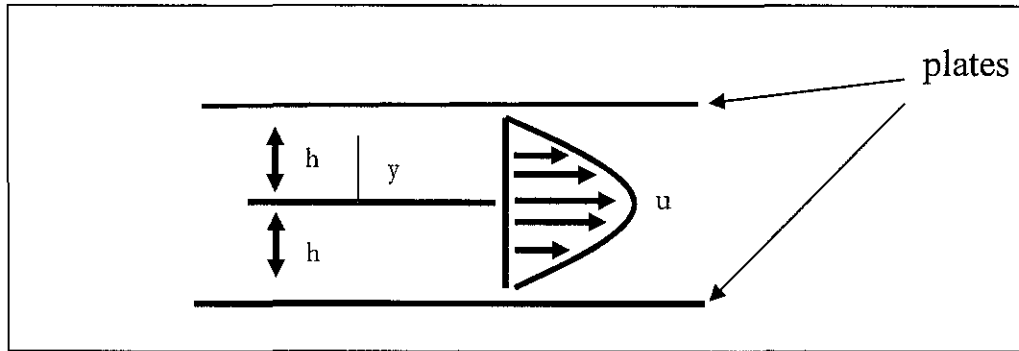


Figure 4.6 : velocity distribution for the flow of a Newtonian fluid between two parallel plates²¹

The equation to determine local velocities is given by

$$U = \frac{3V}{2} [1 - (y/h)^2]$$

Where U = local velocities, m/s

h = radius, m

y = distance from center, m

From the equation, the velocity variations in the test section would be theoretically shape a parabolic form where a zero velocity is obtains near the wall for non-slip condition and maximum velocity is obtained at the center of the test section. The velocity variations in the test section are shown in the next page.

²¹ Young, Donald F, 2000, *A Brief Introduction To Fluid Mechanics*, John Wiley and Sons

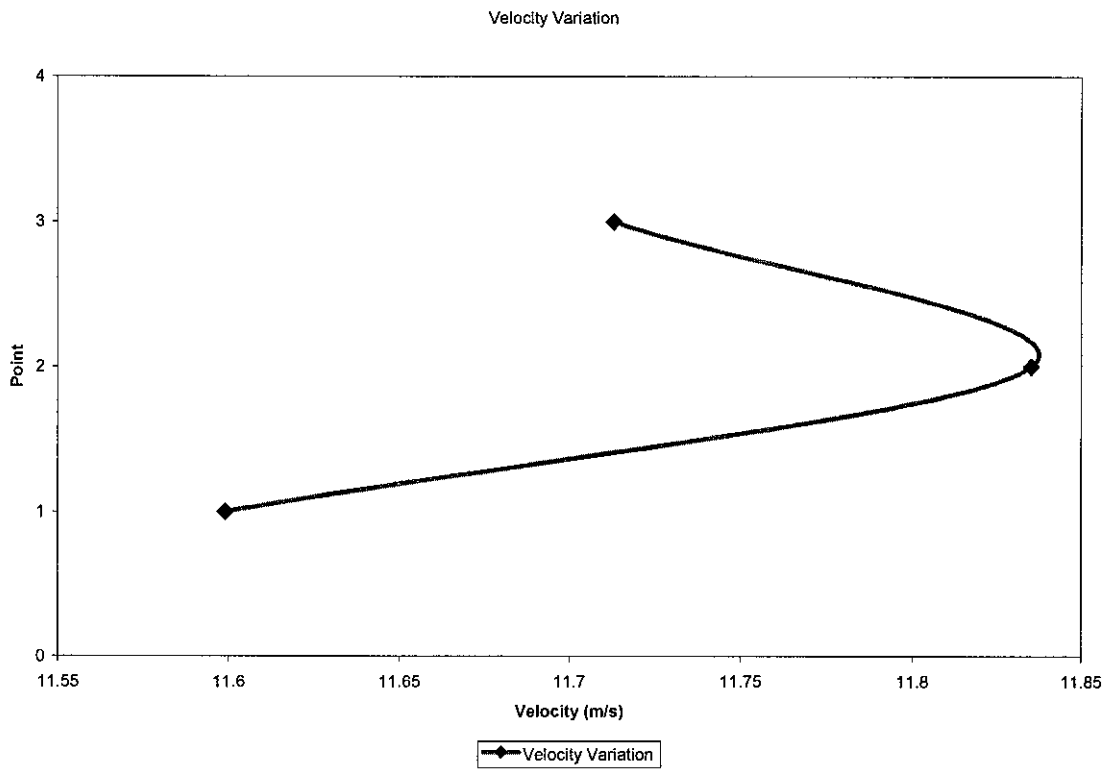


Figure 4.7 : Velocity variation on left side of test section

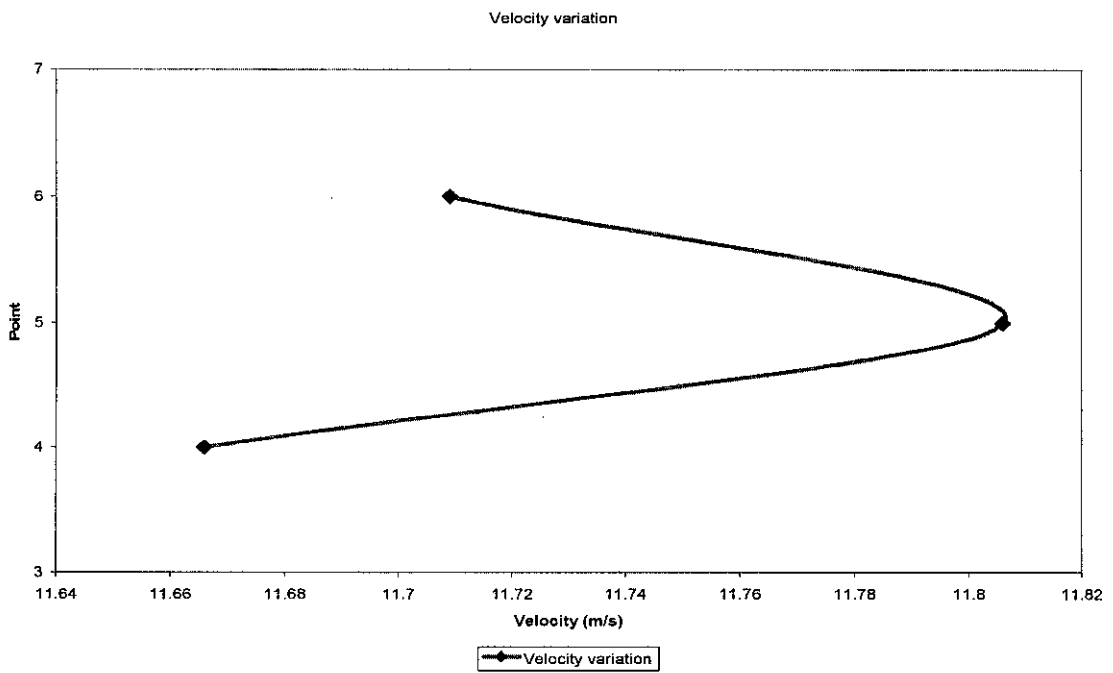


Figure 4.8 : Velocity variations on middle side of test section

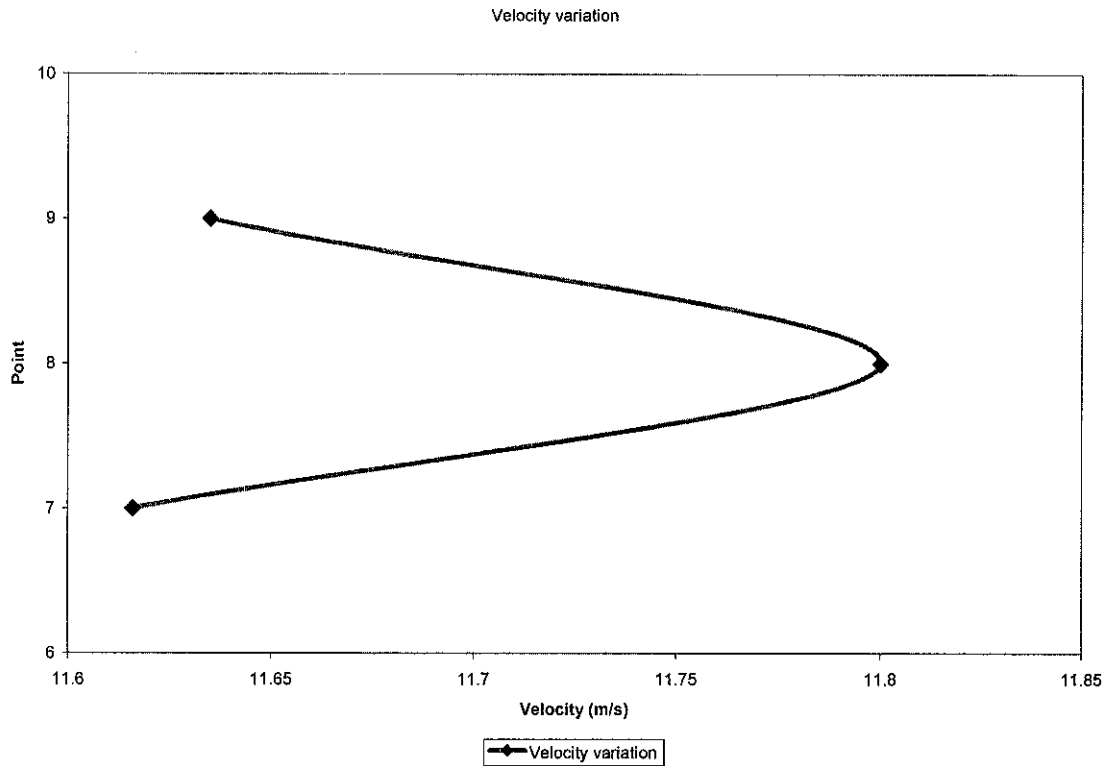


Figure 4.9 : velocity variation on right Side of test section

The velocity variation at the left side shows that it is slightly increased when towards the middle and decrease towards the bottom wall. At center of test section, the velocity increases from top to the center of test section and slightly decreases towards bottom wall. Finally, right side of test section shows an increase in velocity compared to other portion. The velocity is dramatically increasing when towards center but nearly constant when towards the top wall. This is slightly deviates from the theoretical behavior. This might be due to the surrounding disturbances such as excess air and rough surface. The velocity should be slower when flowing near the wall. However, the velocity variations for 3 sides of the test section showed an identical pattern as can be seen through the graphs above.

Turbulence intensities will show the level of turbulence occurred in the test section. The turbulence level was being determined using equation 3.1 and 3.2. Both equation yield the turbulence level at each point and the comparison between two methods was plotted. Sample calculation can be referred at Appendix B-1.

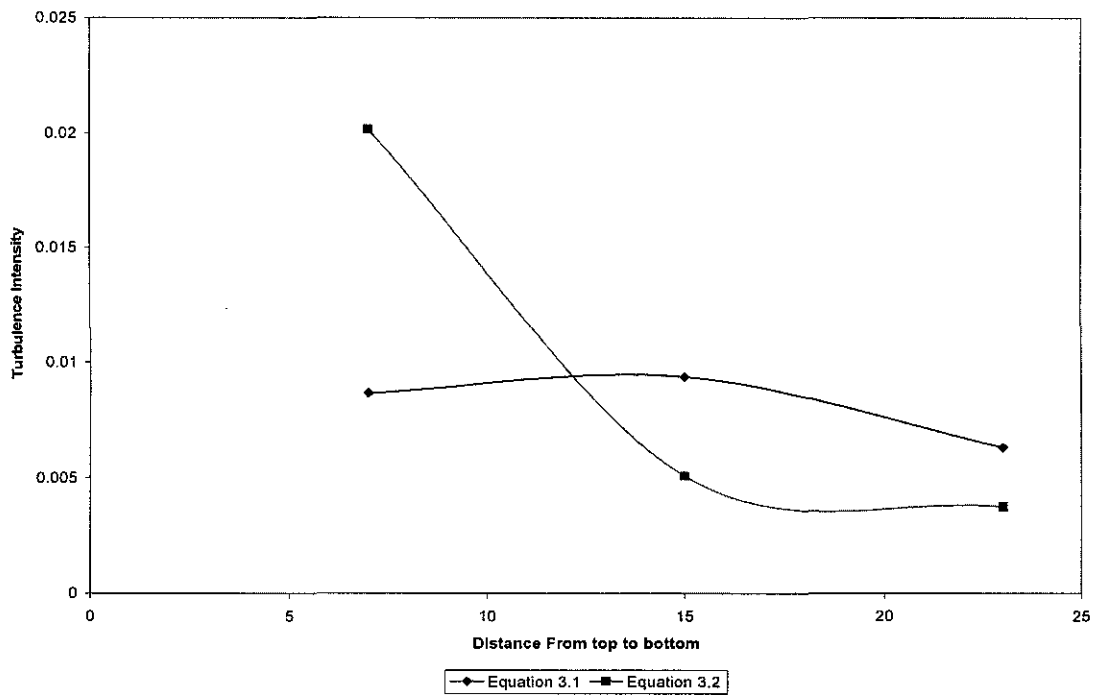


Figure 4.10 : Comparison Between Result of Equation 3.1 and Equation 3.2 (Left Side)

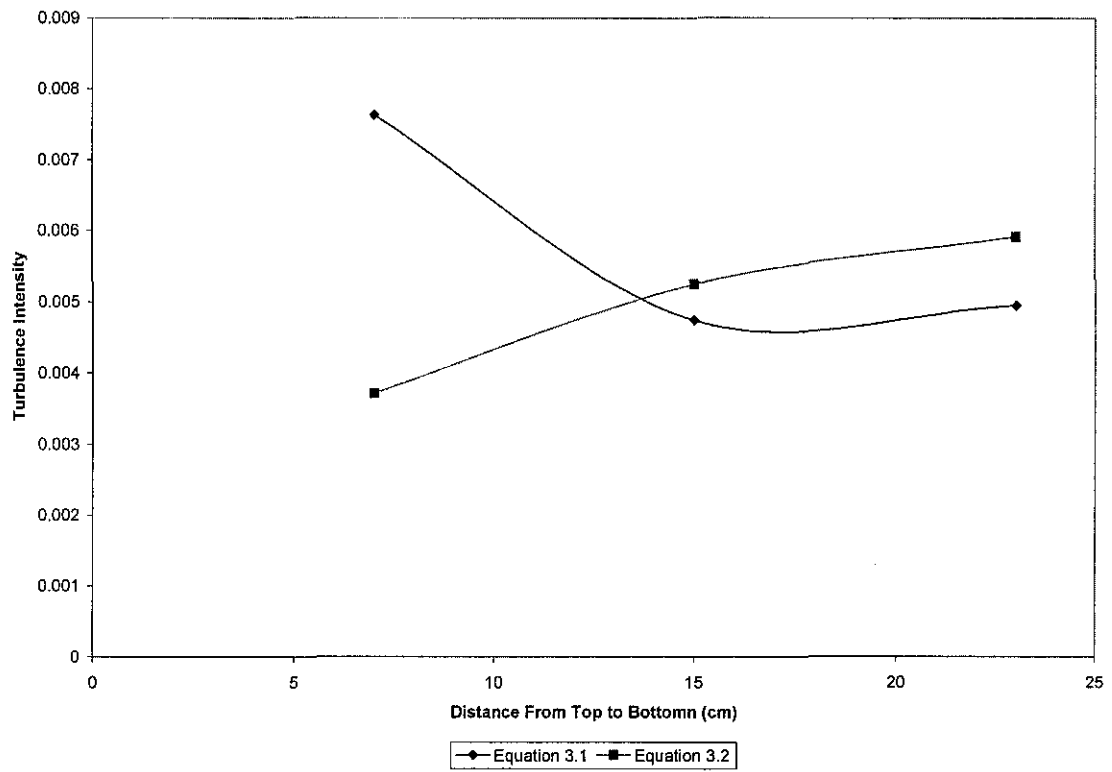


Figure 4.11 : Comparison Between Result of Equation 3.1 and Equation 3.2 (Middle Side)

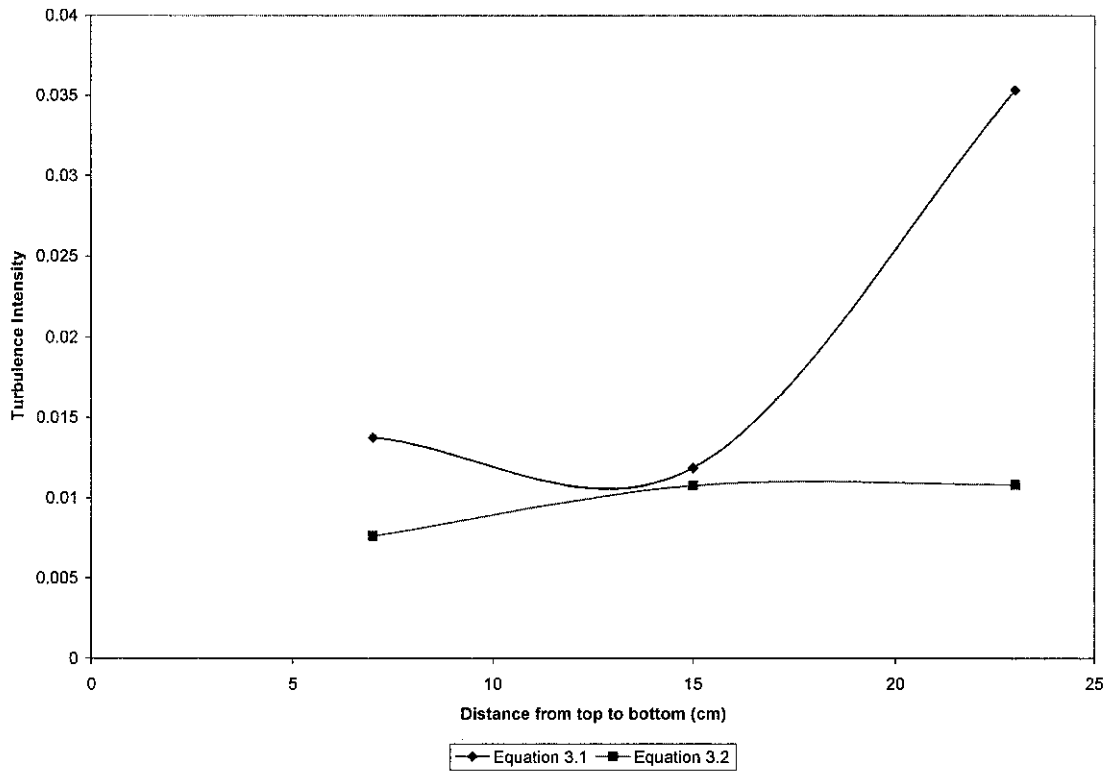


Figure 4.12: Comparison Between Result of Equation 3.1 and Equation 3.2 (Right Side)

From the graph plotted for each point and comparing the two methods, it can be seen that there are differences in the result obtained. The value and the differences percentage compare to the equation 3.1 was tabulated in table 4.4 below.

Table 4.4 : Turbulence Intensity for both method of calculation

Point	Turbulence Intensity, I		Difference (%)
	Equation 3.1	Equation 3.2	
1	0.014656	0.02018	37.69
2	0.009379	0.005088	45.75
3	0.006318	0.003753	40.60
4	0.007629	0.003715	51.30
5	0.004743	0.005251	10.70
6	0.004953	0.00591	19.31
7	0.013752	0.007622	44.58
8	0.011864	0.010751	9.39
9	0.035324	0.010817	69.38

Equation 3.1 relatively calculate the fluctuated value by average value of all fluctuated velocity while equation 3.2 was calculated using the fluctuated velocity at only 5 point of measurement. It was most likely equation 3.1 will derive more accurate result compare to equation 3.2. the RMS value was obtained from Streamline/Streamware software auto generated value.

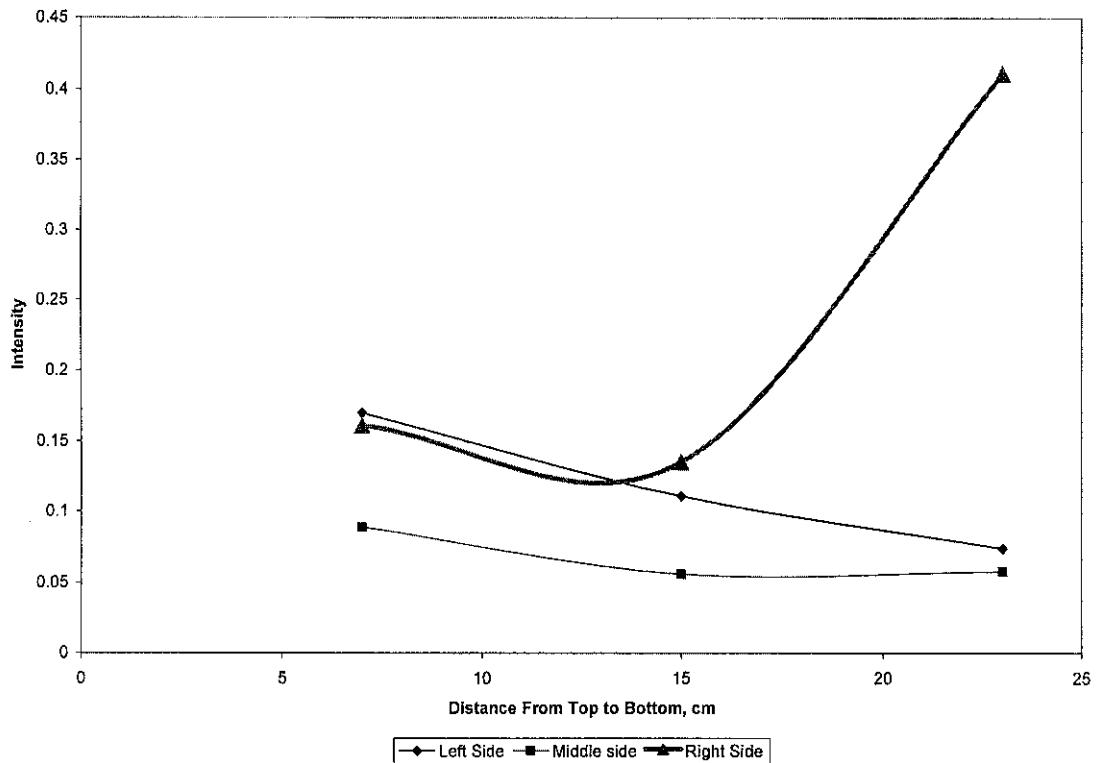


Figure 4.13: Turbulence Intensities distribution in the test section

Comparing the turbulence level for each side, it shows that the highest turbulence level is occurred at the bottom wall at right side of test section. This might be due to the excess air in test section that is coming through the opening section of test section. The poor design has somehow created an opening that might cause unwanted air entering to the test section from side wall and not directly from nozzle. Nevertheless, the turbulence level is shows a same value at the middle of each side of tests the section. In general, turbulence is highly occurred near the wall, which is not theoretically correct. This is probably high due to the poor fabrication of opening wall at all three side of top, left and right test section. However, turbulence is low at the center of the test section, which is

shown on the graph in figure 4.12. The turbulence level at the center is found to be lower compared to the other portion in test section. Beside that, the turbulence level occurred at the middle part of test section is around 0.005.

There is no benchmark for theoretical velocity profile to be referred. But as can be seen from the figure, the turbulence intensity are much more likely the same at all point except regardless point 9(bottom wall right side of test section). The velocity profiles also shows that high speed can be obtained at the middle of the test section and much slower at the wall as can expected theoretically. The overall turbulence intensity level varies from 0.005 to 0.015. This values exceed the preferred turbulence intensities level in the test section ($<0.1\%$) due to the several factors such as the absence of the honeycomb in the settling chamber, swirl wind from the fan and also the current fluctuation from the source that might not stabilize the fan movement.

CHAPTER 5

CONCLUSION AND RECOMMENDATION

5. CONCLUSION AND RECOMMENDATION

5.1 Conclusion

This project has met the objectives of the study, which were to design and fabricate a subsonic wind tunnel in UTP, and also to obtain velocity in the test section in the range of 10 m/s~15 m/s for the given constraint of the test section dimension.

It was obvious that in order to obtain the desired velocity in the test section, a proper consideration and justification on drive section must be made compared to the design of other part in the wind tunnel.

In this project, the only failure was to obtain turbulence intensity level less than 0.1%. As been mentioned before, the experiment of verification of the turbulence intensity level was made in the absent of the honeycomb in the settling chamber. This was due the lack of time to fabricate it by the team project and also other obstacle such as the honeycomb being vandalized by the lack of attention during the process of fabricating it. However, the turbulence intensity level has shown that an acceptable distribution around the test section which means that a well distributed flow occur in the wind tunnel itself.

5.2 Recommendation

Further study is recommended to prepare the better wind tunnel as well as to improve the airflow quality. One of the approaches is to install the honeycomb to improve airflow quality in the test section. A screen or a honeycomb also should be installed in the diffuser to reduce the swirl effect from fan blade rotation. The procedure to determine air flow should be similar as experimentation conducted for current project but can be conducted using 2D sensor to get more accurate result compare 1 D sensor analysis. The experimental work should be done with the use of voltage stabilizer in order to reduce the fluctuated current and lastly to acquired constant speed of fan.

More point should be taken for velocity reading to determine the velocities variations in the test section. It is because a velocity variation in the wind tunnel is a quadratic related to the local velocities and not linearly related. By taking only 3 points a triangle shape of velocity variations is obtained which does not agree theoretically with the expected velocity variations shape between two plates. As been mentioned before,(see section 4.6), supposedly a parabolic shape is obtained from given local velocities taken in the test section. So, it is highly recommended to take at least 5 or more points for each axes x and y so that a more detail velocity variation shape can be determined.

Further study on the effect of honeycomb in local location in the settling chamber to turbulence intensity level also can be conducted in the future. The distance between honeycomb and the test section do give impact to the turbulence intensity level. As an initiator, an article about it has been included in the **Appendix E**.

References:

- Frank P . Bleir, 1998 ,*Fan Handbook, selection,Application and Design*, Mc Graw Hill,
- Frank, M.White. 1999, *Fluid Mechanics, 4th edition*, Mcgrawhill International Editions, United States.p.447
- Finn E. Jorgensen.2002, *How to Measure Turbulence With Hot-Wire Anemometers*, Dantec Dynamic
- George E. Dieter , 2000,*Engineering Design,3rd Edition*, Singapore, Mc Graw Hill
- Jewel B. Barlow, 1999, *Low Speed Wind Tunnel Testing*, John Wiley and Sons,
- Mehta and Bradshaw, 1979, *Design Rules for small low speed wind tunnels*, The Aeronautical Journal of the Royal Aeronautical Society
- Rafan, Nur Aidawaty , June 2003, “Improvement On Subsonic Wind Tunnel Developed In Universiti Teknologi Petronas”
- David B.Deegaff, Jan 1999 ,
<http://vk.stanford.edu/degraaff/thesis/appendices.pdf>
- Engineering Fundamentals, 12th Jan, 2004,
http://www.efunda.com/designstandards/sensors/hot_wire/hot_wires_intro.cfm
- Engineering Fundamentals, 12th Jan, 2004,
http://www.efunda.com/designstandards/sensors/hot_wire/laser_doppler_intro

Engineering Fundamentals, 12th Jan, 2004,

http://www.efunda.com/designstandards/sensors/hot_wire/hot_wires_theory.cfm

Kas Kasravi, 19th August 2003,

<http://www.kasravi/cmu/tech452/aerodynamics/windtunnel.htm>

LDAPS, 5th Aug 2003

<http://ldaps.arc.nasa.gov/curriculum/tunnel.html>

The Engineering Toolbox, 22 October 2003,

<http://www.engineeringtoolbox.com/hvac.htm>

TRW Inc, 10th August 2003,

http://www.observe.arc.nasa.gov/nasa/aero/tunnel_settling.htm

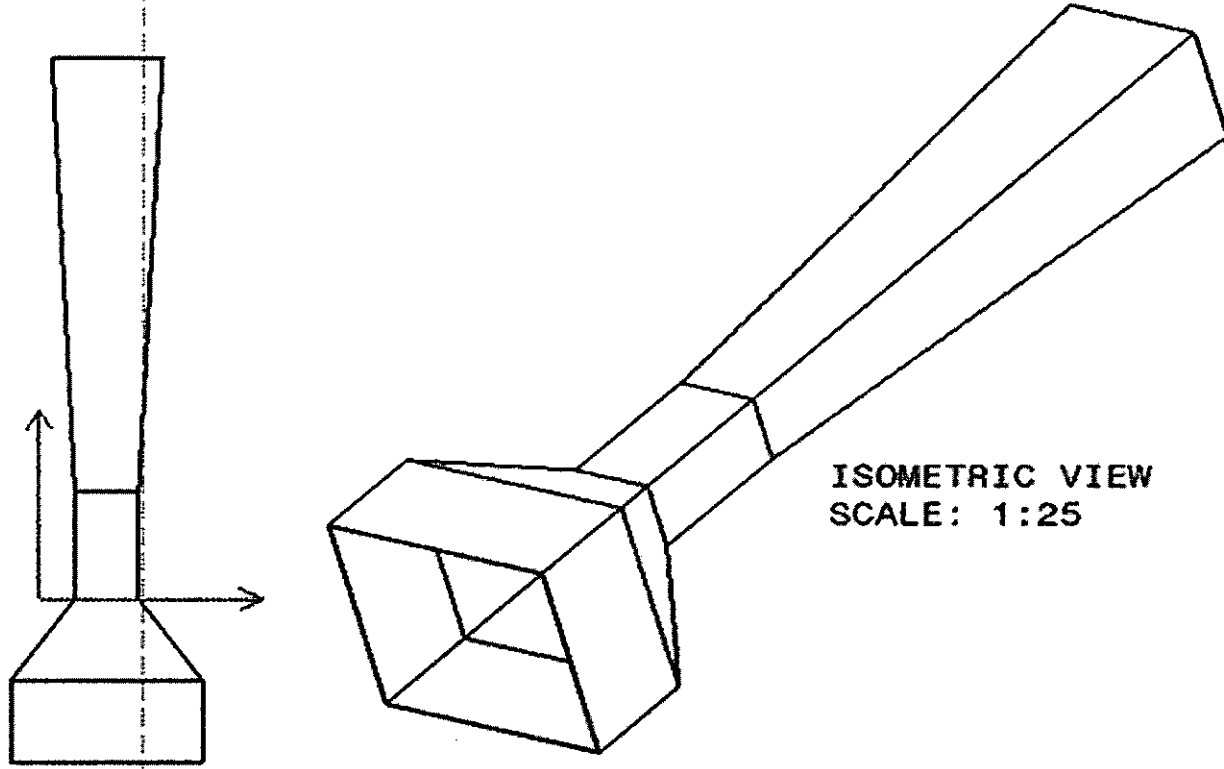
Planned Gantt Chart for Phase I.

o	Weeks	1	2	3	4	5	6	7	8	9	10	11	12	13	14	SW	EW
1	Selection of Project Topic <i>Topic assigned to student</i>																
2	Preliminary Research Work <i>Introduction</i> <i>Objectives</i> <i>List of literature</i> <i>Project planning</i>																
3	Submission of Preliminary Report					15/8											
4	Project work <i>Calculation</i> <i>Design</i>																
5	Submission of Progress Report									22/9							
6	Project work continue <i>Material preparation</i> <i>fabrication/workshop</i>																
7	Submission of Interim Report final draft													20/10			
8	Oral Presentation																
9	Submission of Interim Report																21/11

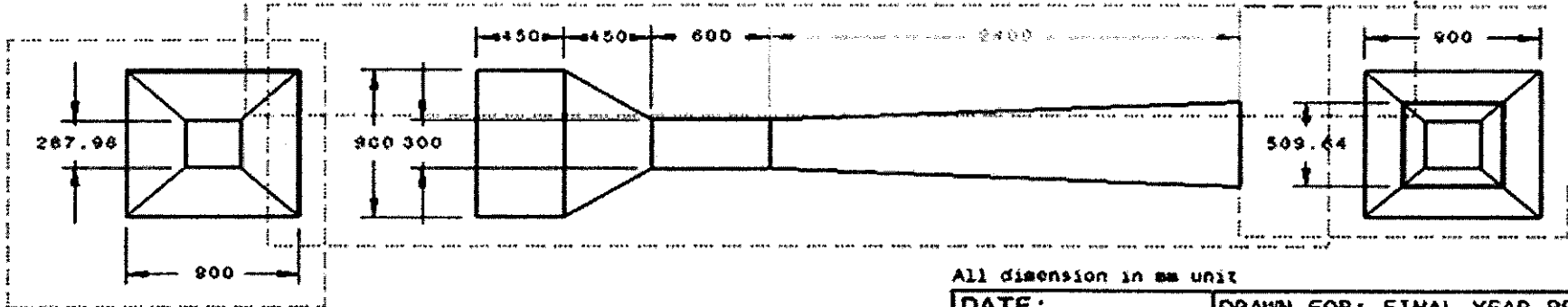
Planned Gantt Chart for Phase II

No	1	2	3	4	5	6	7	8	9	10	11	12	13	14	SW	EW
Preliminary Research Work																
Project planning	■	■														
Introduction (air flow testing methods)	■	■														
Selection of most appropriate method and further study on selected method			■	■												
Submission of progress report 1																
				●												
Project work continue																
Initial development of selected method (redesign test section) and probe holder fabrication					■	■	■									
Preparation of experiment.						■	■	■	■							
Submission of progress report 2																
										●						
										22/3						
Project work continue																
Run the experiment									■	■						
Analysis										■	■	■	■			
Poster submission													12/4			
Submission of Dissertation Final Draft																
														●		
														20/4		
Oral Presentation																
															■	■
Submission of project dissertation																
																●
																31/5

APPENDIX 4 : TECHNICAL DRAWING OF THE SUBSONIC WIND TUNNEL



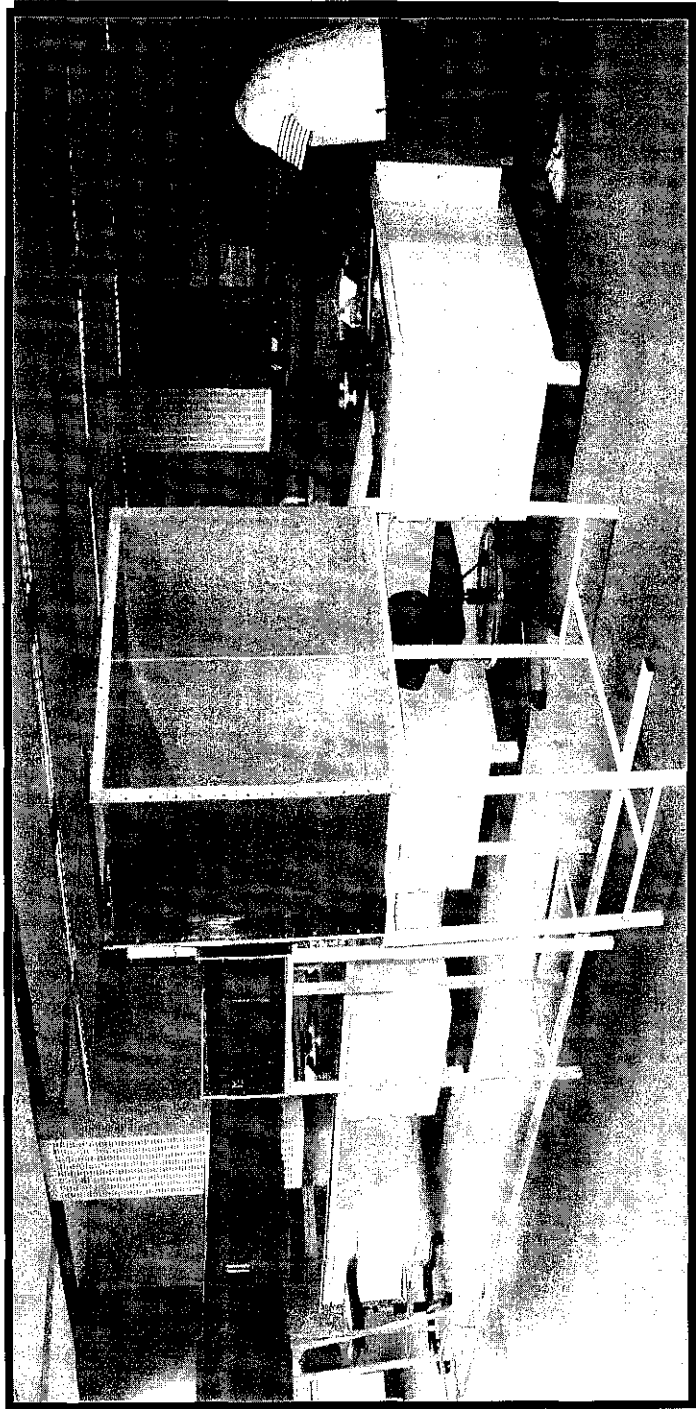
ISOMETRIC VIEW
SCALE: 1:25



All dimension in mm unit

DATE :	DRAWN FOR: FINAL YEAR PROJECT
DESIGN: SYAHIL & AHMAD	DRAWING NAME: SUBSONIC WIND TUNNEL
DRAWN: SYAHIL & AHMAD	NAME: AHMAD KHAIRUDIN ZAINON
 SCALE: 1:35	

Low Speed Wind Tunnel in Universiti Teknologi Petronas



Using equation 3.1,

$$I = \frac{\left(\frac{2}{3} ke \right)^{\frac{1}{2}}}{U_{ref}}$$

$$U_{ref} = (U^2_{mean} + V^2_{mean} + W^2_{mean})^{1/2}$$

$$= 11.599$$

$$\text{kinetic energy, } ke = \frac{1}{2}(0.164367^2)$$

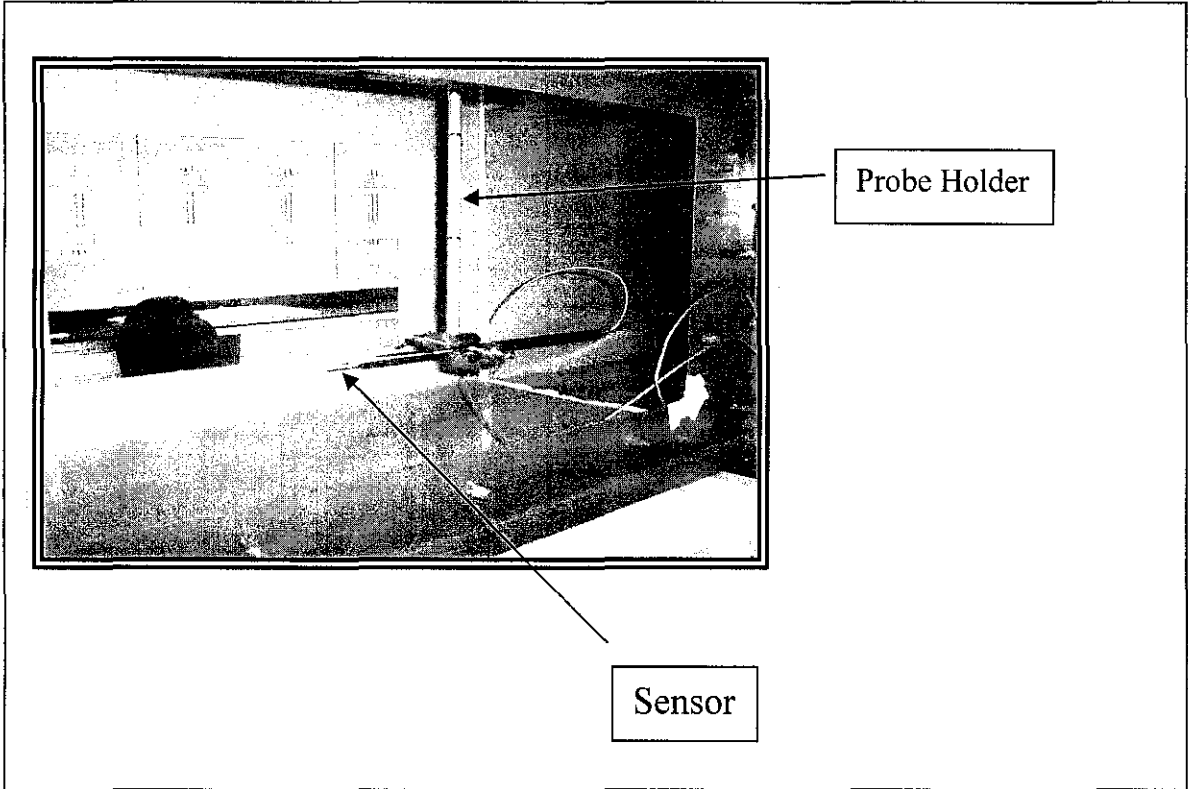
$$= 0.01351$$

Hence,

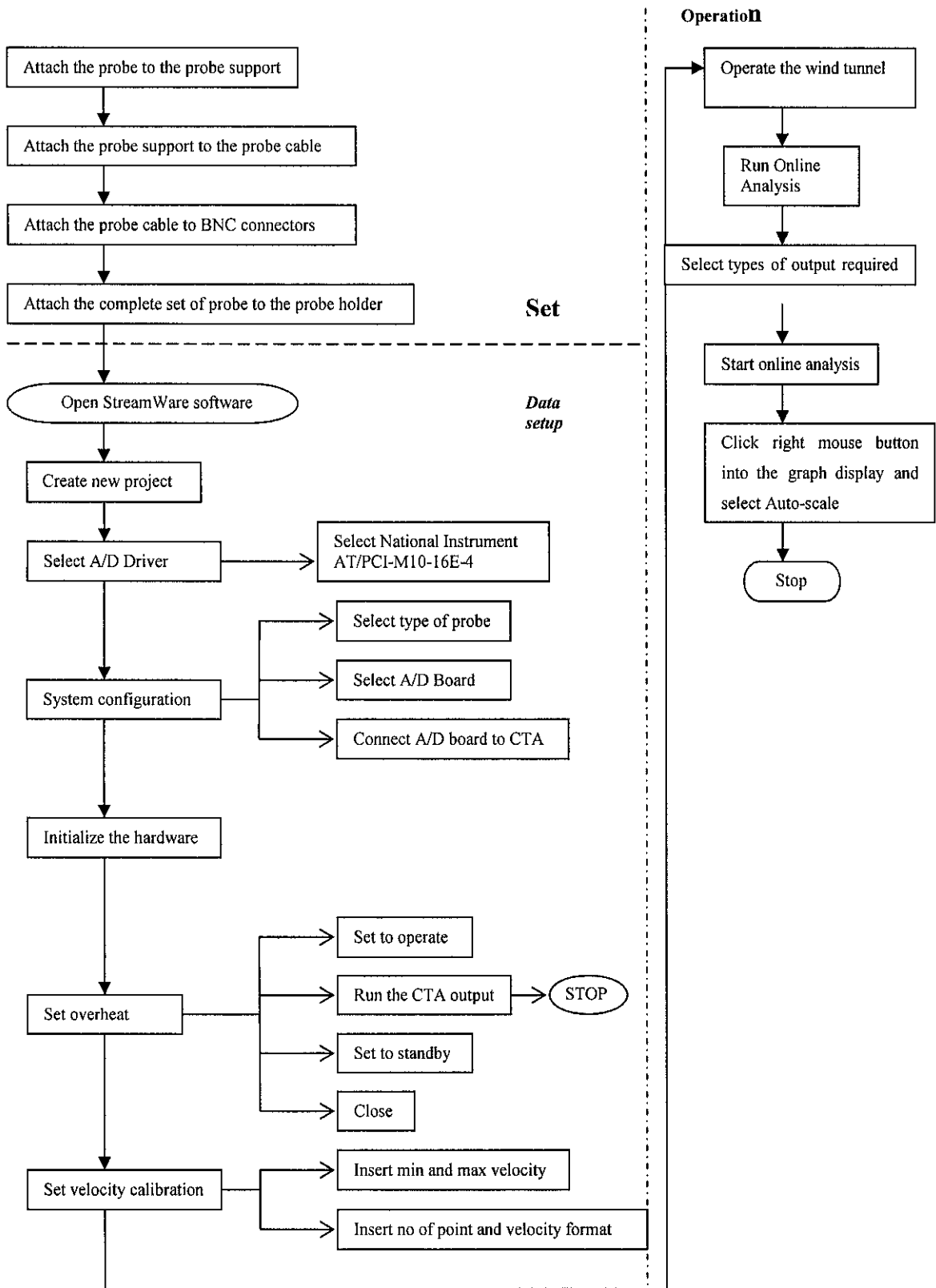
$$I = \frac{\left(\frac{2}{3} (0.0135) \right)^{\frac{1}{2}}}{11.599}$$

$$= 0.02018$$

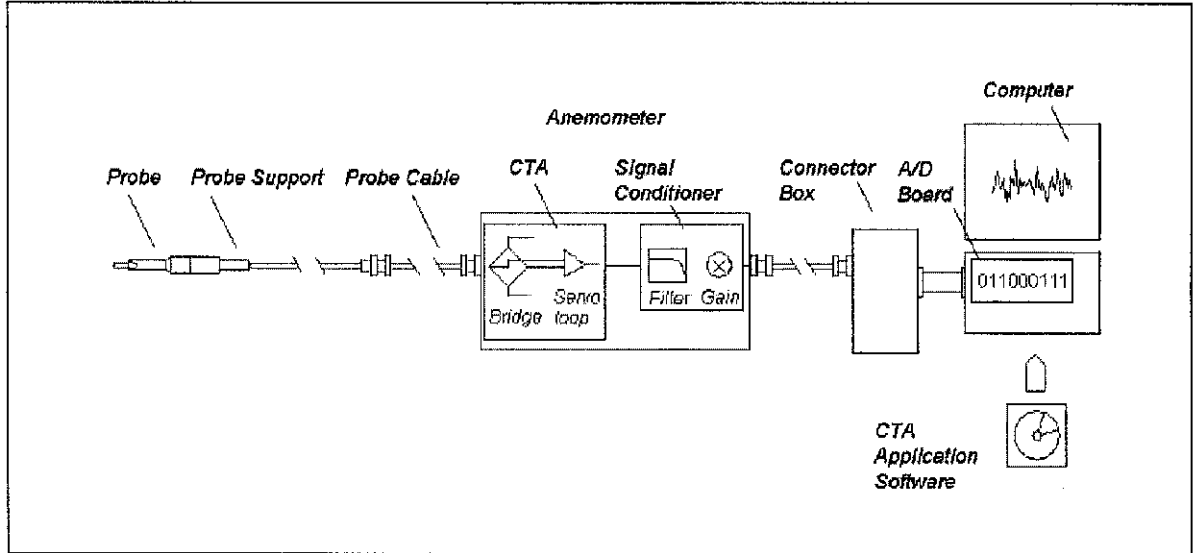
Experimental Hardware Setup in Wind Tunnel



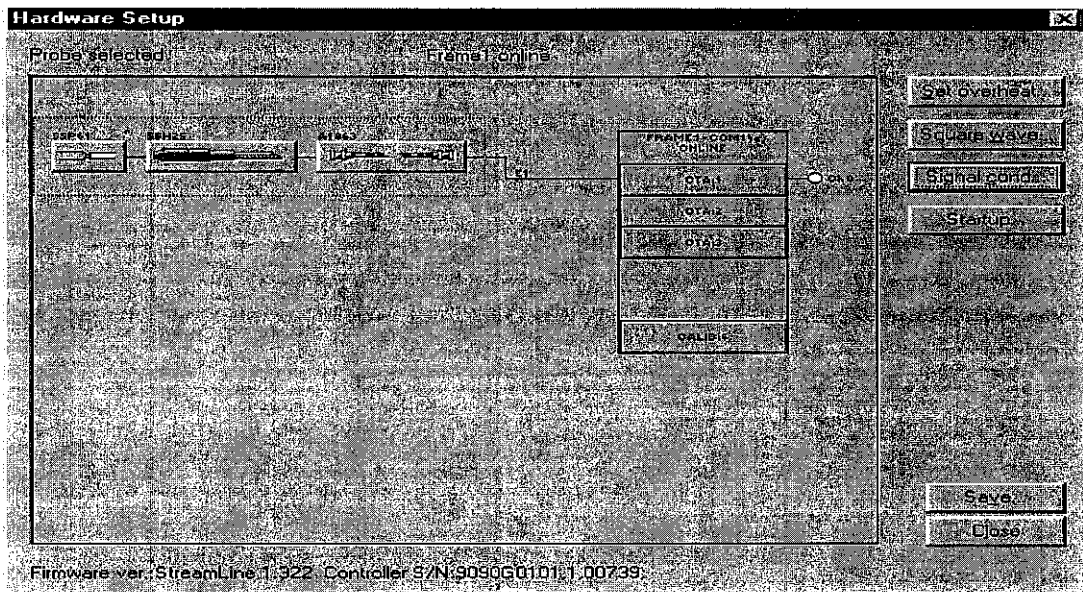
Setup and Operation of Constant Temperature Anemometer (CTA) Flow Chart¹⁰



Components of hot wire anemometer



System Configuration to operate the hot wire anemometer

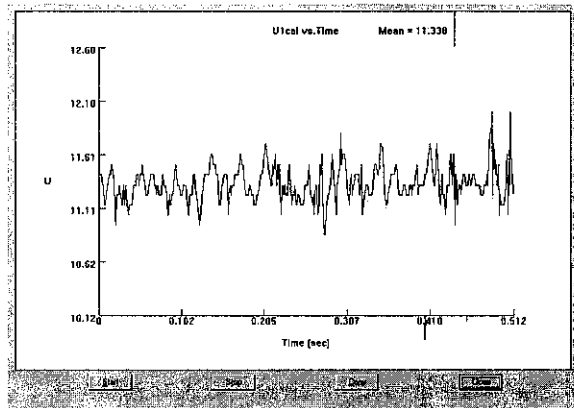


Raw data (in m/s)

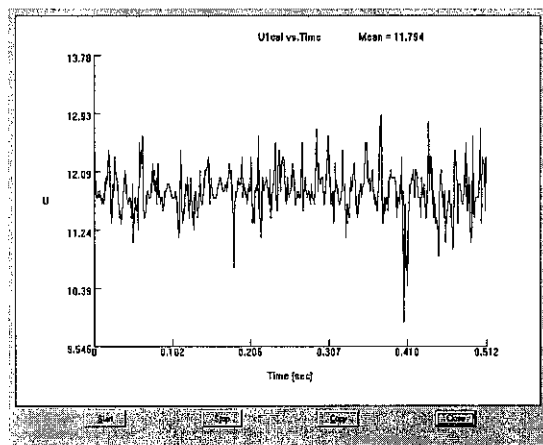
Point	Reading								
	1	2	3	4	5	6	7	8	9
1	0.006889	0.016384	0.0081	0.003025	0.009801	0.036481	0.036481	0.080656	0.005184
2	0.000144	0.001024	3.6E-05	0.018769	9E-06	0.008836	0.037249	0.008649	0.000576
3	0.006889	0.016384	3.6E-05	0.003025	0.009801	0.008836	0	0.035721	0.005184
4	0.801025	0.016384	0.010404	0.001681	9E-06	0.008836	0.036481	0.035721	0.094864
5	0.006889	0.004225	0.010404	0.001681	0.038025	0.008836	0.009216	0.080656	0.131769
$V_{\text{fluctuated Average}}$	0.164367	0.01088	0.005796	0.005636	0.011529	0.014365	0.023885	0.048281	0.047515
V_{mean}	11.599	11.835	11.713	11.666	11.806	11.709	11.707	11.8	11.635
V_{RMS}	0.17	0.111	0.074	0.089	0.056	0.058	0.161	0.14	0.411

Velocity Fluctuation on current wind tunnel

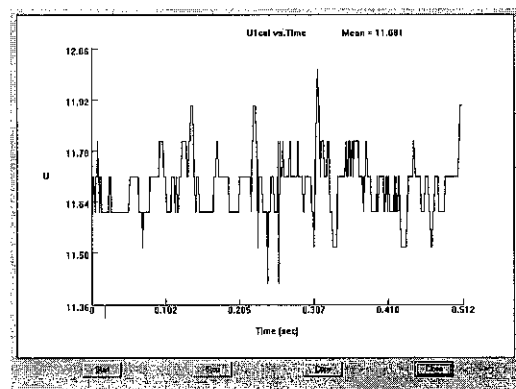
Position 1



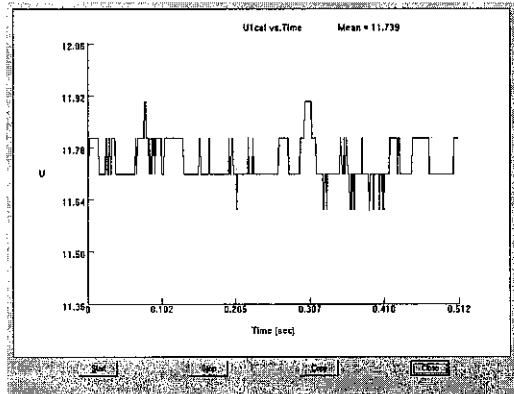
Position 2



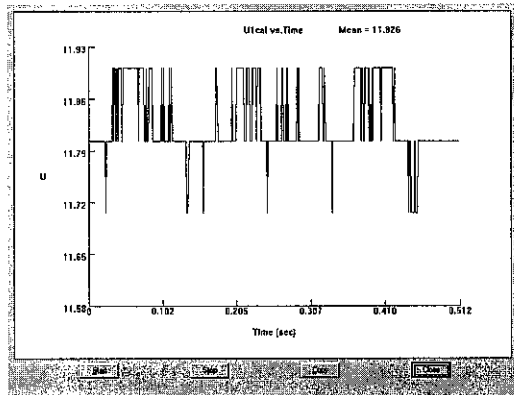
Position 3



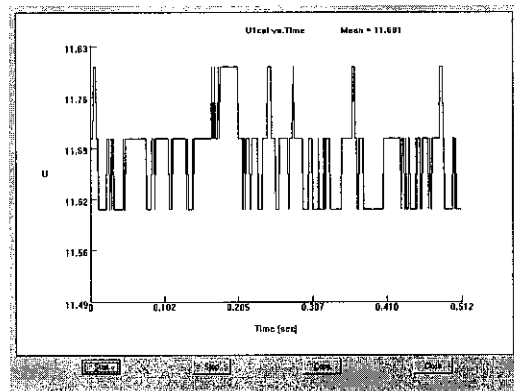
Position 4



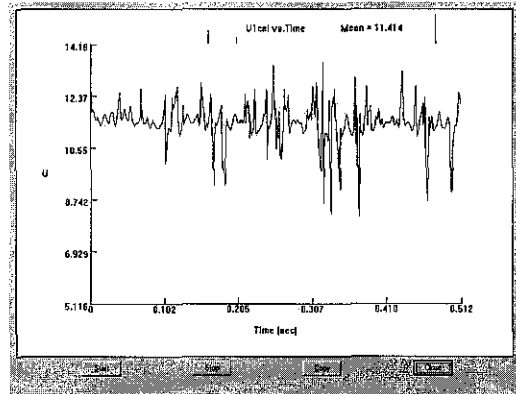
Position 5



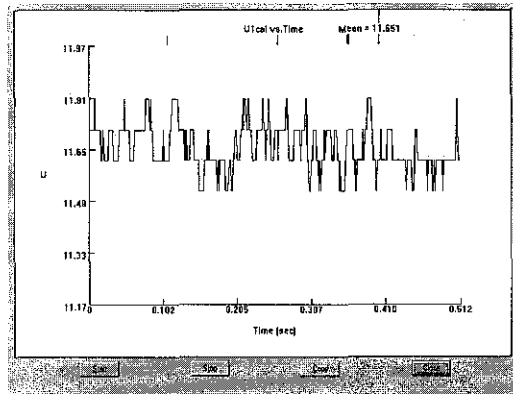
Position 6



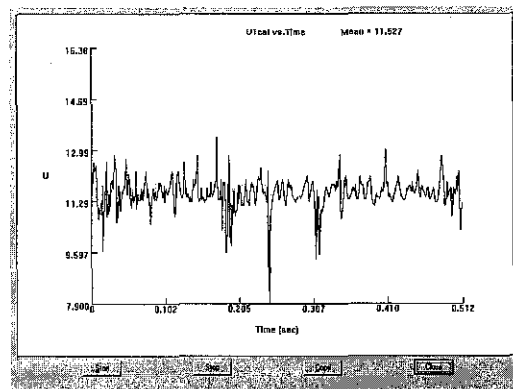
Position 7



Position 8



Position 9



Appendix E : Relevant Journals

Technical Notes

Design rules for small low speed wind tunnels

R. D. MEHTA and P. BRADSHAW

Design rules for small low speed wind tunnels

R. D. MEHTA and P. BRADSHAW

INTRODUCTION

Even with today's computers, a wind tunnel is an essential tool in engineering, both for model tests and basic research. Since the 1930s, when the strong effect of free-stream turbulence on shear layers became apparent, emphasis has been laid on wind tunnels with low levels of turbulence and unsteadiness. Consequently most high performance wind tunnels were designed as closed-circuit types (Fig. 1(a)) to ensure a controlled return flow. However, as will be seen below, it is possible with care to achieve high performance from an open-circuit tunnel, thus saving space and construction cost. 'Blower' tunnels (with the fan at entry to the tunnel, Fig. 1(b)) facilitate large changes in working section arrangements; to cope with the resulting large changes in operating conditions, a centrifugal fan is preferable to an axial one. For ease of changing working sections the exit diffuser is often omitted from small blower tunnels, at the cost of a power factor greater than unity. This paper concentrates on the design of *small blower* tunnels but most of the information is applicable to wind tunnels in general.

A large open-circuit tunnel would be of rather inconvenient dimensions, mainly in length. Also, an open-circuit tunnel requires enough free room around it so that the quality of the return flow is not affected significantly (remember that an open-circuit tunnel in a room is really a closed-circuit tunnel with a poorly-designed return leg). The choice may also be restricted by the maximum available blower size. A working section Re per metre of more than about 3×10^6 (a speed of about 10 ms^{-1}) is rare in blower tunnels of whatever size, and commercial blowers capable of producing such a speed in a section more than about 1 m^2 in area are also rare.

The main advantage of open-circuit tunnels is in the saving of space and cost. They also suffer less from temperature changes (mainly because room volume \gg tunnel volume) and the performance of a fan fitted at the upstream end is not affected by disturbed flow from a working section. One disadvantage of any open-circuit tunnel with an exit diffuser is that the pressure is always less than atmospheric and so spurious jets issue from holes left unpatched, although this can be remedied by obstructing the tunnel outlet and creating an over-pressure in the working section. The main advantage of a centrifugal blower, as distinct from an axial fan, is that it performs well over a large range of loads (the whole range being at the same incidence and hence operating at the same lift coefficient). The only advantage of a closed-circuit tunnel, with a centrifugal or axial fan at exit, is the dubious one that air coming from the tunnel room may be less disturbed than that coming from a fan.

It is difficult and unwise to lay down firm design rules mainly because of the wide variety of requirements and especially the wide variety of working-section configurations. An attempt is made here to present design guide-

lines for the main components of a wind tunnel—the fan, wide-angle diffuser, corner vanes, settling chamber, contraction and exit diffuser (Fig. 1)—based on data from successful designs and some original experiments. For details of the data correlations see Mehta (1977) and for complete details of the experiments and design procedure see Mehta (1978).

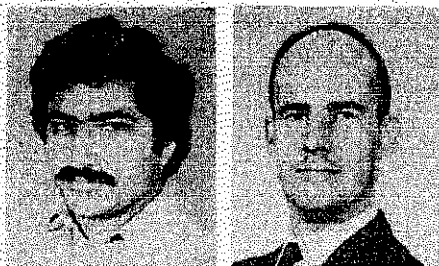
2. FANS

2.1. Axial flow fans

The usual arrangement in a closed-circuit tunnel is a stator ('pre-rotation vanes') upstream of the rotor (the fan proper), designed so that the swirl at exit is zero. In the case of an open-circuit tunnel, swirl present in the flow out of the fan may be dissipated before the flow reaches the intake, but a remaining advantage of pre-rotation vanes is that the flow velocity relative to the fan blades is larger than if the stator is absent or located downstream of the fan.

2.1.1. Fan solidity

The design procedure outlined by Bradshaw and Pankhurst (1964) is still an adequate guide. The only serious problem found in fan design that is not found in the design of wings for low-speed aircraft is the interference between the flow fields of the blades. This interference depends mainly on the 'solidity', the ratio of blade chord to the gap between blades (measured around the circumference). Providing that the solidity is less than unity approximately, interference is small enough to be treated as a small correction to the performance of an isolated aerofoil; for higher solidities the flow cannot be accurately related to that round an isolated aerofoil, and data for 'cascades' (rows of aerofoils arranged in the same manner as corner vanes) must be used instead. The solidity varies with radius, and in order to use the same



The Authors: Dr. R. D. Mehta and Professor P. Bradshaw, BA, Department of Aeronautics, Imperial College of Science and Technology, London.

Paper No 718

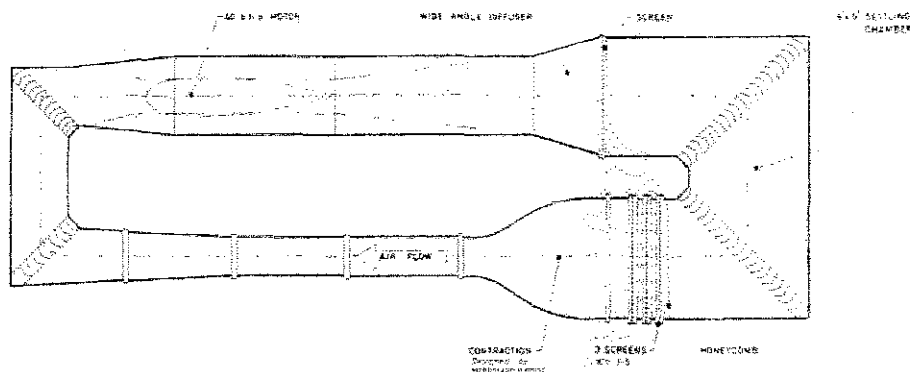


Figure 1(a). The main components of a typical closed-circuit wind tunnel.

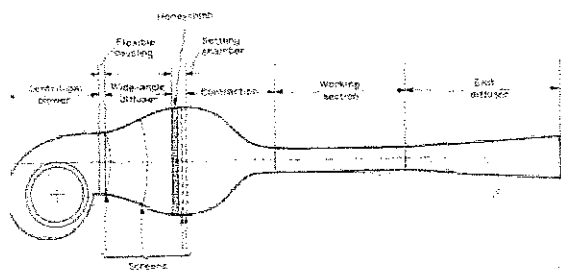


Figure 1(b). The main components of a typical blower tunnel. (Not to scale.)

design procedure for the whole length of the blade it is desirable to keep the solidity at the root below unity by mounting the fan on a central nacelle whose maximum diameter is roughly half the fan diameter.

2. Blade design

Blade efficiencies are of the order of 90% so that minimisation of losses is not usually important, and the usual procedure is to choose the blade lift coefficient to be as high as is safe, irrespective of lift/drag ratio; values 0.7 to 0.9 are typical.

3. Pre-rotation vanes

Pre-rotation vanes should be run at a lift coefficient not far above that for maximum lift/drag ratio because their wakes pass through the fan; to limit the resulting noise, the axial distance between the trailing edge of the pre-rotation vanes and the leading edge of the fan blades should be at least 20% of the vane chord and the number of fan blades should be different from the number of pre-rotation vanes. Pre-rotation vane solidities usually fall into the cascade range.

An alternative to pre-rotation vanes for a lightly loaded fan is a set of straightener vanes downstream of the fan.

For detailed design rules for pre-rotation vanes, fan blades and straighteners see Bradshaw and Pankhurst (64).

4. Centrifugal blowers

Centrifugal blowers are normally used to drive open-circuit tunnels from the upstream end; a blower could be installed at the exit instead but this has no particular advantage. Single-inlet blowers could also be used to drive return-circuit tunnels by installing them in one of the corners. Single-inlet blowers are found to produce a vortex-type flow (due to the asymmetric positioning of the impeller) which would aid wall flow attachment in the wide-angle diffuser. This compensates for the non-

uniformity of the flow (which is also improved by the screens in the wide-angle diffuser and the settling chamber).

2.2.1. Advantages over other fans

Centrifugal blowers run with reasonable steadiness and efficiency over a wide range of flow conditions (i.e. varying tunnel power factor) because the whole blade span operates at nominally the same lift coefficient. The noise and pulsations generated by a centrifugal blower are adequately low, even at off-design conditions, and the uniformity of flow varies less with advance ratio, $U/\omega r$, in the notation of Fig. 2. The swirl (exit vortex) produced by a single-inlet blower is also independent of advance ratio (dependent on the ratio of rotor to casing width).

2.2.2. Types of impeller

The most common type of blading is the backward-facing aerofoil-type (Fig. 2); forward-facing is less efficient. If the blower efficiency is not too important, these blades could be designed in the same way as corner vanes or cascades by choosing a leading edge angle of $4-5^\circ$ and a zero trailing edge angle, but a more efficient blade shape is that of a cambered aerofoil with finite thickness. In the present authors' tests on blowers with aerofoil-type impellers it was found that the flow uniformity deteriorated with increasing loading. However, with backward-facing 'S' shaped blades (Fig. 2) the flow uniformity was found to improve with loading, presumably because these blades stall relatively early, leading to increased mixing. The cost is a higher turbulence level in the outlet flow and a reduced blower efficiency.

2.2.3. Splitter-plate (tongue)

This is an important component which affects the outlet flow uniformity and blower noise characteristics. For minimum interference with the flow uniformity, the ratio of tongue height to casing height needs to be small (<0.3) and the angle and shape carefully designed. The gap between the rotor and tongue needs to be a minimum for aerodynamic reasons but optimised for minimum interaction with the outgoing flow and thus minimum noise level. The tongue design on most commercially available blowers is adequate. A badly angled tongue could be improved upon by adding a cusped fairing downstream, as shown dotted in Fig. 2.

2.2.4. Other features and suggestions

An inlet bellmouth helps to produce a uniform flow and reduces inlet losses, and an inlet filter (helping to reduce inlet swirl) is essential to reduce contamination of hot-wire probes. Large blowers should be mounted on anti-

bration mountings and connected to the tunnel with a flexible coupling to reduce vibration.

Double-inlet blowers (air entering the impeller from both sides) tend to produce a uniformly inclined flow (without a vortex) which takes a longer distance to re-attach to the bottom wall downstream of the tongue. One should therefore be more conservative in designing side-angle diffusers for double-inlet blowers.

On the whole, commercially available single-inlet centrifugal blowers with backward-facing impellers are adequate for driving blower tunnels.

Once the maximum required fan static pressure and volume flow rate have been estimated, the makers' performance charts can be consulted. Optimisation between efficiency, rpm and required power leads to the lower choice (see section 10).

SCREENS

Wind tunnel screens are normally made of metal wires interwoven to form square or rectangular meshes. Screens woven from nylon or polyester threads are also now being used when the wind loads are not expected to be very high (UTS of nylon ~ 70 , steel ~ 1100 , bronze ~ 700 – 1100 MNm $^{-2}$ and E of nylon $\gg 3$, steel ~ 200 , bronze ~ 100 GNm $^{-2}$). The action of the gauze is described in terms of two parameters: the pressure drop coefficient, $K=f_1(\beta, R_o, \theta)$ and the deflection coefficient, $\alpha=f_2(\beta, K, \theta)$, where β is the screen open-area ratio and θ is the flow incidence angle, measured from the normal to the screen.

1. Main effects

(for detailed explanations see Mehta 1978)

Screens make the flow velocity profiles more uniform by imposing a static pressure drop proportional to (speed) 2 and thus reduce the boundary layer thickness so that the ability to withstand a given pressure gradient is increased. A screen with a pressure drop coefficient of about 2 removes nearly all variation in the longitudinal mean velocity. A screen also refracts the incident flow towards the local normal and reduces the turbulence intensity in the whole flow-field. For a given open-area ratio, it is better to have a smaller mesh for the reduction of re-existing turbulence. Plastic screens tend to yield a more uniform flow beyond the boundary layer edge, mainly due to the weaving properties, and produce an 'overshoot' in the velocity profile near the edge, mainly caused by screen deflection angle which is a maximum at the wall. In terms of tackling a given pressure gradient or avoiding separation, this overshoot could be beneficial.

2. Open-area ratio (β)

Flat screens with very low β (~ 0.3) also produce an overshoot but this is caused by streamline inclination near the boundary layer edge. Low β (< 0.57) screens also reduce instabilities resulting from a random coalition of

jets and presumably amalgamating to form longitudinal vortices which persist through the contraction. The coalition process is enhanced by variations in β (i.e. non-uniform weave) and by irregularities in the screen shape (i.e. wrinkles). It is therefore essential to inspect and clean wind tunnel screens regularly.

3.3. Determination of K

(ratio of pressure drop to dynamic pressure)

Although there is no wholly satisfactory method, Wieghardt's (1953) formula $\{K=6.5[1-\beta/\beta^2][Ud/\beta v]^{-1/3}\}$, where d is wire diameter, predicts the right trend; K decreases with increasing speed up to about $Ud/\beta v=600$, after which it is independent of Re . Collar's (1939) formula $\{K=0.9(1-\beta/\beta^2)\}$ usually over-estimates K in the high Re limit. One needs to be more careful in predicting K -values for plastic screens since,

$$K=f(\beta, R_o, \theta, \dots \text{co-planarity} \dots)$$

where θ is angle of screen to incident flow. For $\theta \neq 0$ use

$$K_\theta = K \cos^m \theta, \text{ with } m=1.0 \text{ for screens with } \beta \sim 0.6 \text{ and } m \sim 1.4 \text{ for } \beta \sim 0.3.$$

3.4. Determination of α

(ratio of outlet angle to inlet angle)

For α the form:

$$\alpha = A + \frac{B}{\sqrt{1+K}}$$

where A, B are empirical constants, is a better fit than the generally accepted form:

$$\alpha = \frac{1.1}{\sqrt{1+K}}$$

Note that the refractive index of a screen (μ) defined as in optics is equal to $1/\alpha$ for small θ . For larger θ use

$$\alpha_\theta = \frac{1}{\theta} \tan^{-1} \left\{ \tan \theta - \frac{\theta}{2} \sec^2 \theta \left[C - \frac{D}{\sqrt{1+K_\theta}} \right] (E + F\theta) \right\}$$

C, D, E and F are empirical constants.

Values suggested for the empirical constants by some limited experiments (Mehta, 1978) are: $A=0.66, B=0.31, C=0.68, D=0.62, E=1.0, F=1.5$.

A more complete analysis of the flow through screens can be found in Mehta (1978).

4. DIFFUSERS

The flow through a diffuser depends on its geometry defined by the area ratio (A), diffuser angle (2θ), wall contour and diffuser cross-sectional shapes. Other parameters like the initial conditions, boundary layer control method and the presence of separation could also affect the flow thus making it very difficult to predict. Almost all knowledge acquired about diffusers is empirical. There are two main types:

4.1. Exit diffusers

These are fitted downstream of the working sections and have gentle expansions with a diffuser included angle usually not exceeding 5° (for best flow steadiness, although best pressure recovery is achieved at about 10°) and an area ratio not exceeding about 2.5. It is important to have a reasonable degree of flow steadiness in the exit diffuser, since otherwise the pressure recovery tends to fluctuate with time, and therefore, so does the tunnel speed if the input power is nearly constant. The design

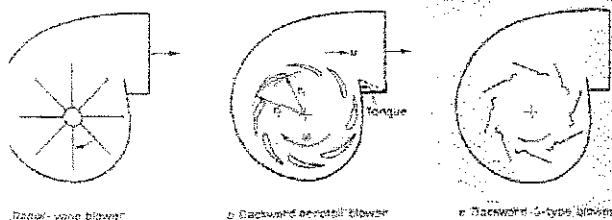


Figure 2. Different impeller types used in centrifugal blowers.

f these diffusers is well catered for by existing methods (see Cockrell and Markland, 1974).

2. Wide-angle diffuser

This type is normally installed between the blower and settling chamber or between the fourth corner and settling chamber of a closed-circuit tunnel; the cross-sectional area increases so rapidly that separation can be avoided only by boundary layer control. A wide-angle diffuser is a means of reducing the length for a given area ratio rather than effecting a pressure recovery; generally the static pressure rise through a screened wide-angle diffuser is negative but small.

2.1. Boundary layer control methods

The most popular means of boundary layer control is the installing of gauze screens. A screen, besides removing the direct effects of layer growth and incipient separation, gives the layer a new lease of life. In a wide-angle diffuser it is better to use several screens of relatively small K (less than about 1.5) because increasing K at one station has little effect on the skin friction at a station much further downstream. Other types of boundary layer control methods include splitters, suction slots, trapped vortices, vortex generators and vanes and may be preferable in diffusers with very severe geometries (> 5 , $2\theta > 50^\circ$). For a review see Mehta (1977).

2.2. Design charts

The four most important parameters in a wide-angle diffuser are A , 2θ , K and n , where n is the number of screens within the diffuser—this includes the screens installed at the inlet and outlet. Data were collected from over a hundred wide-angle diffuser designs, mostly 'successful' (no separation, and uniform outlet flow with an acceptable turbulence level), and charts were plotted of relevant parameters, from which design rules have been derived. In Fig. 3, A is plotted against 2θ ; the curves enclosing successful configurations have an approximately hyperbolic shape. As n increases, the vertex moves to a higher value of 2θ and, to a lesser extent, to a higher value of A , thus implying a stronger dependence of required n on 2θ . Figure 4 is a plot of the sum of pressure drop coefficients of all the screens, $K_{sum} \equiv \sum (1/q)$, vs A . The straight line EF ($A = 1.14 K_{sum} + 1.0$) included the maximum number of successful configurations.

3. Overall design procedure

For a diffuser design to operate successfully it must lie to the left of the relevant curve in Fig. 3, giving the minimum number of screens required in the diffuser, and A

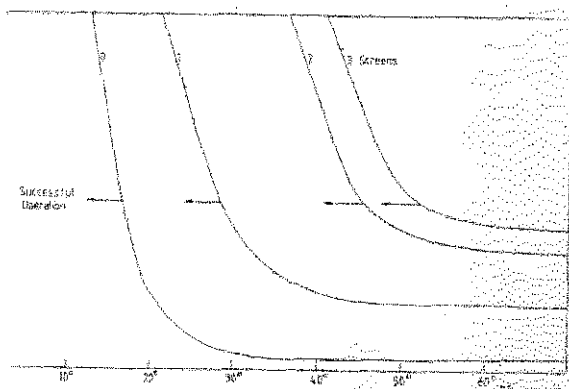


Figure 3. Design boundaries for diffusers with screens.

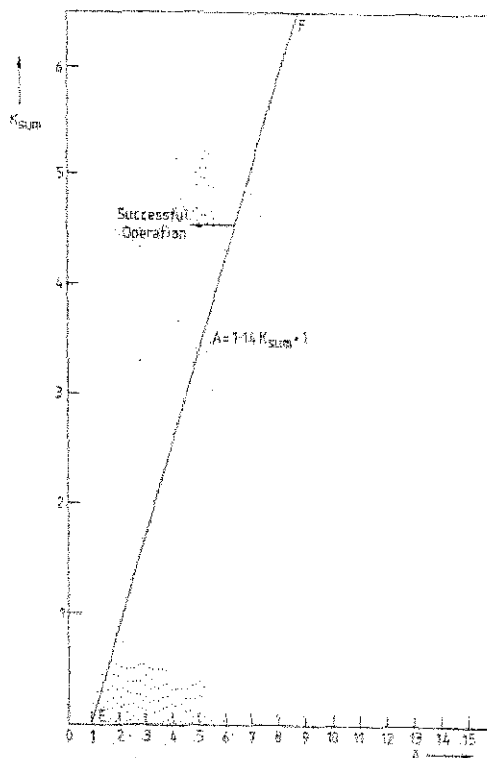


Figure 4. Overall pressure drop coefficient requirements for a diffuser with screens.

must be less than $(1.14 K_{sum} + 1.0)$, giving the minimum required overall pressure drop coefficient. A diffuser configuration satisfying both these curves should perform successfully provided that certain other design factors are kept in mind:

- (i) **Inlet conditions:** Thin boundary layers and steady flow at the inlet are obviously beneficial.
- (ii) **Screen Positioning:** The basic rule is to place screens where the diffuser wall angle changes suddenly, since these are the points where the flow is most likely to separate. In diffusers where no obvious location is indicated screens should be equally spaced, remembering that a screen at the diffuser entry (with a relatively high resistance) is desirable because the angle changes suddenly there.
- (iii) **Wall shape:** The number of screens required in a diffuser could well be reduced, and the efficiency increased, by employing curved walls. Potential flow methods are sometimes used to determine wall shapes but it is often easier to design wall shapes by eye. Straight-walled diffusers (often with curved screens) are, however, often employed, because they are easier and cheaper to construct.
- (iv) **Screen shape:** It is an advantage for the screen to intersect the diverging walls and streamlines at right angles, so that the refraction of the flow by the screens does not itself induce separation. Curved screens can be held in metal frames pressed into circular arcs and lined with wooden strips so that the gauze may be firmly embedded between two frames. It could be more difficult to dish the more flexible plastic screens (see section 3) which may also tend to flutter. Another alternative is to use a plane, 'variable- K ' screen comprising of one screen concentrically superimposed on another.

Technical Notes

Design rules for small low speed wind tunnels

R. D. MEHTA and P. BRADSHAW

Design rules for small low speed wind tunnels

R. D. MEHTA and P. BRADSHAW

INTRODUCTION

With today's computers, a wind tunnel is an essential in engineering, both for model tests and basic research. Since the 1930s, when the strong effect of free-stream turbulence on shear layers became apparent, emphasis has been laid on wind tunnels with low levels of turbulence and unsteadiness. Consequently most high performance wind tunnels were designed as closed-circuit (Fig. 1(a)) to ensure a controlled return flow. However, as will be seen below, it is possible with care to derive high performance from an open-circuit tunnel, saving space and construction cost. 'Blower' tunnels (the fan at entry to the tunnel, Fig. 1(b)) facilitate changes in working section arrangements; to cope with the resulting large changes in operating conditions, a centrifugal fan is preferable to an axial one. For ease of changing working sections the exit diffuser is often fitted from small blower tunnels, at the cost of a power factor greater than unity. This paper concentrates on the design of small blower tunnels but most of the information is applicable to wind tunnels in general.

A large open-circuit tunnel would be of rather inconvenient dimensions, mainly in length. Also, an open-circuit tunnel requires enough free room around it so that the quality of the return flow is not affected significantly (remember that an open-circuit tunnel in a room is equivalent to a closed-circuit tunnel with a poorly-designed re-circulation leg). The choice may also be restricted by the maximum available blower size. A working section Reynolds number of more than about 3×10^6 (a speed of about 30 m s^{-1}) is rare in blower tunnels of whatever size, and commercial blowers capable of producing such a speed in a section more than about 1 m^2 in area are also rare.

The main advantage of open-circuit tunnels is in their saving of space and cost. They also suffer less from temperature changes (mainly because room volume \gg tunnel volume) and the performance of a fan fitted at the upstream end is not affected by disturbed flow from the working section. One disadvantage of any open-circuit tunnel with an exit diffuser is that the pressure is always less than atmospheric and so spurious jets issue from any holes left unpatched, although this can be remedied by obstructing the tunnel outlet and creating an over-pressure in the working section. The main advantage of a centrifugal blower, as distinct from an axial fan, is that it performs well over a large range of loads (the whole range being at the same incidence and hence operating at the same lift coefficient). The only advantage of an open-circuit tunnel, with a centrifugal or axial fan at exit, is a dubious one that air coming from the tunnel room will be less disturbed than that coming from a fan.

It is difficult and unwise to lay down firm design rules generally because of the wide variety of requirements and especially the wide variety of working-section configurations. An attempt is made here to present design guide-

lines for the main components of a wind tunnel—the fan, wide-angle diffuser, corner vanes, settling chamber, contraction and exit diffuser (Fig. 1)—based on data from successful designs and some original experiments. For details of the data correlations see Mehta (1977) and for complete details of the experiments and design procedure see Mehta (1978).

2. FANS

2.1. Axial flow fans

The usual arrangement in a closed-circuit tunnel is a stator ('pre-rotation vanes') upstream of the rotor (the fan proper), designed so that the swirl at exit is zero. In the case of an open-circuit tunnel, swirl present in the flow out of the fan may be dissipated before the flow reaches the intake, but a remaining advantage of pre-rotation vanes is that the flow velocity relative to the fan blades is larger than if the stator is absent or located downstream of the fan.

2.1.1. Fan solidity

The design procedure outlined by Bradshaw and Pankhurst (1964) is still an adequate guide. The only serious problem found in fan design that is not found in the design of wings for low-speed aircraft is the interference between the flow fields of the blades. This interference depends mainly on the 'solidity', the ratio of blade chord to the gap between blades (measured around the circumference). Providing that the solidity is less than unity, approximately, interference is small enough to be treated as a small correction to the performance of an isolated aerofoil; for higher solidities the flow cannot be accurately related to that round an isolated aerofoil, and data for 'cascades' (rows of aerofoils arranged in the same manner as corner vanes) must be used instead. The solidity varies with radius, and in order to use the same



The Authors: Dr. R. D. Mehta and Professor P. Bradshaw, BA, Department of Aeronautics, Imperial College of Science and Technology, London.

Paper No 718.

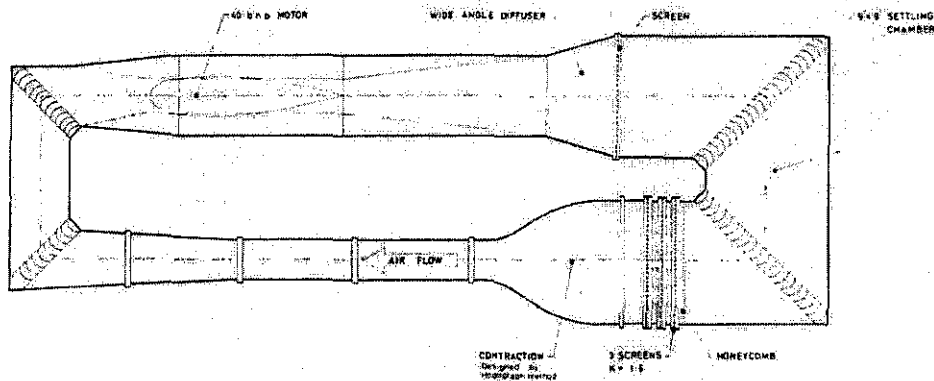
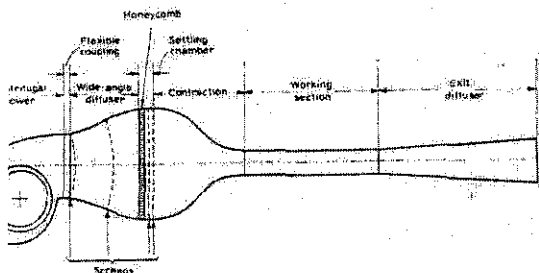


Figure 1(a). The main components of a typical closed-circuit wind tunnel.



1(b). The main components of a typical blower tunnel. (Not to scale.)

procedure for the whole length of the blade it is able to keep the solidity at the root below unity by fixing the fan on a central nacelle whose maximum diameter is roughly half the fan diameter.

Blade design

Fan efficiencies are of the order of 90% so that minimisation of losses is not usually important, and the procedure is to choose the blade lift coefficient to be as high as is safe, irrespective of lift/drag ratio; values between 0.9 are typical.

Pre-rotation vanes

Pre-rotation vanes should be run at a lift coefficient not far above that for maximum lift/drag ratio because the flow passes through the fan; to limit the resulting axial distance between the trailing edge of the pre-rotation vanes and the leading edge of the fan blades should be at least 20% of the vane chord and the number of blades should be different from the number of fan blades. Pre-rotation vane solidities usually fall into the 0.2 to 0.4 range.

An alternative to pre-rotation vanes for a lightly loaded fan is a set of straightener vanes downstream of the fan.

For detailed design rules for pre-rotation vanes, fan vanes and straighteners see Bradshaw and Pankhurst (1977).

Centrifugal blowers

Centrifugal blowers are normally used to drive open-circuit tunnels from the upstream end: a blower could be installed at the exit instead but this has no particular advantage. Single-inlet blowers could also be used to drive return-circuit tunnels by installing them in one of the return ducts. Single-inlet blowers are found to produce a non-uniform flow (due to the asymmetric positioning of the impeller) which would aid wall flow attachment in the inlet diffuser. This compensates for the non-

uniformity of the flow (which is also improved by the screens in the wide-angle diffuser and the settling chamber).

2.2.1. Advantages over other fans

Centrifugal blowers run with reasonable steadiness and efficiency over a wide range of flow conditions (i.e. varying tunnel power factor) because the whole blade span operates at nominally the same lift coefficient. The noise and pulsations generated by a centrifugal blower are adequately low, even at off-design conditions, and the uniformity of flow varies less with advance ratio, $U/\omega r$, in the notation of Fig. 2. The swirl (exit vortex) produced by a single-inlet blower is also independent of advance ratio (dependent on the ratio of rotor to casing width).

2.2.2. Types of impeller

The most common type of blading is the backward-facing aerofoil-type (Fig. 2); forward-facing is less efficient. If the blower efficiency is not too important, these blades could be designed in the same way as corner vanes or cascades by choosing a leading edge angle of $4-5^\circ$ and a zero trailing edge angle, but a more efficient blade shape is that of a cambered aerofoil with finite thickness. In the present authors' tests on blowers with aerofoil-type impellers it was found that the flow uniformity deteriorated with increasing loading. However, with backward-facing 'S' shaped blades (Fig. 2) the flow uniformity was found to improve with loading, presumably because these blades stall relatively early, leading to increased mixing. The cost is a higher turbulence level in the outlet flow and a reduced blower efficiency.

2.2.3. Splitter plate (tongue)

This is an important component which affects the outlet flow uniformity and blower noise characteristics. For minimum interference with the flow uniformity, the ratio of tongue height to casing height needs to be small (< 0.3) and the angle and shape carefully designed. The gap between the rotor and tongue needs to be a minimum for aerodynamic reasons but optimised for minimum interaction with the outgoing flow and thus minimum noise level. The tongue design on most commercially available blowers is adequate. A badly angled tongue could be improved upon by adding a cusped fairing downstream, as shown dotted in Fig. 2.

2.2.4. Other features and suggestions

An inlet bellmouth helps to produce a uniform flow and reduces inlet losses, and an inlet filter (helping to reduce inlet swirl) is essential to reduce contamination of hot-wire probes. Large blowers should be mounted on anti-

tion mountings and connected to the tunnel with a cle coupling to reduce vibration.

ouble-inlet blowers (air entering the impeller from sides) tend to produce a uniformly inclined flow out a vortex) which takes a longer distance to re h to the bottom wall downstream of the tongue. should therefore be more conservative in designing angle diffusers for double-inlet blowers.

n the whole, commercially available single-inlet ifugal blowers with backward-facing impellers are ate for driving blower tunnels.

nce the maximum required fan static pressure and ne flow rate have been estimated, the makers' per- nance charts can be consulted. Optimisation between efficiency, rpm and required power leads to the er choice (see section 10).

SCREENS

l tunnel screens are normally made of metal wires woven to form square or rectangular meshes. ns woven from nylon or polyester threads are also being used when the wind loads are not expected to ry high (UTS of nylon ~ 70, steel ~ 1100, bronze 3-1100 MNm⁻² and E of nylon > 3, steel ~ 200, ze ~ 100 GNm⁻²). The action of the gauze is ibed in terms of two parameters: the pressure drop cient, $K=f_1(\beta, R_o, \theta)$ and the deflection coefficient, $\alpha=f_2(\beta, K, \theta)$, where β is the screen open-area ratio and the flow incidence angle, measured from the normal e screen.

Main effects

(for detailed explanations see Mehta 1978)

ns make the flow velocity profiles more uniform by nsing a static pressure drop proportional to (speed)² thus reduce the boundary layer thickness so that the y to withstand a given pressure gradient is increased. reen with a pressure drop coefficient of about 2 ves nearly all variation in the longitudinal mean y. A screen also refracts the incident flow towards ocal normal and reduces the turbulence intensity in whole flow-field. For a given open-area ratio, it is r to have a smaller mesh for the reduction of xisting turbulence. Plastic screens tend to yield a : uniform flow beyond the boundary layer edge, ly due to the weaving properties, and produce an 'shoot' in the velocity profile near the edge, mainly d by screen deflection angle which is a maximum e wall. In terms of tackling a given pressure gradient voiding separation, this overshoot could be beneficial.

Open-area ratio (β)

l screens with very low β (~0.3) also produce an shoot but this is caused by streamline inclination near boundary layer edge. Low β (<<0.57) screens also ce instabilities resulting from a random coalition of

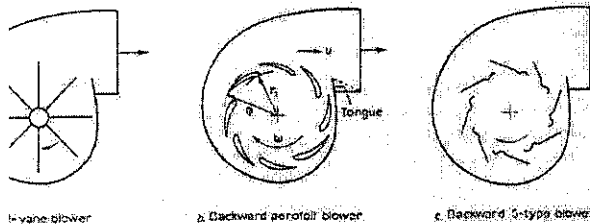


Figure 2. Different impeller types used in centrifugal blowers.

jets and presumably amalgamating to form longitudinal vortices which persist through the contraction. The coalition process is enhanced by variations in β (i.e. non-uniform weave) and by irregularities in the screen shape (i.e. wrinkles). It is therefore essential to inspect and clean wind tunnel screens regularly.

3.3. Determination of K

(ratio of pressure drop to dynamic pressure)

Although there is no wholly satisfactory method, Wiegardt's (1953) formula $\{K=6.5[1-\beta/\beta^2][Ud/\beta v]^{-1.3}\}$, where d is wire diameter, predicts the right trend; K decreases with increasing speed up to about $Ud/\beta v=600$, after which it is independent of Re. Collar's (1939) formula $\{K=0.9(1-\beta/\beta^2)\}$ usually over-estimates K in the high Re limit. One needs to be more careful in predicting K -values for plastic screens since,

$$K=f(\beta, R_o, \theta, \dots \text{co-planarity} \dots)$$

where θ is angle of screen to incident flow. For $\theta \neq 0$ use

$$K_e = K \cos^m \theta, \text{ with } m=1.0 \text{ for screens with } \beta \sim 0.6 \text{ and } m \sim 1.4 \text{ for } \beta \sim 0.3.$$

3.4. Determination of α

(ratio of outlet angle to inlet angle)

For α the form:

$$\alpha = A + \frac{B}{\sqrt{1+K}}$$

where A, B are empirical constants, is a better fit than the generally accepted form:

$$\alpha = \frac{1.1}{\sqrt{1+K}}$$

Note that the refractive index of a screen (μ) defined as in optics is equal to $1/\alpha$ for small θ . For larger θ use

$$\alpha_e = \frac{1}{\theta} \tan^{-1} \left\{ \tan \theta - \frac{\theta}{2} \sec^2 \theta \left[C - \frac{D}{\sqrt{1+K_e}} \right] (E + F\theta) \right\}$$

C, D, E and F are empirical constants.

Values suggested for the empirical constants by some limited experiments (Mehta, 1978) are: $A=0.66, B=0.31, C=0.68, D=0.62, E=1.0, F=1.5$.

A more complete analysis of the flow through screens can be found in Mehta (1978).

4. DIFFUSERS

The flow through a diffuser depends on its geometry defined by the area ratio (A), diffuser angle (2θ), wall contour and diffuser cross-sectional shapes. Other parameters like the initial conditions, boundary layer control method and the presence of separation could also affect the flow thus making it very difficult to predict. Almost all knowledge acquired about diffusers is empirical. There are two main types:

4.1. Exit diffusers

These are fitted downstream of the working sections and have gentle expansions with a diffuser included angle usually not exceeding 5° (for best flow steadiness, although best pressure recovery is achieved at about 10°) and an area ratio not exceeding about 2.5. It is important to have a reasonable degree of flow steadiness in the exit diffuser, since otherwise the pressure recovery tends to fluctuate with time, and, therefore, so does the tunnel speed if the input power is nearly constant. The design

ese diffusers is well catered for by existing methods (Dockrell and Markland, 1974).

Wide-angle diffuser

This type is normally installed between the blower and settling chamber or between the fourth corner and settling chamber of a closed-circuit tunnel; the cross-sectional area increases so rapidly that separation can be avoided by boundary layer control. A wide-angle diffuser is designed in terms of reducing the length for a given area ratio rather than effecting a pressure recovery; generally the pressure rise through a screened wide-angle diffuser is positive but small.

Boundary layer control methods

The most popular means of boundary layer control is the use of stalling gauze screens. A screen, besides removing the adverse effects of layer growth and incipient separation, gives the layer a new lease of life. In a wide-angle diffuser it is better to use several screens of relatively low K (less than about 1.5) because increasing K at a certain station has little effect on the skin friction at a much further downstream. Other types of boundary layer control methods include splitters, suction, trapped vortices, vortex generators and vanes and are preferable in diffusers with very severe geometries ($\theta > 50^\circ$). For a review see Mehta (1977).

Design charts

Four of the most important parameters in a wide-angle diffuser are A , 2θ , K and n , where n is the number of screens within the diffuser—this includes the screens installed at the inlet and outlet. Data were collected from a hundred wide-angle diffuser designs, mostly 'successful' (no separation, and uniform outlet flow with acceptable turbulence level), and charts were plotted in terms of relevant parameters, from which design rules have been derived. In Fig. 3, A is plotted against 2θ ; the enclosing successful configurations have an approximately hyperbolic shape. As n increases, the vertex of the curve shifts to a higher value of 2θ and, to a lesser extent, to a lower value of A , thus implying a stronger dependence of n on 2θ . Figure 4 is a plot of the sum of the pressure drop coefficients of all the screens, $K_{sum} \equiv \sum K_i$, vs A . The straight line EF ($A = 1.14 K_{sum} + 1.0$) defines the maximum number of successful configurations.

Overall design procedure

For a diffuser design to operate successfully it must lie to the left of the relevant curve in Fig. 3, giving the minimum number of screens required in the diffuser, and A

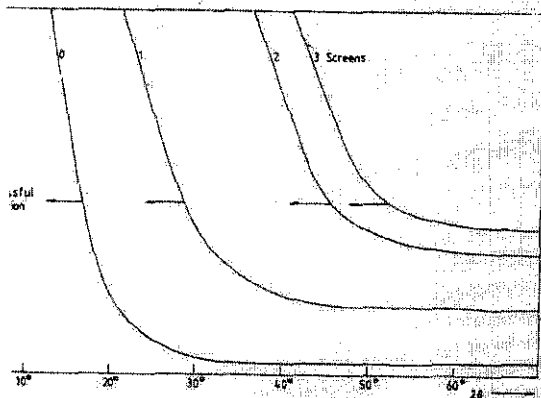


Figure 3. Design boundaries for diffusers with screens.

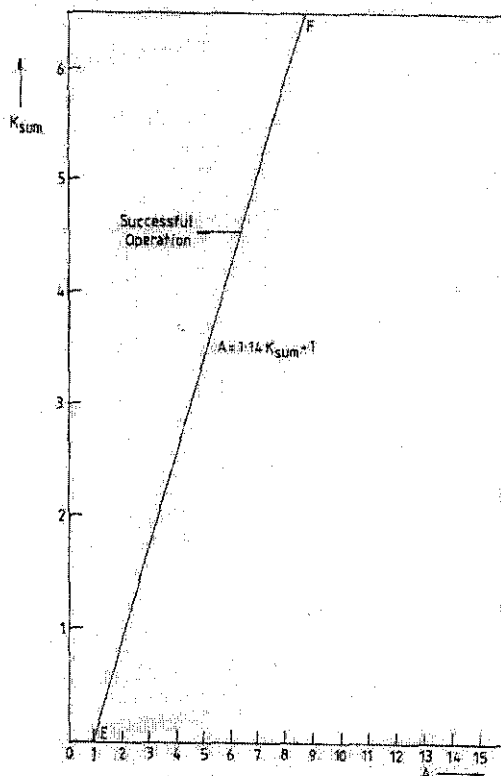


Figure 4. Overall pressure drop coefficient requirements for a diffuser with screens.

must be less than $(1.14 K_{sum} + 1.0)$, giving the minimum required overall pressure drop coefficient. A diffuser configuration satisfying both these curves should perform successfully provided that certain other design factors are kept in mind:

- (i) **Inlet conditions:** Thin boundary layers and steady flow at the inlet are obviously beneficial.
- (ii) **Screen Positioning:** The basic rule is to place screens where the diffuser wall angle changes suddenly, since these are the points where the flow is most likely to separate. In diffusers where no obvious location is indicated screens should be equally spaced, remembering that a screen at the diffuser entry (with a relatively high resistance) is desirable because the angle changes suddenly there.
- (iii) **Wall shape:** The number of screens required in a diffuser could well be reduced, and the efficiency increased, by employing curved walls. Potential flow methods are sometimes used to determine wall shapes but it is often easier to design wall shapes by eye. Straight-walled diffusers (often with curved screens) are, however, often employed, because they are easier and cheaper to construct.
- (iv) **Screen shape:** It is an advantage for the screen to intersect the diverging walls and streamlines at right angles, so that the refraction of the flow by the screens does not itself induce separation. Curved screens can be held in metal frames pressed into circular arcs and lined with wooden strips so that the gauze may be firmly embedded between two frames. It could be more difficult to dish the more flexible plastic screens (see section 3) which may also tend to flutter. Another alternative is to use a plane, 'variable- K ' screen comprising of one screen concentrically superimposed on another.

Cross-sectional shape: Most wide-angle diffusers have either rectangular or square cross-sections for ease of construction and since pressure recovery is not too important. It is advisable to fillet the corners in small tunnels, whose designs are likely to be more adventurous, to reduce the risk of large regions of flow separation.

Comparison and verification of design rules

These design rules compare well with those proposed by *et al* (1957), Schubauer and Spangenberg (1948) and *ire and Hogg* (1944). This is to be expected because many designers have used these rules; evidently the rules are successful, but they may be conservative. The present rules also compare well with some experiments and test results, details of which can be found in Mehta (1977), although there is evidence that the rules are not inflexible.

CORNER VANES

In some open-circuit tunnels have corners, say to deflect the efflux from a horizontal tunnel upwards to clear draughts. Rules for the design of vanes for 90° corners are uncontroversial and probably rather conservative. Thin sheet metal vanes are used on all but the best tunnels and, even in the latter, thick aerofoil-like vanes are used for strength rather than aerodynamic advantage. The ratio of the gap, h , between vanes (measured from leading edge to leading edge) to chord, c , should not exceed about 0.25; the vane lift coefficient is $2h/c$. Usual practice is to make the vane as a circular arc, with short straight extensions at leading and trailing edges for ease of rolling or pressing. The trailing edge is aligned parallel with the axis of the downstream flow and the leading edge is set at a positive 'angle of incidence' of 4° to the axis of the upstream leg. This arrangement has superficial logic but differs from established cascade-design practice, and recently Ermshaus and dascher (1977) have successfully used a hodograph-type design which has a negative angle of incidence at the leading edge and over-turns at the trailing edge so that the included angle is 105° instead of the conventional 86°. It is not clear whether a significantly higher angle can be used with this design.

The pressure drop through thin vanes of standard design is estimated by Bradshaw and Pankhurst (1964) to be about $1.2 (Uc/\nu)^{-1/4}$ times the dynamic pressure.

HONEYCOMBS

Honeycombs are effective for removing swirl and lateral velocity variations, as long as the flow yaw angles are not greater than about 10°. Large yaw angles cause honeycomb cells to 'stall' which reduces their effectiveness besides increasing the pressure loss.

Reduction of turbulence

The incidental effect of honeycombs is to reduce the turbulence level in the flow. Essentially, the lateral components of turbulence, like those of mean velocity, are inhibited by the honeycomb cells and almost complete attenuation is achieved in a length equivalent to about 10 cell diameters. Honeycombs themselves shed small amounts of turbulence, the level of which is found to be higher than the cell flow is laminar than when it is turbulent; this is attributed to a basic instability of the laminar near walls. Note that the cell flow in most wind tunnel honeycombs is laminar and so Lumley and McMahon's (1977) analysis, which assumes turbulent flow, will not apply. With a laminar cell flow the net reduction is tested for the shortest honeycomb (Loehrke and Nagib,

1976). It turns out that the shear layer instability in the near wake has a strength proportional to the shear layer thickness and so for the longest honeycomb, the ratio of turbulence generated to that suppressed is greatest.

6.2. Optimum cell size

For maximum overall benefit the cell length should be about 6-8 times its diameter. The cell size should be smaller than the smallest lateral wavelength of the velocity variation (roughly 150 cells per settling chamber 'diameter', i.e. 25 000 total, are adequate). The cross-sectional shape of the honeycomb cells is usually hexagonal, but sometimes square or triangular, the shape being chosen mainly for ease in construction. Impregnated paper honeycombs are adequate for small tunnels. Aluminium honeycombs made for aircraft sandwich construction have more precise dimensions than paper honeycombs and are to be preferred for high performance tunnels and large tunnels where the wind loads may be expected to be high. The cells of all honeycombs are often partly obstructed by burrs which can be fatigued off with an air hose.

7. SETTLING CHAMBERS

7.1. General arrangement

The usual arrangement consists of a honeycomb (with about 25 000 cells) followed by screens, the number and K -value depending on the turbulence level requirements. If severe yaw or swirl is expected in the flow from the wide-angle diffuser, it is advisable to install one screen upstream of the honeycomb, so that the flow angles are reduced. A screen with $K=1.5$ reduces yaw and swirl angles by a factor of about 0.7 for swirl angles of about 40°. The honeycomb should be installed some way downstream of the wide-angle diffuser exit, so that the flow static pressures and angles have had a chance to become more uniform. Since screens with small β (less than about 0.57) tend to produce instabilities, presumably in the form of longitudinal vortices, at least one screen with a larger β (> 0.57) should be used (in the most downstream position) if a truly two-dimensional boundary layer is required in the working section. Another alternative is to place the honeycomb downstream of the screens but this at best results in a rise in the turbulence level and is not recommended in general.

7.2. Spacing between screens

There are two important properties to consider:

- (i) For the pressure drops through the screens to be completely independent, the spacing should be such that the static pressure has fully recovered from the perturbation before reaching the next screen (i.e. $dp/dy=0$).
- (ii) For full benefits from the turbulence-reduction point of view, the minimum spacing should be of the order of the large energy containing eddies.

It has been found that a screen combination with a spacing equivalent to about 0.2 settling chamber diameters performs successfully. The optimum distance between the last screen and the contraction entry has also been found to be about 0.2 cross-section diameters. If this distance is much shorter significant distortion of the flow through the last screen may be expected. On the other hand, if this distance, or for that matter the overall length of the settling chamber, is too long then unnecessary boundary layer growth occurs.

Installation of components

is are normally tacked onto wooden frames. More is necessary when tacking on plastic screens since being more flexible, tend to wrinkle along the lines. The honeycomb is usually just push-fitted into a frame. A useful arrangement for small tunnels is to use the wide-angle diffuser, screen frames and connect them on a table and clamp them by drawbolts, so that they can be withdrawn easily. On larger tunnels, it is possible to equip the settling chamber (and wide-angle diffuser) components with castors for ease of removal. In tunnels made of metal or concrete, the screens are normally installed in separate frames which can be removed from the tunnel for cleaning or replacement.

CONTRACTIONS

contraction:

increases the mean velocity which allows the honeycomb and screens to be placed in a low speed region, thus reducing pressure losses.

reduces both mean and fluctuating velocity variations to a smaller fraction of the average velocity.

The most important single parameter in determining contraction effects is c , the contraction ratio. The factors of contraction, as derived by Batchelor (1970) for $c \gg 1$,

component mean velocity: $1/c$

or W -component mean velocity: \sqrt{c}

component rms intensity: $1/2c \{3(1+4c^2 - 1)\}^{1/2}$

or w component rms intensity: $(3c)^{1/2}/2$.

factor of reduction of percentage velocity variation can be found by multiplying the above expressions by $100/c$.

The design of a contraction centres on the production of a uniform and steady stream at its outlet, and requires avoidance of flow separation. Two more desirable features include minimum exit boundary layer thickness and minimum contraction length. A design satisfying all these will be such that separation is just avoided and its non-uniformity is equal to the maximum tolerable for a given application (typically $\pm 1\%$ velocity variation on outside the boundary layers).

Contraction lengths

It is always possible to avoid separation in the contraction by making it very long, but this results in an increase of length, cost and exit boundary layer thickness.

Contraction ratio

The power factor contribution of screens in the settling chamber varies as $1/c^2$, large contraction ratios are advantageous. But large contraction ratios mean high construction and running costs besides possible increases of noise and separation near the ends. Therefore, contraction ratios between about 6 and 9 are normally used, at least for the smaller tunnels.

Cross-sectional shape

In a contraction with a non-circular cross-section, the corner walls tend to migrate laterally, especially at the corners of a polygonal section. In any case the boundary layers near the corners will be more liable to separate. However, recent investigations (Mehta, 1978) show that this does not cause a problem in a well-designed contraction; the effect of boundary layer migration in a contraction whose cross-sectional aspect ratio changes with its length can be reduced by adding small 45°

corner fillets, but rapid termination of these in the working section must be avoided.

Two-dimensional contractions are sometimes preferred for tunnels used for boundary layer studies, where the working section is wide but shallow. However, if the boundary layers are thick, the plane walls tend to develop strong secondary flows. Also, 2-D contractions require about 25% more length to attain the same uniformity of pressure distribution as axisymmetric ones.

8.4. Wall shape

8.4.1. Theoretical design

The solution of the Laplace equation or the Stokes-Beltrami equation is relatively easy for simple geometries and many analytical solutions have been derived. With the onset of computers many numerical schemes have also been proposed. For a review see Mehta (1978).

There is no wholly satisfactory method of theoretical wall shape design, as distinct from analysis. The application of all these methods requires the establishment of some criteria and then the application of trial-and-error techniques for which limited guidance is given.

8.4.2. Design by eye

Designers have often used the rather unscientific method of design by eye. Note that the actual form of a contraction contour is not very important except near the ends, and that smoothness in contour shape is much more important than exact dimensions. In general the wall radii of curvature should be less at the narrow end and each end must join the parallel sections so smoothly that at least the first and second derivatives of the curve are zero (or very small) at the ends.

9. WORKING SECTIONS

Working section design is totally dependent on the requirements of the individual experimenter. Blower tunnels are more flexible in accepting a variety of working sections (with and without exit diffusers).

The flow out of a contraction often takes a distance equivalent to about 0.5 diameters before the non-uniformities are reduced below an acceptable level. Also, if a turbulence grid is installed, it may take up to 10-15 mesh lengths before a homogeneous flow is obtained. These requirements often fix the minimum length of the working section. The streamwise pressure gradient is best controlled by installing tapered fillets.

It is advisable to mount removable side panels on pinned hinges on large working sections which makes their 'single-handed' removal easier and safer.

Drag forces, being proportional to (velocity)², change by twice as large a fraction as the mean velocity; lift forces change because of the change in mean velocity and because of the influence of tunnel walls on the effective angle of incidence. Lift interference on a complete aircraft model in a rectangular-section tunnel is minimised if the ratio of working section breadth to height is $\sqrt{2}$ (with model span less than three-quarters of the breadth) so most general purpose aerospace tunnels are made with approximately this aspect ratio. However tunnels for measurements in boundary layers, growing on the tunnel floor say, have an optimum breadth-to-height ratio of about five since all that is necessary is that a reasonable thickness of irrotational flow shall remain between the roof and floor boundary layers at the end of the test section (a diffuser with such a non-uniform entry flow would not be very efficient). Tunnels for testing building complexes or natural terrain at model scale can also have a large breadth/height ratio; conversely, tunnels for testing isolated tower buildings or smokestacks can have a

dth-to-height ratio less than unity, although the ratio model breadth to tunnel breadth must still be kept 1 to minimise interference.

ESTIMATION OF TUNNEL POWER FACTOR

Having decided the size and configuration of a wind tunnel, the next design step is to estimate the tunnel power factor, λ (equal to $H/\frac{1}{2}\rho_o U_o^2 A_o$, where H is the input power and subscript o refers to working conditions) so that the fan and drive unit can be sized. It is difficult, but in fact not essential, to estimate the power factor very accurately; adequate extra power can be installed to cope with a variety of model or wing section configurations, not known in advance. The pressure losses in a wind tunnel are due to diffusers, screens, resistive components such as screens, and friction on the tunnel walls. The total pressure loss due to each component can be estimated separately, and then summed and divided by the blower efficiency η , typically 0.8, to give the tunnel power factor. Typical values for a tunnel are given below.

Losses due to skin friction.

$$\eta\Delta\lambda_1 = \frac{\Delta P}{\frac{1}{2}\rho_o U_o^2} = \left(\frac{A_o}{A}\right)^2 \int C_f \frac{S}{A} dx,$$

where S is the duct local perimeter and remembering that the area ratio is the reciprocal of the velocity ratio. It is normally only necessary to estimate skin friction losses in the working section ($A/A_o=1$). Those in the diffusers are normally accounted for in the efficiency and the other components do not contribute significantly.

Therefore, $\eta\Delta\lambda_1 \approx C_f SL/A$, where L is the working section length. Typical value: $\eta\Delta\lambda_1 \approx 0.07$, assuming $C_f \approx 0.003$.

Losses due to screens, honeycomb and corner-vanes.

$$\eta\Delta\lambda_2 = K \left[\frac{A_o}{A}\right]^2.$$

So for a tunnel with four screens (two in the wide-angle diffuser with $A/A_o=4$ and 6 respectively) each with $K=1.5$ (for $U=5-10$ m/s), and a honeycomb with $K=0.5$ we have, taking $c=9$, typical value: $\eta\Delta\lambda_2=0.18$ (the screen at $A/A_o=4$ contributes 0.094).

Loss of total head in the exit diffuser.

$$\eta\Delta\lambda_3 = (1 - \eta_D) \left[1 - \left(\frac{A_o}{A_{out}}\right) \right],$$

where η_D is the diffuser efficiency. This is a loss due to the inefficiency of the diffuser in transforming kinetic energy into 'pressure energy' and is caused by boundary layer growth and non-uniformity of the flow. The efficiency of a wide-angle diffuser with screens is generally negative but Δp is small.

For a conical diffuser with $A \sim 2.5$ and $2\theta \sim 5^\circ$, Cockrell and Markland (1974) suggest $\eta_D=0.8$, but this may be lower for diffusers with rectangular cross-sections, typical value: $\eta\Delta\lambda_3=0.25$ for $\eta_D=0.7$ and $A=2.5$.

(iv) Loss of total head at the exit of an open-circuit tunnel.

In an open-circuit tunnel, the amount of kinetic energy lost at the exit and dissipated into heat adds to the total losses.

$$\eta\Delta\lambda_4 = \left(\frac{A_o}{A_{out}}\right)^2$$

[=1 for blower tunnels with no exit diffuser], typical value: $\eta\Delta\lambda_4=0.16$ for $A=2.5$.

Therefore the estimated overall tunnel power factor, $\lambda \equiv \sum_{n=1}^4 \Delta\lambda_n / \eta \approx 0.825$ for the tunnel considered (with an exit diffuser), taking $\eta=0.8$.

Once the tunnel power factor has been estimated and the required fan static pressure rise determined, one can set about the selection of the optimum fan size. The dynamic pressure rise through a blower is usually ignored and can be thought of as a safety factor in the calculations.

The fan outlet flow will be least turbulent when the fan is operating near maximum efficiency. Fan efficiency is a function of the dimensionless flow rate; the pressure rise coefficient is a (weak) function of the dimensionless flow rate also, so that requiring maximum efficiency specifies both dimensionless flow rate and pressure rise coefficient. So for a given required flow rate and pressure rise, two equations are obtained which can be solved to give the fan size and optimum operating rpm. In practice the manufacturer's performance charts should be searched for a fan size (and rpm) giving near maximum efficiency for the required flow rate and pressure rise.

ACKNOWLEDGMENTS

We are grateful to R. W. F. Gould, National Maritime Institute, M. C. Welsh, CSIRO Melbourne, and a referee, for helpful comments on a draft of this paper.

REFERENCES

- BATCHELOR, G. K. *The theory of homogeneous turbulence*. Cambridge University Press, pp 55-75, 1970.
- BRADSHAW, P. and PANKHURST, R. C. The design of low-speed wind tunnels. *Prog Aerospace Sci*, Vol 5, p 1, 1964.
- COCKRELL, D. J. and MARKLAND, E. Diffuser behaviour—a review of past experimental work—relevant today. *Aircr Engng*, Vol 46, p 16 (reprint of Vol 35, p 286), 1974.
- COLLAR, A. R. The effect of a gauze on the velocity distribution in a uniform duct. *ARC R & M* 1867, 1939.
- ERMISHAUS, R. and NAUDASCHER, E. Der Niedergeschwindigkeitswindkanal des Instituts für Hydromechanik an der Universität Karlsruhe. *Zeitschrift für Flugwissenschaften und Weltraumforschung*, Vol 1, p 419, 1977.
- KLINE, S. J., MOORE, C. A. and COCHRANE, D. L. Wide-angle diffusers of high performance and diffuser flow mechanisms. *J Aero Sci*, Vol 24, p 469, 1957.
- LOEHRKE, R. I. and NAGIB, H. M. Control of free-stream turbulence by means of honeycombs: A balance between suppression and generation. *ASME J Fluids Engng*, Vol 98, p 342, 1976.
- LUMLEY, J. L. and McMAHON, J. F. Reducing water tunnel turbulence by means of a honeycomb. *ASME J Basic Engng*, Vol 89D, p 764, 1967.
- MEHTA, R. D. The aerodynamic design of blower tunnels with wide-angle diffusers. *Prog Aerospace Sci*, Vol 18, p 59, 1977.
- MEHTA, R. D. Aspects of the design and performance of blower tunnel components. PhD Thesis, Imperial College, University of London, 1978.
- SCHUBAUER, G. B. and SPANGENBERG, W. G. Effect of screens in wide-angle diffusers. *NACA TN-1610*, 1948.
- SQUIRE, H. B. and HOGG, H. Diffuser-resistance combinations in relation to wind tunnel design. *RAE Report No Aero 1933*, 1944.
- WIEGHARDT, K. E. G. On the resistance of screens. *Aero Quarterly*, Vol 4, p 186, 1953.

REPORT No. 392

REDUCTION OF TURBULENCE IN WIND TUNNELS

By HUGH L. DRYDEN

SUMMARY

A nonmathematical outline is given of modern ideas on the nature of the effect of turbulence, and their bearing on the desirability of designing wind tunnels for large turbulence. Experiments made on a parabolic tunnel for the purpose of reducing the turbulence described, to illustrate the influence of certain factors on the magnitude of the turbulence. Moderate changes in the size, shape, and wall thickness of cells in a honeycomb were found to have little effect. The use of a room honeycomb at the entrance was also of little effect in reducing the turbulence. The turbulence was reduced with increasing distance between the honeycomb and the measuring station. A further decrease was obtained by using a large area reduction in the entrance to the honeycomb at the extreme entrance end. Measurements of turbulence were made by the use of a hot wire anemometer and also by the use of the hot wire anemometer bed in Reference 5. The present work was conducted with the cooperation and financial assistance of the National Advisory Committee for Aeronautics.

INTRODUCTION

The subject of turbulence is one of great interest in the field of aerodynamics, and many investigations are in progress in the aerodynamical laboratories of the various countries. The recent developments in various aspects of the subject. The recent international cooperative measurements inaugurated in the auspices of the National Physical Laboratory Great Britain have shown that turbulence is a factor of considerable importance in determining the drag on bodies in an air stream, and the chief question of the day is whether it is desirable to have a minimum of turbulence in wind tunnels.

The recognition of the effect of turbulence in wind tunnel experiments came about somewhat as follows: In the year 1911, Eiffel (reference 1) measured the resistance of a sphere in his newly constructed wind tunnel and published the value of the resistance coefficient as 0.18.¹ A year later, Föppl of the Aerodynamical Institute at Göttingen (reference 2), in a comparison of results with the Eiffel Laboratory,

stated that Eiffel's published value was obviously in error, probably a misprint, and that the true value was 0.44 or nearly three times as great. Eiffel replied that the published value was correct and made further experiments on spheres of different diameters at several wind speeds which showed certain anomalous features, now familiar to students of aerodynamics.

The first clue to the explanation of the discrepancy was given by Wieselsberger (reference 3) who showed that he could obtain results in the Göttingen wind tunnel similar to those obtained by Eiffel. He accomplished this by producing a disturbance ahead of the sphere by placing an open-mesh screen across the air stream in front of the sphere, or by placing a wire ring on the surface of the sphere in a plane perpendicular to the wind direction. By these and numerous other experiments it has been established that the air resistance of a sphere depends not only on the diameter of the sphere, the speed, density, and viscosity of the air but also on the turbulence of the air stream.

Another type of body for which widely varying results have been obtained in different wind tunnels is the streamline body exemplified by the airplane strut and the airship hull. Values obtained at the National Physical Laboratory for the resistance of streamline bodies appeared to be on a lower level than values obtained at the wind tunnel of the Washington Navy Yard, and the nature of the scale effect was quite different. In 1923 the National Physical Laboratory began the circulation of two airship models for comparative tests in a large number of the wind tunnels of the world. The results in the United States wind tunnels (reference 4) show variations of 50 per cent from a mean value and it has recently been shown by experiment (reference 5) that these differences are due to differences in the turbulence of the several wind tunnels.

While these two examples illustrate the large effects of turbulence in wind tunnel experiments, the discovery of the effect itself is much older. Osborne Reynolds (reference 6), in his study of flow in pipes, records the first observations of the effect. For a sufficiently small Reynolds Number (product of the mean speed by the diameter divided by the kinematic viscosity), the flow in a pipe is laminar and takes place

¹ Resistance coefficient equals the force divided by the product of cross-sectional area and velocity squared.

in accordance with the laws of hydrodynamics for the steady flow of a viscous liquid. At large Reynolds Numbers, the flow is eddying and the movements of finite "molar" masses of the fluid as well as movements of single molecules transfer momentum from one layer of the fluid to another. In a definite experimental arrangement, the transition from one régime of flow to the other occurs at a definite value of the Reynolds Number, irrespective of the individual values of the speed, diameter of the pipe, and viscosity and density of the fluid. When a disturbance (turbulence) is present in the incoming flow, the value of the critical Reynolds Number is found to depend on the magnitude of the disturbance, decreasing as the turbulence increases until a certain lower limit is reached, beyond which further increase of turbulence has little effect. The turbulence in the incoming flow may be produced by objects placed near the entrance of the pipe, by honeycombs across the pipe, or by the shape of the entrance itself. The resistance coefficient of a pipe is a function of the turbulence as well as of the Reynolds Number, and for a certain range of Reynolds Numbers the effect is very large indeed.

The information now available on the effect of turbulence clears up many puzzling discrepancies in wind tunnel results, and indicates that no standardization of wind tunnels can result until a standard value of the turbulence is adopted and methods are known for controlling the turbulence in a given wind tunnel. The title of this paper suggests that the turbulence in wind tunnels should be as small as possible, a view that is not at all unanimously accepted, and the object of this paper is to present the arguments for and against this view and to indicate by experiments on a particular wind tunnel how a small turbulence may be secured.

The turbulence in a given wind tunnel has far-reaching effects on the results of measurements made in that tunnel. Not only will the value of the force coefficients at a given Reynolds Number be dependent on the value of the turbulence, but the whole nature of the variation of the force coefficient with Reynolds Number (i. e., the scale effect curve), on which the extrapolation to full scale depends, is governed by the amount of the turbulence. As is well known, the scale effect on an airship model in a wind tunnel of large turbulence shows a coefficient decreasing as the Reynolds Number increases, whereas in a tunnel of small turbulence the coefficient is much lower and usually increases with increasing Reynolds Number at the higher Reynolds Numbers. While the effects of turbulence are large only for certain types of bodies, it is reasonably certain that an effect is present in all cases, although often its magnitude is extremely small. Under these circumstances the importance of knowing the value of the turbulence in every wind tunnel experiment is obvious.

Modern views as to the nature of the effect of turbulence.—As a background for the discussion of the relative advantages and disadvantages of having small or large turbulence in wind tunnels, it is necessary to outline briefly the modern conception of the nature of the effect of turbulence. The views here presented hardly have the status of a well-developed theory, and some of the details may be subject to controversy. The outline, however, is believed to be substantially correct, and represents a combination of the contributions of many investigators including Prandtl, von Kármán, Burgers, and others.

The starting point is the boundary layer theory of Prandtl. It had long been noted that in a large part of the field of flow of air or water at moderately large Reynolds Numbers, the dissipation of energy is negligible and therefore that the effects of the viscosity of the fluid are negligible. There must, however, be some effect of viscosity on the flow, else there would be no drag. It occurred to Prandtl to assume that the effects of viscosity are confined to a thin layer or skin close to the surface of the body and to introduce this assumption in the general equations of motion of a viscous fluid. The result is a series of equations giving the velocity distribution in the layer, the thickness of the layer or equivalent parameter, and the skin friction on the surface when the pressure distribution along the body is known. The results of this theory have been abundantly confirmed by experiment for parts of the layer not too far from the point of origin at the nose or leading edge of the body.

Two phenomena intervene to make the formulas invalid for the entire boundary layer. The first is the phenomenon of separation, which takes place when the pressure outside the layer increases downstream. The fluid particles near the wall are dragged along by the friction of the neighboring particles but are retarded by the pressure. As the boundary layer thickens the retarding effect becomes predominant and finally causes a reversal of the flow. The reversal of flow, on account of the consequent accumulation of fluid, separates the flow from the surface, as observed on cylinders, and on airfoils at large angles of attack. The onset of separation is predicted by the equations of Prandtl, but the phenomena following the occurrence of separation introduce wide departures from the assumptions on which Prandtl's equations are derived.

The second phenomenon not contemplated in the basic assumptions is the onset of eddying flow in the boundary layer. The flow described by Prandtl's equations is laminar. Momentum is transferred from one layer to another by the motions of single molecules whose total effect is integrated in the viscosity coefficient. The experiments of Burgers and his pupil v. d. Hegge Zijnen show that the flow becomes eddying and that so long as the turbulence of the approaching

is not altered, the transition occurs when the Reynolds Number formed from the speed at the edge of the boundary layer and the thickness of the boundary layer reaches a certain critical value. This critical value depends, however, on the turbulence of the approaching stream, decreasing as the speed increases.

The onset of eddying flow in the boundary layer, if it occurs long before separation of the layer, modifies the point of separation. In the eddying motion there is thorough mixing of the air particles, and the action of the outer layers on the inner layers (near the surface of the body) is greater. The air in the boundary layer is thus enabled to flow farther against an adverse pressure gradient and the process of separation is delayed. The delayed separation caused by the eddying motion in the boundary layer is responsible for the great variation of the drag coefficient of spheres and cylinders in the critical Reynolds Number range.

The hastening of the onset of eddying flow in the boundary layer is responsible for the effect of turbulence on the air resistance of spheres.

The preceding matters are presented in a more technical manner in reference 5, which includes a detailed discussion of the transition to spheres and airship models. It should be noted here that the mechanism of the breakdown of the laminar boundary layer and of the effect of turbulence is not yet fully understood. The author believes that the mechanism is essentially the same as occurring in the phenomenon of separation, and that the breakdown would not occur if there were no turbulence in the air stream at the edge of the boundary layer.

The observed fluctuations of speed at a fixed point may be taken as an indication that at any one point there are variations of speed along the outer edge of the boundary layer. With the speed variations there will be associated variations of pressure, and in regions where the speed is decreasing, the pressure is increasing. The magnitude of the pressure fluctuations depends on the amplitude and frequency of the speed fluctuations, increasing as either increases. At sufficient distance from the leading edge, the thickness of the boundary layer will be such that there is a reversal of the direction of flow near the surface in those places where the pressure is increasing in the stream. Larger speed fluctuations bring larger pressure gradients and an earlier reversal of flow. It is very probable that such a reversal would give rise to the formation of eddies. This theory has not been subjected to any mathematical check, and will be discussed in another paper.

Is small turbulence desirable?—In the light of this discussion of the action of turbulence, the question arises as to the amount of turbulence that is most to be desired in wind tunnel experiments. At the large Reynolds Numbers encountered in full-scale airplanes and ships, the flow in the boundary layer is bound to

be eddying over most of the body since the critical Reynolds Number is reached at a comparatively short distance from the nose. In wind-tunnel experiments, the flow in the boundary layer is likely to be laminar over most of the surface, especially if the turbulence is small. This difference in the character of the flow in the boundary layer often gives rise to large differences between force coefficients observed for the model and for the full-scale body. For example, the angle of attack at which burbling (i. e. separation) occurs on airfoils, especially thick airfoils, is often much smaller for the model.

The first suggestion which occurs to anyone receiving this information for the first time is to build wind tunnels with a high degree of turbulence, so that eddying flow will be established throughout most of the boundary layer. It is assumed that this procedure will give at small Reynolds Numbers a flow more like the flow of a nonturbulent air stream at large Reynolds Numbers than is the flow which is obtained at the same small Reynolds Numbers with small turbulence. Or it may be argued that turbulence is always present in the atmosphere and that this condition should be represented in the model experiments. It has been claimed for several wind tunnels that the turbulence in them is exactly that of the atmosphere, because of the agreement of extrapolated model coefficients with full-scale coefficients in a few cases. This is a specious argument, for the turbulence in the atmosphere is a highly variable quantity, and at any one place is different at different times. Furthermore, because of the effect of turbulence on the form of the "scale-effect" curve, it is possible to obtain the same extrapolated full-scale value from model values observed in different wind tunnels, even when the model values differ widely. For example, if the drag of an airship model is measured in a highly turbulent wind tunnel, the drag coefficient will be found to decrease with increasing Reynolds Number, and the extrapolated value for the full-scale Reynolds Number will be considerably lower than any of the measured values. If the drag of the same model is measured in a wind tunnel with small turbulence, the drag coefficient will be found to be lower than in the highly turbulent wind tunnel and the variation with Reynolds Number will be small. The full-scale value will then be assumed the same as the measured value, and it may happen that this value agrees closely with the full-scale value extrapolated from the turbulent wind-tunnel observations.

The argument for the use of wind tunnels with large turbulence is based on a great simplification of the actual phenomena, a simplification which is helpful at the beginning of a study of the problem, and is useful to nontechnical readers, but which often leads to misunderstanding. The words "laminar" and "eddy-ing" are used to distinguish between two general types of flow as rough classifications, but all "eddy-ing" flows

re not identical; furthermore, different parts of one and the same boundary layer having eddying flow are not identical. The skin friction per unit area, the thickness, and the velocity distribution vary from point to point. The classification of flows into laminar and eddying is only a very rough and general classification; there is always a transition region between the two, in which the flow can not be unambiguously assigned to either classification. Thus while in a very general way, an increase in turbulence has an effect similar to the effect of an increase of Reynolds Number, a detailed examination (see for example reference 5) shows that the resemblance is only superficial.

Wieselsberger (reference 7) presents the arguments for or a small turbulence as follows. "It has not yet been definitely ascertained as to whether, in the case of experiments with models, the turbulence is an advantage under all circumstances and has the same effect as the increasing of the Reynolds Number, since the information on this subject is still (1925) insufficient. It is quite conceivable, however (and this possibility must be taken into account), that, in certain cases, the air stream is affected by the turbulence in quite a different and perhaps undesirable manner. Besides, we often have to test in the wind tunnel full-scale objects, such as radiators, spars, and landing gear parts. In these cases, a turbulent stream would give a wrong idea of the actual relations. A turbulence-free air stream is also necessary for testing and calibrating instruments (for example, air-speed meters). Lastly, it may be remarked that a nonturbulent flow is very easily rendered turbulent to any desired degree by the interposition of a screen of wire or thread, if required for certain experiments, while the reverse is not so easily accomplished. We see, therefore, that the reference must unquestionably be given a wind tunnel with as smooth an air flow as possible."

Little needs to be added to this clear statement. It emphasizes again that turbulence is an important factor, whose value needs to be known. The adoption of small turbulence as an ideal to be sought in the design of wind tunnels does not preclude the possibility and desirability in many cases of carrying on experiments with a large turbulence.

The measurement of turbulence.—In the preceding discussion the word turbulence has been used, without precise definition, in the general sense of any departure from the ideal conditions of steady and uniform flow. In the absence of more complete knowledge of the mechanism of the breakdown of laminar flow and the onset of eddying flow, no completely satisfactory definition can be given. At any point in the air stream, the speed varies with the time in a very regular manner, about some mean value, \bar{V} . At any instant the speed differs from the mean value by an amount ΔV , which varies from instant to instant.

Let \bar{u} form the average value, dV , taken without regard to sign, in accordance with the definition

$$dV = \sqrt{\frac{1}{T} \int_0^T \Delta V^2 dt}$$

where t is the time and T is a time interval which is large in comparison with the period of the fluctuations of speed. dV is nothing more than a particular kind of average value of the deviation of the speed from

its mean value, \bar{V} ; $1/2 \rho dV^2$, ρ being the density of the air, is the amount by which the kinetic energy of the air exceeds what it would have been had the velocity been constant and of value \bar{V} . In reference 5, the quantity $\frac{dV}{\bar{V}}$ was defined as the turbulence, and it was shown that the forces on spheres and streamline models can be correlated with its value.

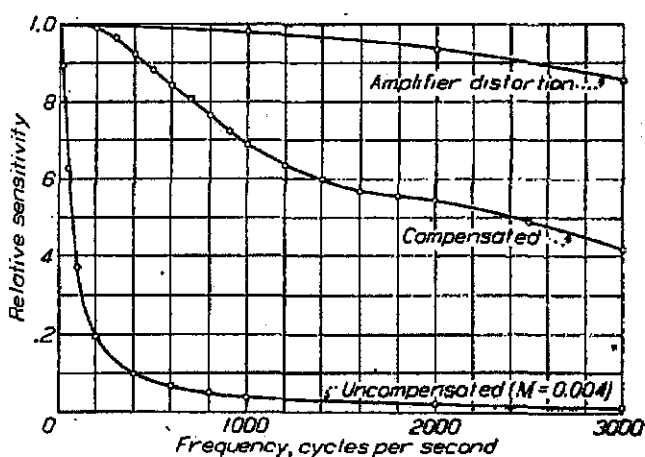


FIGURE 1.—Relative sensitivity of hot-wire anemometer to periodic variations in speed. The curves apply to the apparatus described in N. A. C. A. Technical Report No. 342, and the one of chief interest is that labeled compensated. The uppermost curve indicates the loss due to distortion in the amplifier; the remaining loss is due to defects of the compensating circuit. The lower curve shows the response when no compensation is introduced.

The turbulence was measured by a hot-wire anemometer and associated apparatus. The sensitivity of such apparatus to variations in speed is constant up to a frequency of 100 per second, and then decreases rapidly, somewhat as shown in Figure 1. (Consequently, when used in a stream containing variations of widely different frequencies, its indications refer mainly to the variations having the lower frequencies.) This curve was determined by the method of reference 8.

The considerations at the end of the section on "Modern views as to the nature of the effect of turbulence" lead to the conclusion that fluctuations of high frequency are more effective in causing breakdown of the laminar flow than are those of low frequency, and it has been suggested by other investigators that the frequencies of importance are much higher than 100 cycles per second. The correlation of the force

rements with the mean amplitude of fluctuation asured is, then, to be regarded as indicating that both the forces and the mean amplitude of frequency fluctuations vary with the "real" ance. This interpretation may be the correct As yet, we have no experimental evidence for or t it. Experiments are now in progress at the 1 of Standards, and also in Holland (reference an attempt to extend the frequency range determine the "spectral distribution" of the tions.

surements on spheres have often been used as a tive method for the comparison of the tur- e in different wind tunnels. It was suggested rence 5 that sphere results be expressed by the Reynolds Number for which the drag ent of the sphere is 0.3. For the experimental o be described in this paper, both methods of ing turbulence have been used, namely, the method, and that of the hot-wire anemometer. ription of wind tunnel and modifications.—The lar wind tunnel selected for experiments on duction of turbulence was the 54-inch wind of the Bureau of Standards, which was known e a fairly large turbulence. When the measure- were begun, the tunnel was in the condition ed in reference 5 and as shown in arrange- No. 1 on Figure 2. The features to be noted are atively small and abrupt area reduction in the ce cone and the presence of an upstream honey- n the straight portion of the tunnel. In ar- ent No. 2 a honeycomb of paper tubes 1 inch eter and 4 inches long was installed in the room o the tunnel inlet. This honeycomb was a te of the one already in place at the exit end. ngement No. 3 the upstream honeycomb in ight portion of the tunnel was removed. In nment No. 4 an upstream honeycomb of round f galvanized iron 3 inches in diameter and 12 long was installed as far upstream as practicable. ngement No. 5 the upstream honeycomb of round cells was removed and replaced by a omb made of paper tubes 1 inch in diameter and s long. In arrangement No. 6 the entrance as completely rebuilt. The entrance was made ial in cross section, 10 feet between opposite and a honeycomb of 4-inch square cells, 12 long, was placed immediately at the entrance. rance was placed in the plane of the room omb already in place. It will be noted that erences between arrangements 1, 2, 3, 4, and 1 the honeycombs alone, whereas arrangement s a radical change in the form of the entrance

RESULTS

drag of a sphere was measured for a number of ds at each of the positions designated as up-

stream, working section, and downstream in Figure 2, except for arrangement No. 3 where only the up- stream and downstream runs were made. For ar- rangements 1, 2, 4, and 5 a 5-inch sphere was used, whereas for arrangements 3 and 6 a sphere 8.6 inches in diameter was used. The same experimental arrange- ment was used for both spheres, namely, that shown in Figure 4 of reference 5 for the 8.6-inch sphere, a downstream spindle suspended by 4 wires arranged in 2 V's, with a shielded counterweight from a fifth wire. The drag was computed from the downstream deflec- tion of the system and the weight. The drag of the spindle was measured with the sphere detached but supported in front of the spindle. The results are expressed in the usual manner as a plot of the drag coefficient, C_A , against the logarithm to base 10 of the Reynolds Number, R .

$$C_A = \frac{F}{\frac{\pi D^2}{4} \frac{1}{2} \rho V^2}$$

$$R = \frac{VD}{\nu}$$

where F is the drag force, D the diameter of the sphere, V the air speed, ρ the density of the air, and ν the kinematic viscosity of the air. The results for the six arrangements are given in Figures 3 to 8, inclusive.

It was suggested in reference 5 that the critical Reynolds Number for a sphere be defined as the value of the Reynolds Number at which the drag coefficient is 0.3. The values so obtained from the curves shown in Figures 3 to 8 are given in Table I.

Table I also contains the turbulence as measured by the hot-wire anemometer. The values given are the mean fluctuation of the speed at a given point expressed as a percentage of the mean speed. Each value represents the mean of two or more runs, each run consisting of observations at 6 to 10 speeds. For example, the value for arrangement 4, upstream, namely, 1.6, is the mean of the following results for 6 runs, 1.67, 1.68, 1.61, 1.77, 1.28, 1.31. The value for the fifth run, 1.28, is the mean of the following values, 1.55, 1.28, 1.10, 1.27, 1.27, 1.26, 1.45, 1.29, 1.23, 1.22, 1.27, while that for the fourth run, 1.77, is the mean of 1.64, 1.87, 1.78, 1.86, 1.80, 1.72, 1.75, and 1.73. As stated in reference 5, the values for a given run are in general more consistent among themselves than the values for different runs. The averages are given only to the first decimal place and it is believed that they are correct to ± 0.2 .

The information in the table needs to be supple- mented, especially for arrangements 3 and 5. The sphere results apparently indicate that a tunnel without a honeycomb is the least turbulent. The observations in Figure 5 do not, however, tell the complete story. The drag of the sphere varied in

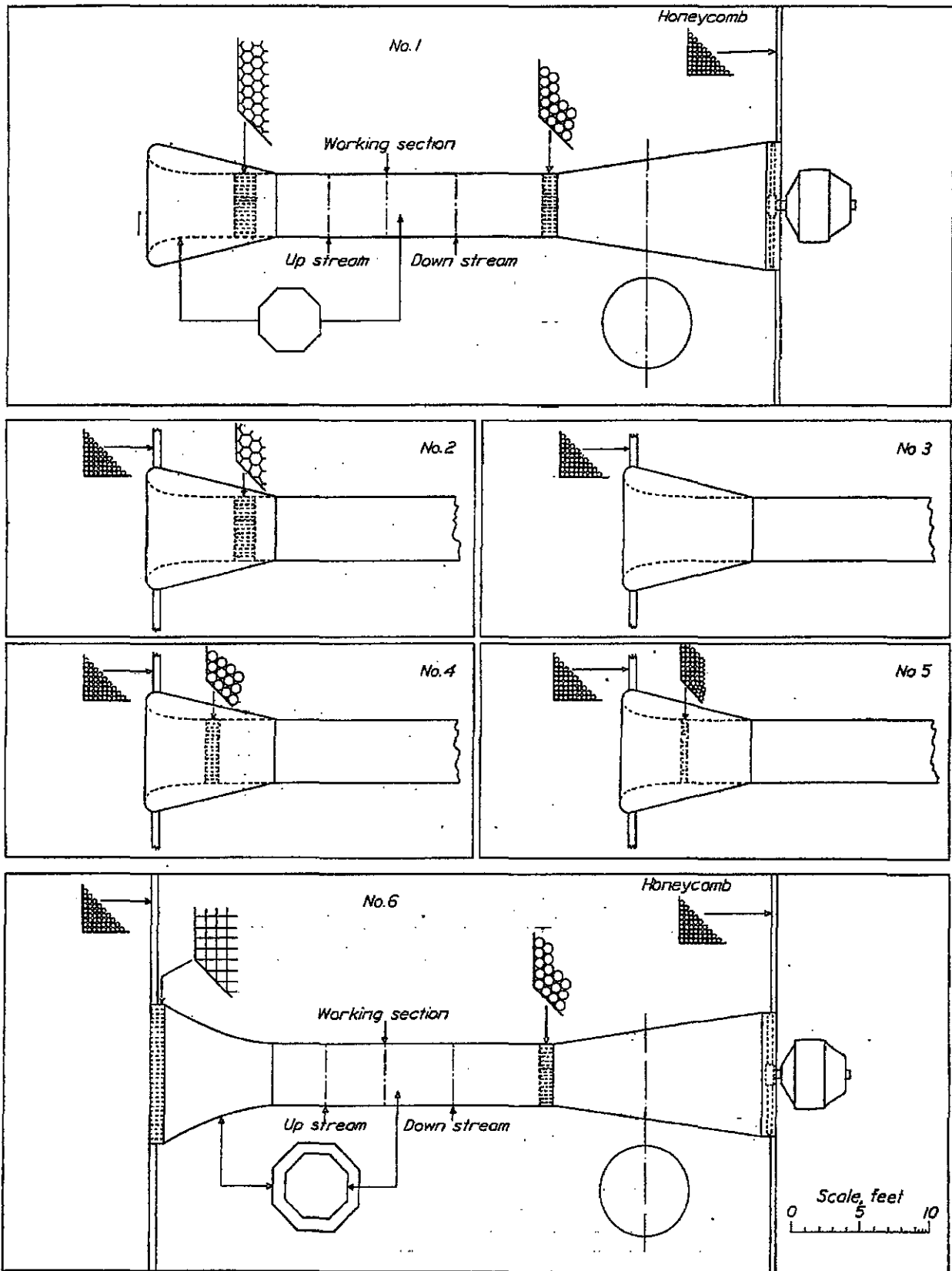


FIGURE 2.—Arrangement of parts of wind tunnel for various tests

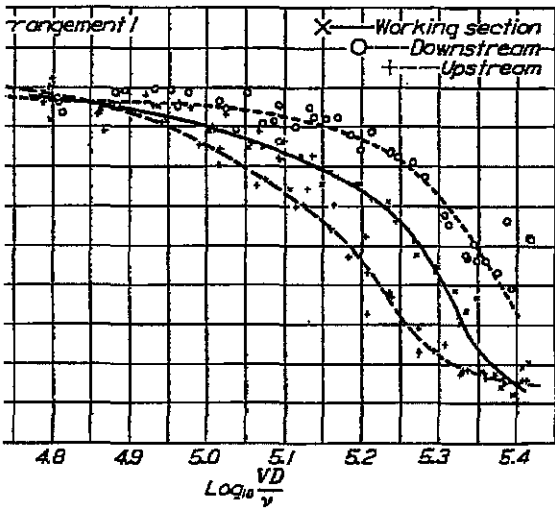


FIGURE 3.—Resistance coefficient of a sphere for arrangement 1

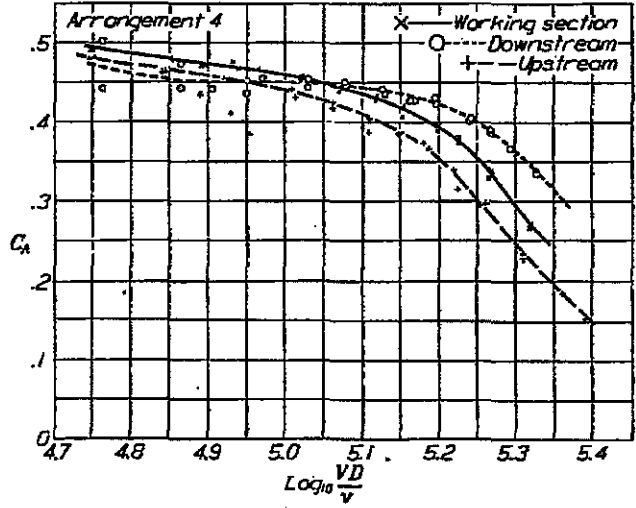


FIGURE 6.—Resistance coefficient of a sphere for arrangement 4

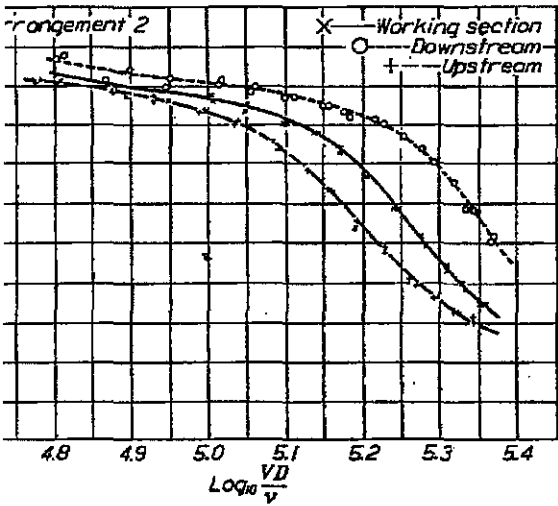


FIGURE 4.—Resistance coefficient of a sphere for arrangement 2

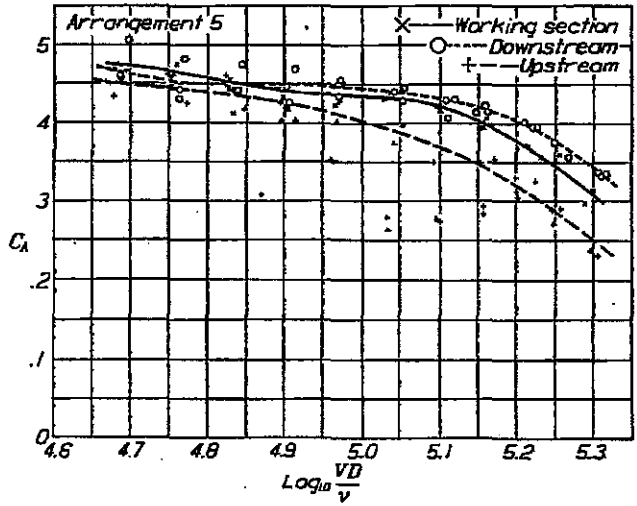


FIGURE 7.—Resistance coefficient of a sphere for arrangement 5

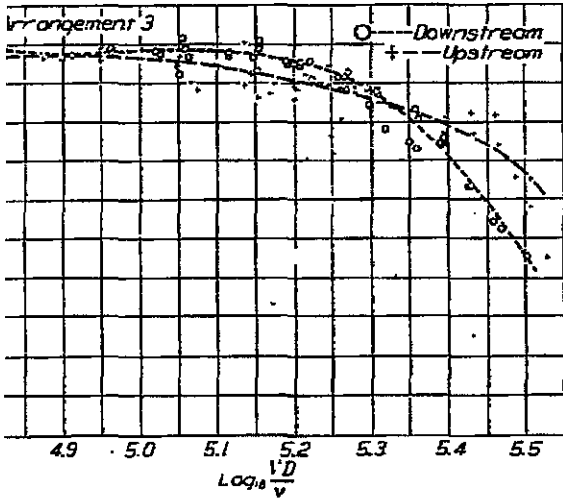


FIGURE 5.—Resistance coefficient of a sphere for arrangement 3

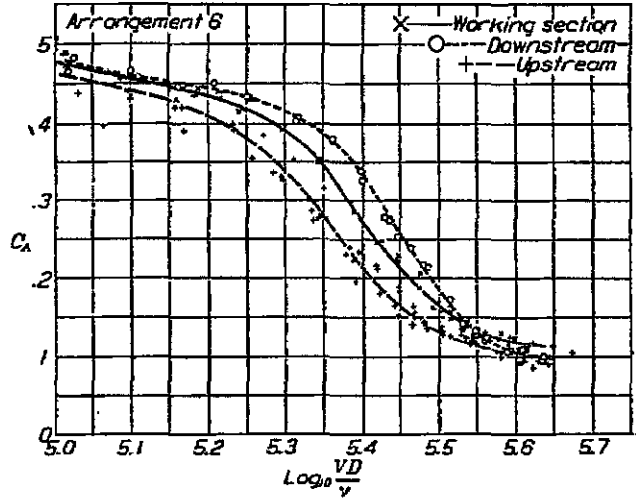


FIGURE 8.—Resistance coefficient of a sphere for arrangement 6

very interesting manner, the sphere moving in jumps from one position of equilibrium to another. The observations represent the condition prevailing for the longest time. It is believed that the turbulence is very small in general, but that frequent disturbances sweep through the tunnel and break down the laminar flow in the boundary layer of the

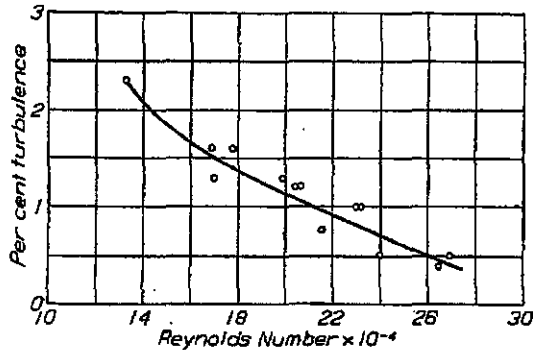


FIGURE 9.—Reynolds Number when C_d for sphere is 0.3, as a function of the turbulence

where. The taking of observations was difficult and time-consuming. The same behavior was indicated by the hot wire. Here, however, the period of the apparatus was so great (30 seconds or more) that the w values were never recorded. The sphere suspension was such that its period was only a few seconds, and the fluctuations could be more accurately observed. The operation of the tunnel in this condition was found to be impractical.

A great deal of difficulty was also experienced with arrangement 5 as indicated by the scattering of the results in Figure 7, especially for the upstream position. The trouble was found to be due in part to motion of the honeycomb under the action of the wind. The paper tubes forming the honeycomb were usually glued together and additional bracing was provided but the trouble never disappeared completely. We consider this honeycomb, or any type of honeycomb which changes position or deforms, to be completely unsatisfactory. The hot wire value for the downstream position with this arrangement is considered unreliable. It is based on a single run taken just before trouble developed with the amplifier and through an oversight no further measurements were made in this position.

Some of the measurements on arrangement 1 (fig. 3) do show a large spread. This arrangement has always shown a peculiar kind of unsteadiness of flow which the speed as recorded by a Pitot tube drops several per cent for periods as long as 15 to 30 seconds. Calibration runs have shown individual values of the ratio of the Pitot-static head to the static-pressure head differing from the mean by as much as 4 per cent and mean deviations for 15 or 20 readings of as much as 1.5 to 2 per cent, so that a large number of runs would be made to secure a precision of 1 per cent.

This behavior was in marked contrast to that of arrangement 6. The fluctuations of the manometers for arrangement 6 are reduced to a fraction of those observed for arrangement 1. Maximum deviations in calibration runs are rarely as much as 1 per cent, and mean deviations are only 0.3 per cent.

The observations in Table I give new data on the calibration of a sphere as an instrument for measuring turbulence. The data, excluding the points marked "b," which have already been discussed, are plotted in Figure 9, together with the two points for the other wind tunnels at the Bureau of Standards as given in reference 5. All of the points fit a smooth curve (slightly different from that of reference 5) within the accuracy claimed for the observations. Six of the thirteen points are near the estimated maximum deviation and lend a little support to the view that the frequencies of the fluctuations may be of importance.

The effect of the various modifications on the turbulence may be seen from Table I to be as follows: The addition of a room honeycomb at the entrance gave a measurable but small reduction in turbulence. The complete removal of the honeycomb gives the least turbulence, but the flow is subject to temporary disturbances following each other in rapid succession, which make operation in this condition impractical. Arrangement 4 gives some reduction, but as shown in Figure 10, the reduction is entirely due to increasing the distance from the honeycomb. Arrangement 5

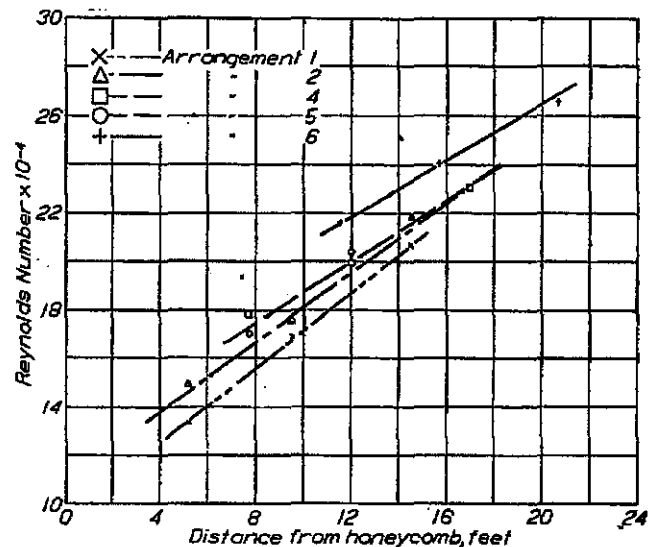


FIGURE 10.—Reynolds Number when C_d for sphere is 0.3, as a function of distance from the honeycomb for the several arrangements

gives results substantially identical with arrangement 4. From Figure 10 it appears that the value of the Reynolds Number when C_d for the sphere is 0.3 in the upstream position of arrangement 4 is somewhat high, a result also indicated by the hot-wire value. Arrangement 6 gives considerable improvement. A large part of the effect (at least half) is again due to

increased distance from the honeycomb as shown in figure 10. The remainder is probably to be attributed to the lower initial intensity produced by the speed at the honeycomb.

CONCLUSION

The turbulence in the Bureau of Standards 54-inch tunnel at a fixed distance from the honeycomb is not greatly reduced by modifications of the diameter, wall thickness, or shape of the honeycomb cells or the addition of a room honeycomb. Working at a greater distance from the honeycomb or moving the honeycomb upstream is effective in reducing the turbulence. The use of a large area reduction in the entrance cone with the honeycomb in the slow-speed section gives an additional reduction of turbulence and greatly improves the general operating conditions.

ACKNOWLEDGMENT

The measurements described in this paper were made numerous times over a period of 18 months by the members of the section of aerodynamics of the Bureau of Standards. Practically every member of the section took part in the work, and acknowledgment is made of their cooperation.

BUREAU OF STANDARDS,
WASHINGTON, D. C., March 7, 1931.

REFERENCES

1. Eiffel, G.: La résistance de l'air et l'aviation, p. 76 (Dunod et Cie, Paris), 1911. See also Sur la résistance des sphères dans l'air en mouvement, Comptes Rendus, 155, 1912, p. 597.
2. Prandtl, O.: Ergebnisse der aerodynamischen Versuchsanstalt von Eiffel, verglichen mit den Göttinger Resultaten. Zeitschrift für Flugtechnik und Motorluftschiffahrt, 3, no. 9, 1912, p. 118.

3. Wieselsberger, C.: Der Luftwiderstand von Kugeln. Zeitschrift für Flugtechnik und Motorluftschiffahrt, 5, No. 9, 1914, p. 140.
4. Higgins, George J.: Tests of the N. P. L. Airship Models in the Variable Density Wind Tunnel. N. A. C. A. Technical Note No. 264, 1927.
5. Dryden, H. L., and Kuethe, A. M.: Effect of Turbulence in Wind Tunnel Measurements. N. A. C. A. Technical Report No. 342, 1930.
6. Reynolds, O.: An Experimental Investigation of the Circumstances which Determine whether the Motion of Water Shall Be Direct or Sinuous and of the Law of Resistance in Parallel Channels. Phil. Trans. Roy. Soc. 1833, Part III, 174, p. 935.
7. Wieselsberger, C.: On the Improvement of Air Flow in Wind Tunnels. N. A. C. A. Technical Memorandum No. 470, 1928. Translation from Journal Soc. Mech. Eng. of Japan, 28, No. 98, June, 1925.
8. Ziegler, M.: The Application of the Hot-Wire Anemometer for the Investigation of the Turbulence of an Air Stream. Proc. Koninklijke Akademie van Wetenschappen te Amsterdam, 33, No. 7, 1930, p. 723.

TABLE I.—REYNOLDS NUMBERS WHEN C_d FOR SPHERE IS 0.3 FOR THE SEVERAL ARRANGEMENTS, IN ORDER OF INCREASING VALUES OF R (DECREASING VALUES OF TURBULENCE).

Arrangement	Reynolds Number for sphere when C_d is 0.3	Average hot-wire value of turbulence (per cent)
1, upstream.....	128000	2.3
2, upstream.....	150000	
1, working section.....	168000	1.5
2, upstream.....	170000	1.8
2, working section.....	175000	
4, upstream.....	178000	1.6
4, working section.....	180000	1.8
5, working section.....	204000	1.2
1, downstream.....	206000	1.2
6, upstream.....	215000	0.75
2, downstream.....	218000	
4, downstream.....	230000	1.0
5, downstream.....	230000	1.4
6, working section.....	240000	0.5
6, downstream.....	250000	0.4
3, downstream.....	281000	0.8-1.4
3, upstream.....	338000	0.5-1.4

¹ These values differ slightly from those of Reference 5 as more points have been added and the curves redrawn.
² Extrapolated.
³ Omitted from Figure 6.
⁴ Omitted from Figure 9, erratic.